

# A modelling methodology to quantify the impact of plant anomalies on ID fan capacity in coal fired power plants

---



## **Prepared by:**

Rendani Yaw-Boateng Sean Khobo  
KHBREN001

Department of Mechanical Engineering  
University of Cape Town

## **Supervisor:**

Professor Pieter Rousseau

## **Co-Supervisor:**

Mr. Priyesh Gosai

**January 2020**

Submitted to the Department of Mechanical Engineering at the University of Cape Town in partial fulfilment of the academic requirements for a Master's of Science degree in Mechanical Engineering

## **Key Words:**

Induced Draft Fan; Draught plant, anomaly detection, Fan Capacity Limitations,

The copyright of this thesis vests in the author. No quotation from it or information derived from it is to be published without full acknowledgement of the source. The thesis is to be used for private study or non-commercial research purposes only.

Published by the University of Cape Town (UCT) in terms of the non-exclusive license granted to UCT by the author.

## *Abstract*

In South Africa, nearly 80 % of electricity is generated from coal fired power plants. Due to the complexity of the interconnected systems that make up a typical power plant, analysis of the root causes of load losses is not a straightforward process. This often leads to losses incorrectly being ascribed to the Induced Draught (ID) fan, where detection occurs, while the problem actually originates elsewhere in the plant.

The focus of this study was to develop and demonstrate a modelling methodology to quantify the effects of major plant anomalies on the capacity of ID fans in coal fired power plants. The ensuing model calculates the operating point of the ID fan that is a result of anomalies experienced elsewhere in the plant. This model can be applied in conjunction with performance test data as part of a root cause analysis procedure.

The model has three main sections that are integrated to determine the ID fan operating point. The first section is a water/steam cycle model that was pre-configured in VirtualPlant™. The steam plant model was verified via energy balance calculations and validated against original heat balance diagrams. The second is a draught group model developed using FlownexSE™. This one-dimensional network is a simplification of the flue gas side of the five main draught group components, from the furnace inlet to the chimney exit, characterising only the aggregate heat transfer and pressure loss in the system. The designated ID fan model is based on the original fan performance curves. The third section is a Boiler Mass and Energy Balance (BMEB) specifically created for this purpose to: (1) translate the VirtualPlant results for the steam cycle into applicable boundary conditions for the Flownex draught group model; and (2) to calculate the fluid properties applicable to the draught group based on the coal characteristics and combustion process.

The integrated modelling methodology was applied to a 600 MW class coal fired power plant to investigate the impact of six major anomalies that are typically encountered. These are: changes in coal quality; increased boiler flue gas exit temperatures; air ingress into the boiler; air heater in-leakage to the flue gas stream; feed water heaters out-of-service; and condenser backpressure degradation.

It was inter alia found that a low calorific value (CV) coal of 14 MJ/kg compared to a typical 17 MJ/kg reduced the fan's capacity by 2.1 %. Also, having both HP FWH out of service decreased the fan's capacity by 16.2 %

## *Declaration*

I, Rendani Yaw-Boateng Sean Khobo, hereby declare the work contained in this dissertation to be my own. All information which has been gained from various journal articles, text books or other sources has been referenced accordingly. I have not allowed, and will not allow, anyone to copy my work with the intention of passing it off as their own work or part thereof.

2020/01/30

Signed by candidate

Name

Date

## *Acknowledgements*

Firstly, I would like to thank the Eskom Power Plant Engineering Institute and more directly the Applied Thermodynamic Process Modelling Research Unit for affording me the funding and opportunity to pursue this Masters.

I would like to thank my supervisors Prof Pieter Rousseau and Mr Priyesh Gosai whose experience, constant pushing and mentoring saw me through some difficult times, and without whom this could not have continued to where it is now.

Thank you, Associate Professor Wim Fuls, for helping me very early on to crack the secrets to the VirtualPlant Software.

I would like to thank my industrial mentor Ravendra Govindsamy whose insight to the plant illuminated many dark corners of this research.

A big thank you to the staff at Plant A, whose willingness to help me get the information I needed, made investigations less stressful.

My fellow students at UCT have my gratitude for extending helping hands on those long nights. Especially Patrick Akpan, Excellent Gwebu and Geoff Raikes who guidance made me feel like I had two older brothers (and a little one) looking out for me.

To my brilliant editor, Renata Briajraj, for trudging through all my spelling and grammar issues. I really appreciate it.

Mother, Father, Brother, Sister. Thank you for being yourselves and the support I can never hope to ever payback.

Finally, I would like to thank God for helping me carry on till this day. All things are possible with a little faith.

# Table of Contents

|   |      |
|---|------|
| List of figures .....                                 | vi   |
| List of tables .....                                  | ix   |
| List of acronyms and abbreviations .....              | x    |
| List of nomenclature .....                            | xii  |
| List of equations .....                               | xiii |
| 1. Introduction .....                                 | 1    |
| 1.1 Background.....                                   | 1    |
| 1.2 Research problem .....                            | 4    |
| 1.3 Objectives of this study .....                    | 5    |
| 1.4 Scope and limitations .....                       | 5    |
| 2. Literature review.....                             | 6    |
| 2.1 Overview of literature .....                      | 6    |
| 2.2 Fan fault detection .....                         | 8    |
| 2.3 Power plant efficiency improvement.....           | 9    |
| 2.4 Water/steam modelling .....                       | 13   |
| 2.5 Draught group modelling .....                     | 14   |
| 2.6 ID fan anomalies.....                             | 15   |
| 3. Model development .....                            | 23   |
| 3.1 Rankine cycle model.....                          | 24   |
| 3.2 Boiler mass and energy balance tool .....         | 33   |
| 3.3 Draught group model .....                         | 39   |
| 3.4 Model integration methodology .....               | 47   |
| 4. Application case studies.....                      | 49   |
| 4.1 Coal quality effects .....                        | 51   |
| 4.2 Increased boiler flue gas exit temperatures ..... | 53   |
| 4.3 Air ingress into the boiler .....                 | 54   |
| 4.4 Air heater inleakage to flue gas stream .....     | 55   |
| 4.5 Feed water heaters out-of-service .....           | 56   |
| 4.6 Condenser backpressure degradation .....          | 58   |

|  |     |
|--|-----|
| 5. Conclusions and recommendations.....      | 59  |
| 5.1 Conclusions.....                         | 59  |
| 5.2 Recommendations .....                    | 60  |
| 6. List of references.....                   | 61  |
| Appendix A. Mathematical derivation.....     | 64  |
| A.1 – Complete BMEB .....                    | 64  |
| A.2 – Excess air calculation.....            | 86  |
| Appendix B. Program code .....               | 90  |
| B.1 - MEB C# script .....                    | 90  |
| B.2 - VirtualPlant C# script.....            | 110 |
| Appendix C. Model design .....               | 120 |
| C -1 Steady state controller flowchart ..... | 120 |

# List of figures

|   |    |
|---|----|
| Figure 1: Eskom's electricity generation installed capacity/production 2017 (Left) and planned 2030 generation (Right) for South Africa ..... | 1  |
| Figure 2: Typical CFPP layout .....   | 2  |
| Figure 3: Top 5 UCLF Contributors. Adapted from [6] .....   | 3  |
| Figure 4: Cause and of effect of Condenser on ID fan .....  | 4  |
| Figure 5: Comparison of Achievable and Actual Performance .....   | 8  |
| Figure 6: Heat Rate Logic Tree - Main Diagram [15] .....  | 10 |
| Figure 7: Heat Rate Logic Tree - Electrical Auxiliary Losses - Change in ID Fan Efficiency [15] .....   | 11 |
| Figure 8: Coal use in South Africa 2010 (excludes exports)[21] .....  | 15 |
| Figure 9: Air heater schematic[33].....   | 19 |
| Figure 10: Impact of number of feedwater heaters on the steam cycle efficiency [7] .....  | 20 |
| Figure 11: Feedwater heater banks .....   | 20 |
| Figure 12: Full Model Flowchart .....   | 23 |
| Figure 13: Steam cycle model inputs and outputs .....   | 24 |
| Figure 14: Fossil Boiler as in VirtualPlant.....  | 26 |
| Figure 15: High-pressure turbine as in VirtualPlant.....  | 27 |
| Figure 16: HP Turbine Inputs and Outputs .....  | 27 |
| Figure 17: IP/LP turbine as in VirtualPlant.....  | 28 |
| Figure 18: IP/LP Turbine Inputs and Outputs .....   | 28 |
| Figure 19: Main Condenser as in VirtualPlant .....  | 29 |
| Figure 20: Condenser Inputs and Outputs.....  | 30 |
| Figure 21: Closed (left) and Open (right) feedwater heater as in VirtualPlant .....   | 30 |
| Figure 22: HP FWH Inputs and Outputs .....  | 31 |
| Figure 23:HP inlet steam mass flow vs Plant load .....  | 32 |
| Figure 24: Total turbine power vs Plant load.....   | 32 |
| Figure 25: BMEB Boundary .....  | 35 |



|   |    |
|---|----|
| Figure 26: High level schematic of BMEB .....   | 35 |
| Figure 27: Air heater schematic .....   | 36 |
| Figure 28: BMEB high level calculation flow .....   | 36 |
| Figure 29: BMEB tool inputs and outputs .....   | 37 |
| Figure 30: Draught group diagram .....  | 39 |
| Figure 31: Draught group model inputs and output .....  | 40 |
| Figure 32: Draught group representative boundary .....  | 40 |
| Figure 33: Variable Speed Fan .....   | 41 |
| Figure 34: Flow resistance .....  | 41 |
| Figure 35: General empirical relationship .....   | 41 |
| Figure 36: Script .....   | 41 |
| Figure 37: Boundary Condition .....   | 41 |
| Figure 38: Node .....   | 41 |
| Figure 39: Illustration of fan chart with two vane angle curves .....                           | 42 |
| Figure 40: Prototype air heater (with leakage) .....  | 45 |
| Figure 41: Full draught group model .....   | 46 |
| Figure 42: Final connected model .....  | 47 |
| Figure 43: Excel model setup .....  | 48 |
| Figure 44: Anomaly locations .....  | 49 |
| Figure 45: ID fan capacity loss at varying loads schematic .....                                | 50 |
| Figure 46: Normalised capacity lost due to coal quality (CV Measured) .....                     | 52 |
| Figure 47: Normalised capacity lost due to coal quality (CV Calculated) .....                   | 52 |
| Figure 48: Normalised capacity lost by boiler flue gas exit temperature .....                   | 53 |
| Figure 49: Normalised capacity lost by air ingress into the boiler .....                        | 54 |
| Figure 50: Normalised capacity lost by air leakage into the flue gas stream of air heater ..... | 55 |
| Figure 51: Feedwater heater train of Plant A .....  | 56 |
| Figure 52: Normalised capacity lost by out of service HP FWH at various boiler loads .....      | 57 |

|  |     |
|--|-----|
| Figure 53: Normalised capacity lost by condenser backpressure degradation..... | 58  |
| Figure 54: Steady-state controller program flowchart .....                     | 120 |

# List of tables

|   |    |
|---|----|
| Table 1: Sensitivity of Performance Parameter Deviation on Heat Rate [15] ..... | 12 |
| Table 2: Factors influencing combustion efficiency of coal[22] .....            | 16 |
| Table 3: HP Turbine Mass and Energy Balance Results .....                       | 27 |
| Table 4: IP/LP Turbine Mass and Energy Balance Results .....                    | 29 |
| Table 5: Condenser Mass and Energy Balance Results.....                         | 30 |
| Table 6: HP FWH Mass and Energy Balance Results .....                           | 31 |
| Table 7: Residuals between BMEB and baseline information .....                  | 37 |
| Table 8: FlownexSE component icons.....   | 41 |
| Table 9: The composition of the coals examined .....                            | 51 |
| Table 10: Runs carried out for out of service HP FWHs.....                      | 56 |

# List of acronyms and abbreviations

|                 |   |
|-----------------|---|
| ASME            | American Society of Mechanical Engineers                                  |
| API             | Application Programming Interface   |
| ASHRAE          | American Society of Heating, Refrigerating and Air-conditioning Engineers |
| BMCR            | Boiler Maximum Continuous Rating  |
| BMEB            | Boiler Mass and Energy Balance  |
| CFPP            | Coal-Fired Power Plants   |
| CM              | Condition Monitoring  |
| CV              | Calorific Value   |
| CVCalc          | Calculated Calorific Value  |
| CVMeasured      | Measured Calorific Value  |
| EAF             | Energy Availability Factor  |
| EPPEI           | Eskom Power Plant Engineering Institute                                   |
| FD              | Forced Draught  |
| FET             | Furnace Exit Temperature  |
| FWH             | Feed Water Heater   |
| HBD             | Heat Balance Diagram  |
| HEI             | Heat Exchange Institute   |
| HHV             | Higher Heating Value  |
| HP              | High-Pressure   |
| HVAC            | Heating, Ventilation, And Air Conditioning                                |
| ID fan          | Induced Draught Fan   |
| IP              | Intermediate Pressure   |
| LHV             | Lower Heating Value   |
| LP              | Low Pressure  |
| MEB             | Mass & Energy Balance   |
| MEV             | Map Entered Variable  |
| NIST            | National Institute of Standards and Technology                            |
| NO <sub>x</sub> | Nitrogen Oxides   |
| NPP             | Nuclear Power Plant   |
| OEM             | Original Equipment Manufacturer   |
| PA fan          | Primary Air Fan   |
| PCLF            | Planned Capability Loss Factor  |
| PF              | Pulverised Fuel   |
| PM              | Performance Monitoring  |
| PTC             | Performance Test Codes  |
| SO <sub>x</sub> | Sulphur Oxides  |

|        |  |
|--------|--|
| TCMR   | Turbine Maximum Continuous Rating                                      |
| UCLF   | Unplanned Capability Loss Factor                                       |
| UNIPED | International Union of Producers and Distributors of Electrical Energy |
| VP     | VirtualPlant   |
| YTD    | Year-To-Date   |

# List of nomenclature

## Greek symbols

|                  |                                 |          |
|------------------|---------------------------------|----------|
| $\alpha$         | Pressure drop constant          |          |
| $\beta$          | Pressure drop constant          |          |
| $\delta, \Delta$ | Change in or Difference between |          |
| $\theta$         | Vane opening percentage         | %        |
| $\rho$           | Fluid density                   | $kg/m^3$ |

## General symbols

|                     |   |                |
|---------------------|---|----------------|
| cfm                 | Cubic feet per minute   |                |
| A                   | Flow area   | $m^2$          |
| $A_f$               | Flow admittance   | $m^4$          |
| $c_k$               | Pressure drop constant  |                |
| D                   | Inside diameter of pipe   | m              |
| $f$                 | Friction factor   |                |
| g                   | Gravitational acceleration constant   | $m/s^2$        |
| H                   | Pressure rise   | kPa            |
| $I_{abnormal}$      | Abnormal operational current  | A              |
| $I_{limit}$         | Operational current limit   | A              |
| $I_{ref}$           | Reference current   | A              |
| L                   | Length of pipe  | m              |
| $\dot{m}$           | Fluid mass flow   | $kg/s$         |
| Q                   | Volume flow rate  | $m^3/s$        |
| $q_{formation}$     | Formation energy of stable element  | $kJ/kg$        |
| $q_{latent}$        | Latent heat   | $kJ/kg$        |
| rpm                 | Revolution per minute   |                |
| s                   | Specific Entropy  | $J/kg \cdot K$ |
| T                   | Temperature   | $^{\circ}C$    |
| V                   | Mean fluid velocity   | $m/s$          |
| $x_i$               | Mass fraction of i  | %              |
| $\delta_{capacity}$ | Normalised capacity loss  | %              |
| $\Delta I_{ab}$     | Difference between abnormal operational current and Operational current limit | A              |
| $\Delta I_{ref}$    | Difference between Reference current and Operational current limit            | A              |
| $\Delta P$          | Change in pressure  | kPa            |
| $\Delta Z$          | Height difference between inlet and outlet                                    | m              |

## List of equations

|      |  |
|------|--|
| (1)  | % Fan capacity remaining                 |
| (2)  | Expected full load calculation           |
| (3)  | Percentage change in auxiliary power     |
| (4)  | Higher heating value of coal calculation |
| (5)  | Fan operating point derivation (part 1)  |
| (6)  | Fan operating point derivation (part 2)  |
| (7)  | Fan operating point derivation (part 3)  |
| (8)  | Fan operating point derivation (part 4)  |
| (9)  | Pressure drop equation                   |
| (10) | Mass flow                                |
| (11) | Mass flow rearranged                     |
| (12) | Pressure drop equation rearranged        |
| (13) | Flow admittance derivation               |
| (14) | Pressure drop equation (version 2)       |
| (15) | Normalised capacity loss equation        |

# 1. Introduction

## 1.1 Background

Eskom produces nearly 95 % of the electricity generated in South Africa and also provides power to neighbouring countries [1]. As Jeffery [2] noted, South Africa's abundant coal reserves is the main source for power production using Coal Fired Power Plants (CFPP). Figure 1 shows Eskom's energy mix in 2017 and the expected energy mix for 2030 based on the Integrated Resource Plan[3].

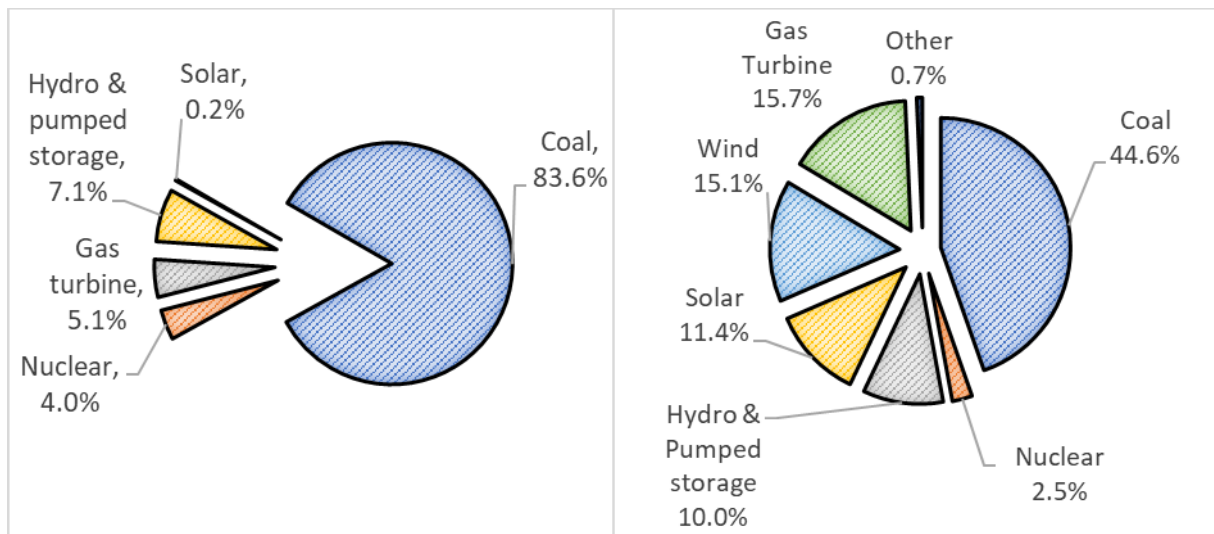


Figure 1: Eskom's electricity generation installed capacity/production 2017 (Left) and planned 2030 generation (Right) for South Africa

It is expected that the proportion of electricity generated from other sources of energy will increase in the decades to come. However, CFPP's are most likely to continue producing most of South Africa's electricity for the foreseeable future. The misleading percentage drop of CFPPs from 83.6% to 44.6% translates to an actual installed generation capacity from 39 GW to 34 GW [3]. Excluding the two new plants under construction (Medupi and Kusile power stations), most of Eskom's CFPP's have passed mid-life with some approaching, if not passing, the end of their design life. This aged power plant fleet is now more likely to have more components fail or, having deteriorated, operate inefficiently. Developing tools to enable condition-based maintenance will contribute to lower maintenance costs and allow utilities to prioritise maintenance.

The typical CFPP is based on an ideal water/steam Rankine cycle. The technology, which was first commercially established around 1884 [4], has seen developments in technology which have led to increased efficiency and larger capacity power plants, while decreasing lifecycle costs.



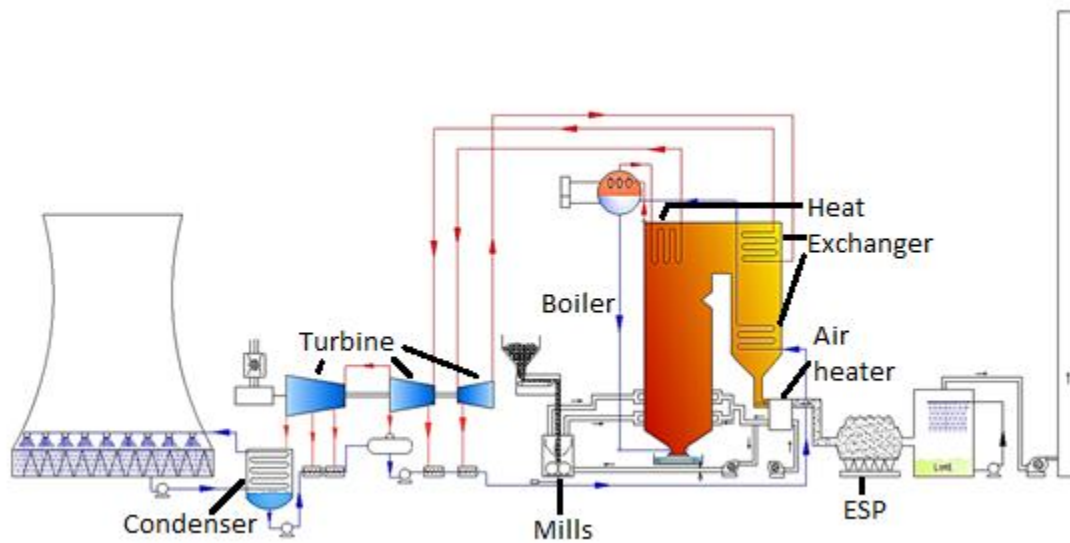


Figure 2: Typical CFPP layout

The typical layout of a modern day CFPP is depicted in Figure 2 above. The method by which electricity is generated can be explained with respect to the coal/flue gas cycle and the water/steam cycle.

In the coal/flue gas stream, the coal is pulverised in mills and then transported to the boiler where it is mixed with air to combust. The resulting flue gas is drawn through a series of heat exchangers to generate high temperature steam. At the boiler's exhaust, the flue gas is still above ambient temperatures. The energy contained in the exhaust gasses would normally be completely lost as it is discharged into the atmosphere. While it still has the potential to be used for heating ambient fresh air entering the boiler. The remaining heat in the flue gas is therefore used to pre-heat the incoming air in the air heaters, thereby contributing to reducing the heat demand from the boiler. Before being discharged to atmosphere, pollutants such as particulates and Sulphur Oxides ( $\text{SO}_x$ ) are removed using various pollutant abatement technologies. Figure 2 uses electrostatic precipitators (ESP).

On the water/steam side, shown by the blue and red arrows in Figure 2, superheated steam produced in the boiler is delivered to a steam turbine that converts thermal energy to mechanical energy which is in turn used to generate electricity. Latent heat in the steam leaving the turbine is rejected via a condenser to atmosphere and the resulting condensate is pumped back to the boiler. To improve cycle efficiency steam is extracted at various points along the turbine train to supply feed water heaters which pre-heat feedwater before entering the boiler.

Anomalies in any single component are not always obvious. Other components in the system are impacted by the anomaly and the resulting symptoms are seen in other seemingly unconnected

components. Anomalies affect overall plant performance, and their impact is typically quantified using performance metrics such as the Energy Availability Factor (EAF) and Unplanned Capability Loss Factor (UCLF), as defined by UNIPED [5]. An increase in anomaly occurrences, increases the UCLF. This thus decreases the EAF.

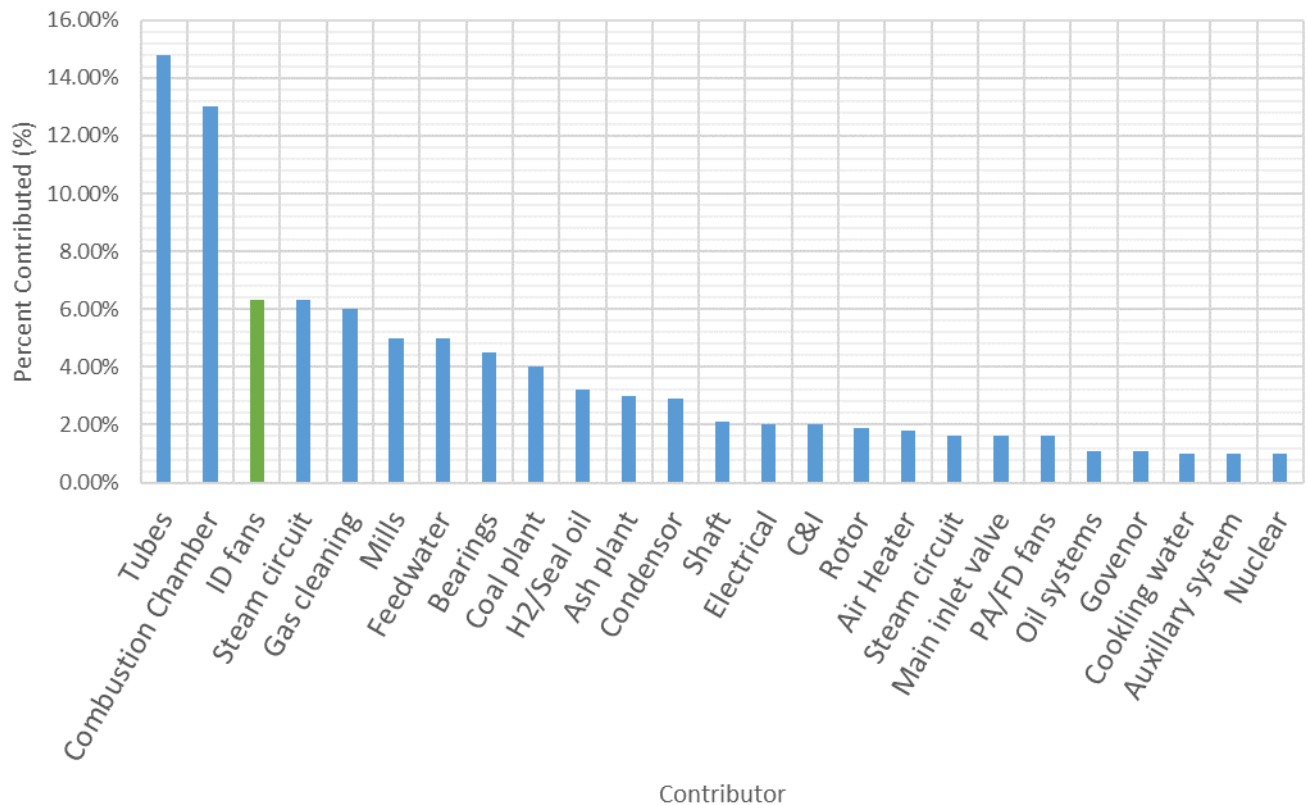


Figure 3: Top 5 UCLF Contributors. Adapted from [6]

As shown in Figure 3, the induced draught (ID) fan is recorded as having the third most significant impact on the UCLF at about 6.25 %. Of all the faults recorded for the ID fan, the most common issue is that of the fan running out of capacity.

The ID fan is controlled with the aim to maintain pressure in the boiler furnace slightly below atmospheric conditions [7]. This is achieved by throttling the gas flow or varying fan speed. The fan's capacity is thus the amount of flue gas the fan can draw through the system given the inherent pressure losses. When the fan is unable to draw the desired air flow for maintaining the required generating load, it is reported as a bottleneck.

One typical cause for a fan not being able to meet demand could be that the fan has physically deteriorated and is unable to perform as designed. However, this is not the only cause and can be demonstrated as follows:

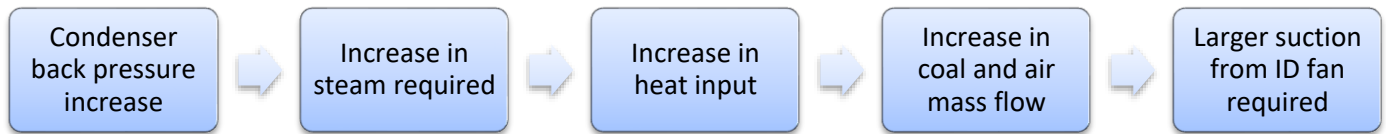


Figure 4: Cause and effect of Condenser on ID fan

An increase in condenser pressure from inter alia adverse atmospheric conditions or scaling in condenser tubes will lead to increased steam demand. This in turn will lead to increased heat required to meet the expected generating load. To supply this energy, operators would increase coal flow and the corresponding air flow, which adds additional demand on the ID fan. This is graphically shown in Figure 4.

Similarly, other plant anomalies also increase the demand on the ID fan. Understanding and quantifying the relationship between those anomalies and their impact on the ID fan can vastly improve load forecasting, performance monitoring and support condition-based maintenance. This is further supported by utilities increasingly adopting centralised data historians making online monitoring more easily accessible. A systematic study of various well-defined anomalies, and their effects on the ID fan, would yield results that help in the understanding of capacity limitations.

## 1.2 Research problem

Modelling this inter-connected complex system to quantify the impact of anomalies on the ID fan requires a sensible approach with regard to the level of detail needed. Having too much detail would lead to a model which cannot be validated or is impractical, while too little detail will not capture the governing physics affecting this problem. Therefore, the study will involve the use of various tools available commercially to the power plant industry. These tools are integrated such that the impact of anomalies is appropriately quantified.

Three tools available to engineers are:

- FlownexSE<sup>TM</sup> (referred to as FlownexSE hereafter), which solves for mass, momentum and energy conservation using a one-dimensional network-based modelling approach.
- VirtualPlant (VP), which performs mass and energy balances applied to power generation cycles.
- Boiler Mass and Energy Balance (BMEB), which can be used to determine the quantity of heat generated from coal supplied to the furnace.

## 1.3 Objectives of this study

The primary objective of this project is to develop a modelling methodology that can be used to conduct a systematic study of the impact of various anomalies within the power plant that impact the ID fan.

The enabling objectives will be to:

- Identify and quantify power plant anomalies that could result in altered air flow requirements.
- Develop a model of the draught group with the appropriate level of detail using FlownexSE.
- Evaluate the validity of a VP model for full and part load conditions with various anomalies.
- Implement the BMEB methodology to determine flue gas properties for the draught group model.
- Demonstrate the integrated model by simulating different scenarios of anomalies and generation loads to quantify the effect on the ID fan operating point.

## 1.4 Scope and limitations

The study is limited to using the FlownexSE and VP software for the creation of a methodology to model a power plant. VP software is ideal for the water/steam cycle model. The water/steam side model need only solve the conservation equations of mass and energy which VirtualPlant does solely. This saves time by neglecting the conservation of momentum equations. FlownexSE will be used to model the draught group as it contains all three conservation equations built into its solver. VP and FlownexSE are readily available in Eskom and can be used to follow the methodology described here.

The study will perform case study calculations on an Eskom power plant, referred to as *Plant A* from here on.

The methodology is limited to modelling six anomalies, identified through consultation with industry experts, and is thus not an exhaustive study on all possible anomalies.

This tool can help as a building block towards creating a platform for root cause analysis and on-line condition monitoring schemes. The project as it is now, is not a way to solve the anomalies investigated.

## 2. Literature review

### 2.1 Overview of literature

A collaboration between GP Strategies and Westar Energy (USA) involved the development of a tool to model the ID fan. The application of this model would be to overcome and predict ID fan capacity limitations [9]. The model was applied to an 800MW coal fired power plant based in Kansas (USA).

Initially the input data to be used was the: boiler gas exit flow; boiler air in-leakage and air heater air-in leakage; ID fan suction pressure; ID fan gas inlet temperature; ID fan discharge pressure; ID fan gas outlet temperature; and ID fan vane position. The boiler gas exit flow was calculated using the EtaPRO's combustion calculations while the leakage values were calculated using the oxygen measurements. All the other inputs came from live data from pressure transmitters, thermocouple transmitters and the ID fan vane position has its own position transmitter.

Original Equipment Manufacturers (OEMs) performance curves of the ID fan were also obtained to investigate how the inlet vane position effects the fan's performance. During the study, it was discovered that the current fan performance was significantly lower than the original fan curves. This was later verified by the OEM via empirical data and a CFD model. The results showed that the fan running at fully open guide vanes, functioning at a 15% volume flow deficit.

Once the above inputs were verified, the tool was developed with the following equation (eq (1)) used to determine the remaining fan capacity (derived from the work done by Godre[9]):

$$\% \text{ Fan capacity remaining} = 100\% * \left[ \frac{\text{Maximum volumetric flow} - \text{Actual volumetric flow}}{\text{Maximum volumetric flow}} \right] \quad (1)$$

A second calculation (eq (2)) was also incorporated to calculate the expected capacity at full load given the current conditions (derived from the word done by Godre[9]):

$$\text{Full Load} = \text{Gross MW} * \left[ \frac{\text{Maximum volumetric flow} + \text{Excess Capacity}}{\text{Maximum volumetric flow}} \right] \quad (2)$$

Having completed the tool, the next step was to quantify the individual effects of plant issues such as, boiler convection fouling, boiler gas path air in leakages, air heater fouling, air heater leakage, and physical ID fan problems. They noted that the end goal was to help the plant staff by providing them with the ability to better focus their resources to mitigate large economic impacts.

Godre, et. al [9] identified that the fan performance curve can be significantly different to the actual operating point. If plant operators are using these curves for analyses, it would be important to determine the actual capacity available. However, a more pressing matter concerning some

operators was not only the maximum capacity, but the impact of anomalies on the fan. A more practical first step, in the South African context, is to determine the relative contribution of anomalies to enable maintenance prioritisation.

The application of a monitoring system in power plants has been heavily improved due to advances in integrated information technology solutions. Kim, Na and Heo [10] focused on creating a framework for in-situ performance analysis based on Nuclear Power Plants (NPP). The technologies in NPP, are comparable to that of CFPPs and, as such, many of the concepts described in the paper are of value. The first concept to differentiate between them is the terminology of performance testing and performance monitoring. Performance monitoring aims to detect changes in performance metrics of cycles or components, unlike performance testing whereby the goal is to accurately quantify the performance metrics in a highly controlled environment. Another distinction can be made with the types of losses a power plant can incur. Controllable losses are those due to degradation of a component or system in a way that can be remedied while an uncontrollable loss is due to aging. The understanding that uncontrollable losses occur in power plants means that system engineers should expect an actual performance lower than the rated performance. Performance tests are run in environments with an aim to eliminate any controllable losses and create good reference material for the plant to run off of. One commonly used standard for this is the ASME PTC 6 standard. In performance monitoring, because only the changes in performance metrics are calculated, the differentiation between controllable and uncontrollable losses is hard to differentiate without a good reference and commonly guided by the PTC 6M. The only definite result that can come from performance monitoring is whether actions on the plant are degrading the plants performance.

The following figure depicts the idea of actual performance versus achievable performance. It must be noted that the achievable performance curve is that of a plant in which degradation and aging are not factors.

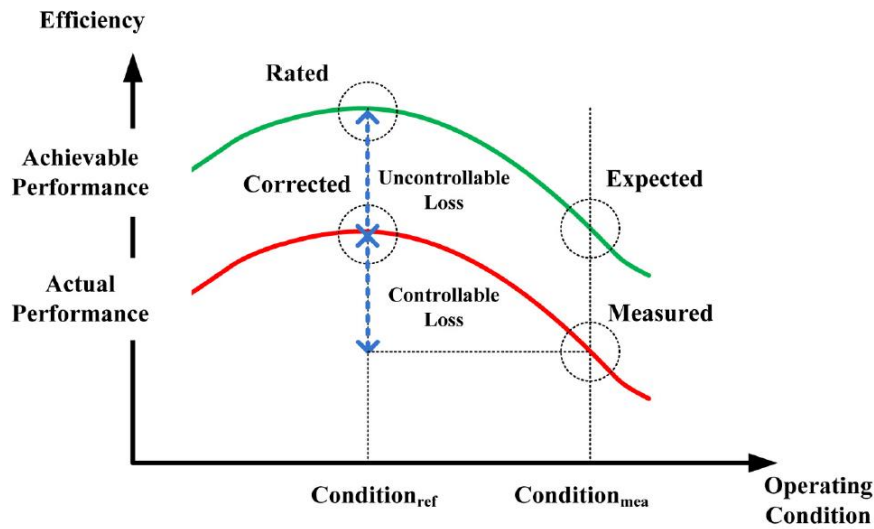


Figure 5: Comparison of Achievable and Actual Performance

The advantage in condition monitoring helps show when systems are deteriorating however identifying their causes requires information on how the system reacts in the different situations. The model approach to quantifying the impacts will not only help identify when things are not working optimally, but also help in diagnosing and ultimately rectifying whatever fault may have occurred.

The impacts to the system can be broadly categorized into real and effective issues. Real issues related to physical anomalies with the component in question. This can be rectified by typical maintenance, if possible, or replacement. Effective issues are those that are not seen to directly cause performance issues on a component. Effective issues on a power plant would be seen as a component limiting generation even though there are no discernible real issues. The root cause of this is typically not from the component in question. Real issues are not the focus of the study however, it is important to know some common mechanisms of failure and how they can be seen in a condition monitoring system. Real issues are easily identified; however, their impacts are not always known. That is aside from the component in question not operating correctly.

## 2.2 Fan fault detection

Commonly reported damage mechanisms are focused on fan blade integrity. This microscopic view of inefficiency is important as it can give clues into identifying real issues from effective issues. Thus, the following selection of studies has been presented.

Kazempour-Liacy, et.al [11], carried out a study on forced draught (FD) fan blade failure mechanisms. The blade design for the FD and ID fan are very similar and as such the findings are

applicable. The power plant investigated was near the sea, and it was ultimately concluded that chlorine ions in the air caused pitting on the surface of the blades. This initial weakness caused the blades to experience both fatigue and corrosion at the same time thus drastically reducing their lifetimes. The active loss in performance could be seen in the volume flow and a lack of pressure rise across the fan.

Bulloch and Callagy[12] investigated fan blade coating as a source for reduced service life. Standard fan blade coating *Metco 447*, was tested against Alumina/Titania 87/13, Nicrome 80/20 and Hastalloy G30. During their investigation it was found that their case study was performed under an acidic environment which greatly diminished expected service life times. The Nicrome 80/20 coated blades lasted around three times longer than the other coatings. A further result from the study saw that the smaller grain sizes in the coating was linked to smaller depths of damage zones.

One study was very focused on the malfunctions experienced on fans (ID fans, PA fans, and FD fans), and its impact on service intervals. Ramos[13] used a parametric study to observe the effects of typical fan malfunction types on the time till the next required maintenance. The malfunction types were: High vibrations, inlet damper obstructions and higher temperature at reels. The Weibull Distribution was utilised; and with plant data from two Fossil power units the required parameters were determined. Unit reliability at varying operating times from 1000 to 10 000 hours was calculated and deviations between the units were interrogated to identify what may have caused the discrepancies.

EPRI did a study that focused on root cause failure analysis of fossil fired power plants draught fan [14]. The study was an extensive and detailed one, covering around 360 different fans in fossil fired power plants with 26 different causes being classified. It is noted that generation loss due to above design flow rate or pressure rise as one of the highest issues being recorded.

## 2.3 Power plant efficiency improvement

One of the leading documents in power plant efficiency improvements is the Heat Rate Improvement Guideline[15]. The project was aimed to improve the state of the American power plant industry by setting up generic guidelines to decrease the heat rate found in its power plants. The generic guidelines were created with aims to not only introduce different concepts on how to improve the power plants efficiency, but to also lay down a structure to work within for an effective heat rate improvement program to be created in any power plant.

One of the useful outputs from the project was a series of logic trees breaking down the plant into the various components and identifying their impacts on the heat rate. Figure 6 is one of the main diagrams from the study that depicts various plant sectors affecting the heat rate.



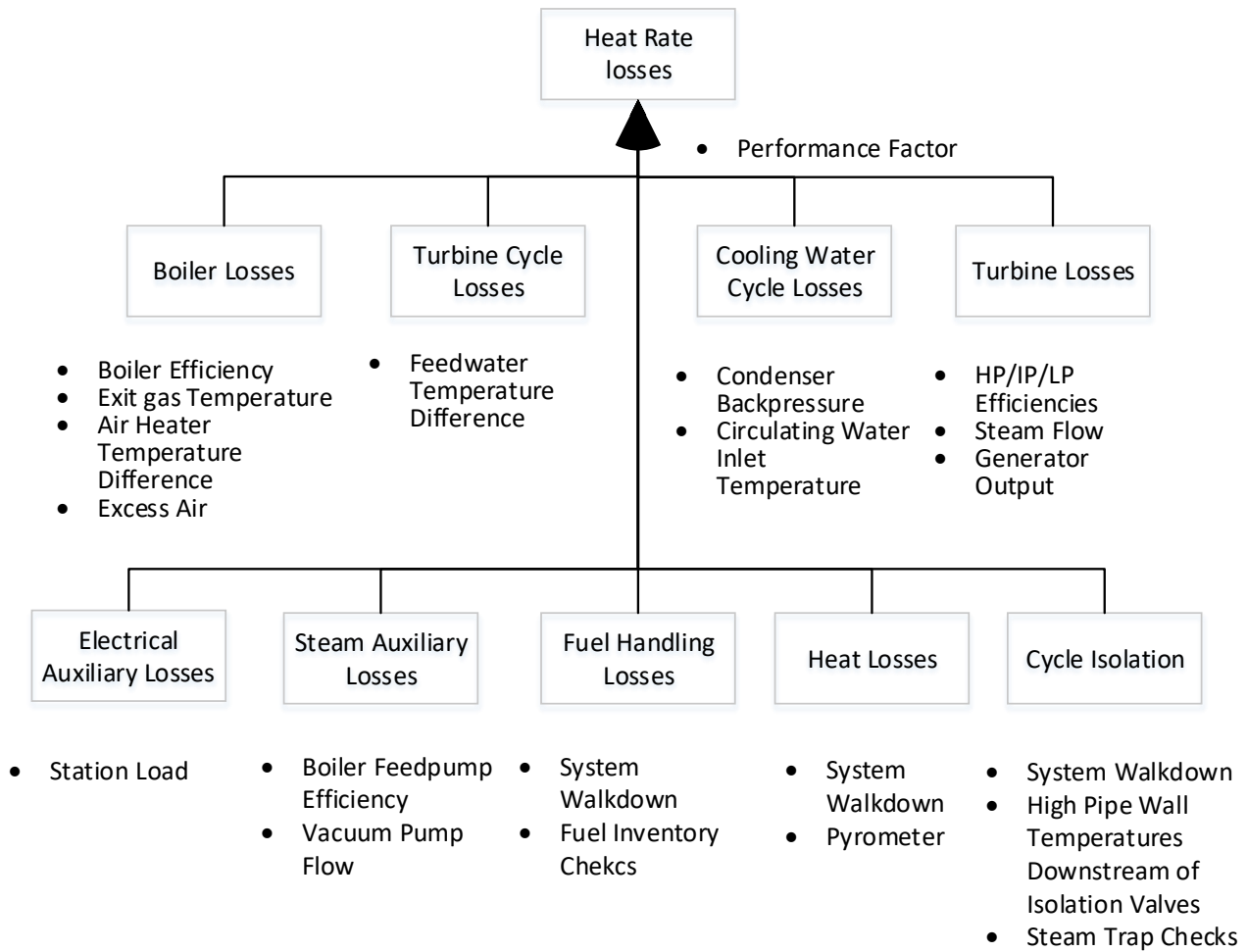


Figure 6: Heat Rate Logic Tree - Main Diagram [15]

Under each subsection are bullet points indicating the different methods/indicators the engineer can use to identify the type of loss impacting the heat rate. For example, the turbine losses can be identified by investigating changes in the following parameters: HP, IP, and LP turbine efficiencies; the steam flow rate into and out of the turbines and; the generators' electrical output.

Under further perusal of the document, it was found that the ID fans effect was listed under "Electrical Auxiliary Losses". Furthermore, it was under a sub-division of total fan efficiency. Figure 7 is a modified version of the total Electrical Auxiliary Losses diagram.

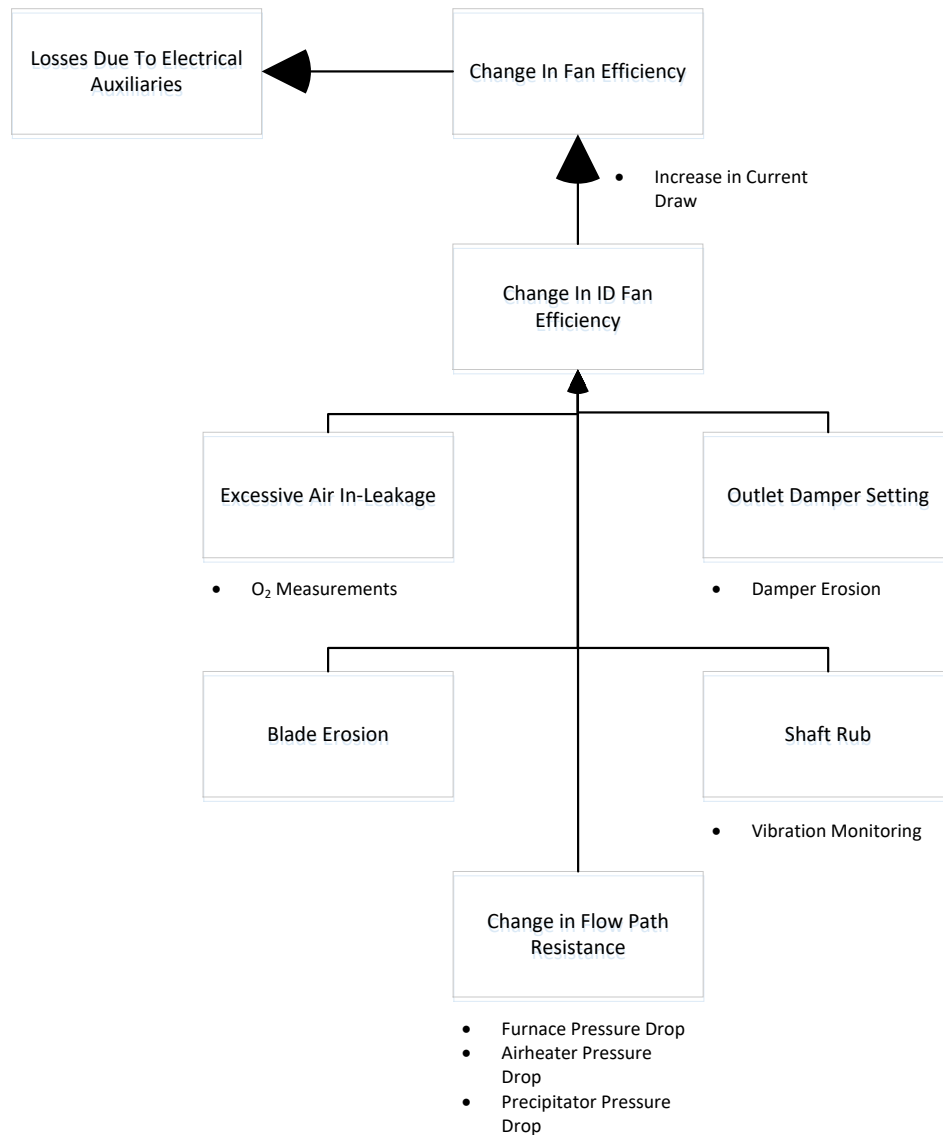


Figure 7: Heat Rate Logic Tree - Electrical Auxiliary Losses - Change in ID Fan Efficiency [15]

As can be seen from Figure 7 above, the project quantified the changes in upstream component pressure drops as a change in the ID Fans efficiency. It did not go further into looking at other systems effect on the flow path resistance and ultimately the fan's performance. It is noted that the study was intended to quantify the root causes and classify their effects on the heat rate and not how they can cause other issues down the line.

The Heat Rate Improvement Guideline also quantified the effect of key performance parameters on the variation of heat rate. Table 1 shows how a change of one unit of the stated parameter can influence the heat rate.

**Table 1: Sensitivity of Performance Parameter Deviation on Heat Rate [15]**

| Performance Parameter       | Engineering Units:<br>E. U | Variation:<br>Heat Rate/E.U. |
|-----------------------------|----------------------------|------------------------------|
| Auxiliary Power             | %                          | 90.7                         |
| Condenser Backpressure      | kPa                        | 63.6                         |
| L.P Turbine Efficiency      | %                          | 60.1                         |
| Excess Oxygen               | %                          | 31.0                         |
| Makeup                      | %                          | 25.3                         |
| H.P Turbine Efficiency      | %                          | 19.8                         |
| Feedwater Inlet Temperature | °C                         | 16.5                         |
| I.P Turbine Efficiency      | %                          | 15.3                         |
| Unburned Carbon             | %                          | 12.3                         |
| Coal Moisture               | %                          | 8.2                          |
| Flue Gas Temperature        | °C                         | 5.1                          |
| Main Steam Temperature      | °C                         | 2.7                          |
| Hot Reheat Temperature      | °C                         | 2.5                          |
| Main Steam Pressure         | kPa                        | 0.1                          |

The heat rate is measured in kJ/kWh. It should be noted the deviation for each of the parameters is measured with reference to their optimum value. For instance, auxiliary power % change (equation (3)) is calculated as:

$$\Delta \text{Auxiliary Power \%} = \frac{\text{Current Power} - \text{Optimum Power}}{\text{Optimum Power}} * 100 \quad (3)$$

As a reference guide, this type of correlation can be useful to operators. Table 1 shows that for each performance parameter, if its characteristic measurement (engineering unit) deviates from norm by one, then the corresponding variation can be seen in the heat rate. For example, a 1 kPa increase in condenser backpressure will cause an increase of 63.6 kJ/kWh. An increase in the heat rate means that the system requires more primary energy/coal in to create electrical energy out.

The macro scale of the results does not help when more specific problems are at hand when it comes to the auxiliary power. As the ID fan contributes to auxiliary power, it is not possible to determine its individual effect. The study does confirm that there is concern when it comes to auxiliary power

The study does not have a singular quantity for the ID Fan and is combined with auxiliary power. Nevertheless, it can be seen that the UCLF contributors do reappear in the EPRI table showing the concern for such issues [6].

For the system proposed by Godre et al. [9] to work, the fan performance curves and any in situ flue gas flow rate measurements need to be valid and accurate at all times. This enabled the resistance curve to be created.

Although OEMs provide their own characteristic curves for bought fans, these graphs sometimes do not correspond to the equipment's current performance levels. Factors such as the fan's age, mechanical wear of parts, as well as initial installation and retrofits are just some of the things that would make the characteristic curves differ from those of the manufacturer. Lui and Lui [16] initially proposed to research a cost-effective and accurate way of measuring the air flow within a heating, ventilation and air conditioning (HVAC) system. It was noted that accurate fan curves are imperative for any results to be valid. The writers noted that their method, even though valid for their purposes, still relied heavily on the OEM's fan curves.

Hauschke and Leithner [17] aimed to optimize the soot blowing intervals in a hard coal fired power plant using a dynamic simulation in ENBIPRO. They noted that the improper functioning of the soot blowers causes many problems, such as decreasing boiler efficiency and increasing fuel consumption for constant load. They also related the build-up of ash/slag to the increase in ID fan power consumption but did not go further to quantify this effect.

Kier and Potgieter [18] conducted an engineering investigation to state the benefits of optimising boiler air flows for the best efficiency. In the report it was stated that the reduction in fan power was an important benefit into the overall improvement to boiler efficiency. They explained a procedure they created to achieve boiler optimisation to be further expanded in Eskom systems. Kier and Potgieter presented nothing more on quantifying this improvement for fan power usage.

## 2.4 Water/steam modelling

A water/steam model is needed to calculate the thermodynamic changes in the Rankine water/steam cycle. The Plant A has a model, developed by GP Strategies, that helps with the online monitoring of systems. The model was configured to work online with predefined plant data and algorithms and first principles to calculate the ideal values. It then calculates the deviations in the measured values to those it calculates to display to the operator. The software can be repurposed to work offline as a simple design tool.

The water/steam cycle in a power plant is based on the ideal Rankine cycle. The cycle is composed of four processes namely:

- Isentropic compression of water by the pump
- Constant pressure heating of water into steam in the boiler
- Isentropic expansion of steam in the turbine to convert energy
- Constant pressure heat rejection to condense steam to water by the condenser

Alobaid, et.al.[19] wrote a review on various thermodynamic models built on various software platforms. This was done with the aim to highlight current efforts and future developments in the

dynamic simulation field of power generation. An extensive search was done on various studies for different thermal power plant technologies including coal-fired power. The programs involved for the CFPPs are APROS, ASPEN and gPROMS platform, to name a few. The models listed all had their advantages and advantages but ultimately focused on dynamic modelling of start-up and load change scenarios. Furthermore, there was a lack of available data for validation during the development of these models. It was noted that the use of models was needed in the energy sector as there is potential for further improvements to the way power plants are run.

## 2.5 Draught group modelling

The focus on the study is towards the ID fan. As such, the modelling of the draught group would have a pivotal role to play. The draught group's main components are the fans, boiler, precipitators, air heater, and mills. As a system, these components alter the main fluid, pre- and post-combustion gases, flowing through the network of ducting. The fans, for example, can be said to promote the flow of the gases at specific pressures throughout system. The mills can be thought to change the composition of the working fluid by adding pulverised fuel into the mixture. With that in mind, modelling the proper interactions being done to the fluid flow is key in quantifying the load requirement of the ID fan as it is the last component in the draught group. Literature on draught group modelling is not prevalent, however Heating, Ventilation and Air Conditioning (HVAC) modelling is well documented. The degree to which an HVAC system needs to maintain a specific environment in an enclosed area is similar to that of a power plant's boiler.

Afram and Janabi-Sharifi wrote a review on the different methodologies used to model HVAC systems [20]. In the study, the modelling methodologies were split into data driven, physics based and grey box methods. It was noted that the data driven model performed well when an ample amount of measurements was constantly given, and the behaviour of the system approximated linear and non-linear functions. On the other hand, physics-based models have their benefits by having a better generalisation capability. On the downside, physics-based models tend to deviate when conditions vary from training data. The intersection of these two methodologies is the grey box model.

With that in mind, the FlownexSE software is a physics-based modelling tool that allows for external data to be fed into it if needs be. This would be considered as a grey box model. A model of the draught group can be modelled and tuned using design data as a bass and simulated plant data for boundary conditions can be fed into the model to calculate ID fan performance. FlownexSE modelling environment also allows for inclusion of parameters to function as anomaly inputs.

## 2.6 ID fan anomalies

The following section aims to describe the six anomalies being investigated. A brief description of the surrounding area is given in some instances and an explanation on the mechanism of how the anomaly can influence the ID fan's performance. The six anomalies are: coal quality, increased boiler flue gas exit temperature, air ingress into the boiler, air heater inleakage into flue gas stream, feed water heaters out-of-service, and condenser backpressure degradation.

The anomalies have some connection to the performance parameters presented in Table 1. Coal quality encompasses the parameter for coal moisture and unburnt carbon, but this study will include more of the coal's chemical composition. The flue gas temperature anomaly is studied with reference to its temperature at the boiler exit. Air ingress into the boiler and air heater inleakages is associated with excess oxygen, however that could also refer to the combustion process. The feedwater heaters being out of service would cause low feed water inlet temperatures. Finally, the clearest anomaly is the condenser backpressure degradations which has the second highest impact per engineering unit change.

### 2.6.1 Coal quality

South Africa has a large quantity of coal and as such has based its electricity production on this. Other than for exportation, it was estimated that the power utility Eskom consumed 70 % of the coal produced for internal use. The coal usage split can be seen in Figure 8

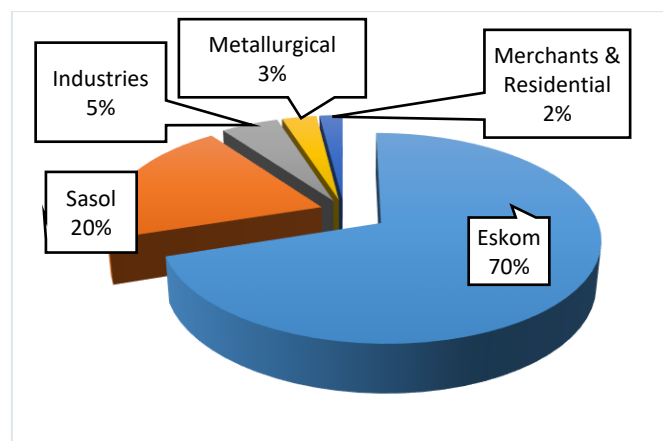


Figure 8: Coal use in South Africa 2010 (excludes exports)[21]

For combustion to take place, the many factors that influence its efficiency can be divided into external factors and inherent/intrinsic. The external factors are characterised by that which influence the combustion process, specifically occurring in the furnace region. The intrinsic factors have to do with chemical composition of the coal and its ability to burn. These factors are shown in Table 2.

**Table 2: Factors influencing combustion efficiency of coal[22]**

| Intrinsic Factors                              | External Factor  |
|--|--|
| Organic and Inorganic Composition              | Particle size  |
| Degree of maturity                             | Throughput   |
| Porosity                                       | Environmental temperature                                  |
| Exposed surface area                           | Temperature and velocity of combustion air                 |
| Moisture content                               | Nature of mixing solid and gas                             |
| Degree of weathering or heat effect            | Design and spacing of the burners                          |
| Size of particle                               | Residence time of the combustible particles in the furnace |
| State of oxidation                             |  |
| Characteristic initial or ignition temperature |  |
| Peak combustion temperature                    |  |

Under intrinsic factors, the organic and inorganic composition of the coal is the factor being studied. The chemical composition can be used to calculate how much coal needs to be burnt to gain the desired energy output. This in turn, is linked to the amount of air needing to be supplied. The Calorific Value (CV) is used to measure the energy that can be expended during combustion. The Higher Heating Value (HHV), or gross CV, is the limit of how much energy one can extract from the coal combustion. This is the energy includes the energy needed to produce steam and evaporate the inherent moisture in the coal. The value excluding the evaporation energy is called the Lower Heating Value (LHV). Equation (4) can be used to calculate the HHV:

$$HHV = \sum_{i=C,H,O,N,S} (q_{formation,i} + q_{Latent,i}) * x_i \quad (4)$$

Where C, H, O, N, S corresponds to carbon, hydrogen, oxygen, nitrogen, and sulphur. The variable  $q_{formation}$  is the formation energy,  $q_{latent}$  is the latent heat, and  $x_i$  refers to the mass fraction of each constituent. The units are kJ/kg for formation energy and latent heat. [23]

The composition of the coal will also determine the resultant flue gas composition which effects its heat capacity and its density. The heat capacity will affect the temperatures that will be seen by the various heat exchangers.

An important factor to consider is the ash content in the coal. The coal used in Southern Africa has a very high ash content compared to that of Europe, Asia, and America. Furthermore, coal with lower ash content is running out in our reserves and we will soon be forced to consistently use higher ash content coal [24].

The effects of ash content on performance of power plants can be detrimental to many parts of a power plant. These issues are usually seen if the power plant is not specifically designed to burn the higher ash content coal. For example, the ID fan's blades can experience erosion since an increase in ash content could rise above the precipitators' working envelope, reducing its effectiveness (especially in the case of electro static precipitators).

The most applicable effect to this study is the increased coal mass flow. An increase in coal mass flow is associated with an increased requirement of combustion air. This results in the PA and FD fan motors to draw more current. The resultant flue gas mass flow will also be increased, causing an increase in current drawn by the ID fan. Generally, the required heating surface would also need to be increased as the heat transfer rate decreases due to the flue gas composition. The building up of ash on the heat exchangers, especially when there is a neglect for proper soot blowing, can have a major effect on lower heat transfer. Taking all these into consideration, some power plants are forced to run at partial loads and as such the overall efficiency takes a significant knock compared to design[25]–[27]. Proof of this can also be seen by studies by Rousseau & Laubscher, where there is a great difference in the performance due to what is currently being burnt vs what the station was designed to burn.[28]

## 2.6.2 Increased boiler flue gas exit temperature

The boiler is a large vessel enclosing all the components for the combustion of coal and the generation of steam. The generation of steam is done by various heat exchangers that take energy from the flue gas and transfer it to the water/steam.

An important aspect of designing boilers is the upper and lower limits of the Furnace Exit Temperature (FET). The furnace exit has the highest temperature in the boiler and must be maintained else damage may occur to the heating elements. Measuring the temperature in that area is a difficult task as the tumultuous environment leaves traditional techniques useless.

A high back end temperature can mean a high FET which comes with issues such as ash fusion causing slagging on the heat exchangers. The slagging would cause a lower boiler efficiency. Hotter flue gas through the system would also cause the tube metal temperatures to also increase. At very high temperatures, thermal excursion can occur thus rapidly decreasing the remaining life of the pipes. Ultimately, the whole system would have accelerated tube failures due to long-term overheating, fatigue cracking and corrosion.

The temperatures seen by successive heat exchangers naturally decrease proportionally to the increase of water/steam temperatures. A measure of how much energy was extracted by the heat exchanger train is the boiler flue gas exit temperature. If the temperatures are higher due to



operational constraints, this indicates a larger needed input to the system thus decreasing the overall efficiency of the boiler. The larger load requirement will also affect the required performance level of the ID fans with a larger pressure head and volume flow requirement.

The failure of tubes ranks high among power plant failures and studying the deviations of flue gas temperatures can help to mitigate their occurrence. Yin, Rosendahl and Condra, studied these deviations by creating simulations that compared well with available site operation records. Thereafter, some effects were studied to determine their impact.[29]

### 2.6.3 Air ingress into the boiler

Controlling furnace pressure is vital to maintaining a safe environment by keeping the hot gasses, within the boiler and the rest of the draught group, under vacuum environment. The prevailing draught mechanism to keep this vacuum, and encourage the flow of flue gases, can be split into four main categories: natural draught, forced draught, induced draught, and balanced draught[30].

The natural draught system solely relies on the difference in density of the hot flue gases within the chimney and the colder atmospheric air. The forced draught and induced draught systems rely on a mechanical fan upstream and downstream of the boiler respectively. The balanced draught uses a combination of all three systems with a forced draught fan preceding the boiler and an induced draught fan proceeding the boiler.

The effects of this incoming air into the system was studied by Bhatt for high ash content coal fired power plants (35% - 45%). In his study he found Oxygen values of 10% in refractory type boilers where the optimal levels are around 3.5%. This high oxygen level is a severe sign of leakage and has a serious effect on combustion. Overall plant efficiency can be dropped by approximately 3%.[31]

The power plant being modelled in this study, Plant A, is designed as a balanced draught system. The balanced system provides more control, however leaks within the system can drastically affect the induced draught fan loading. The immediate effects to the boiler would be that the additional mass to the flow stream will cool down the overall flue gas temperature.

### 2.6.4 Air heater inleakage to flue gas stream

The air heaters of a power plant are heat exchangers used to preheat the incoming combustion air. Residual energy from the combustion gases are typically utilised for this, but some systems can be configured to use extraction steam or other sources of energy [32] . Among the various types of air heaters used by Eskom, the most notable is the rotary type air heater depicted in Figure 9. The rotating matrix transfers heat from the flue gas to the inlet air.

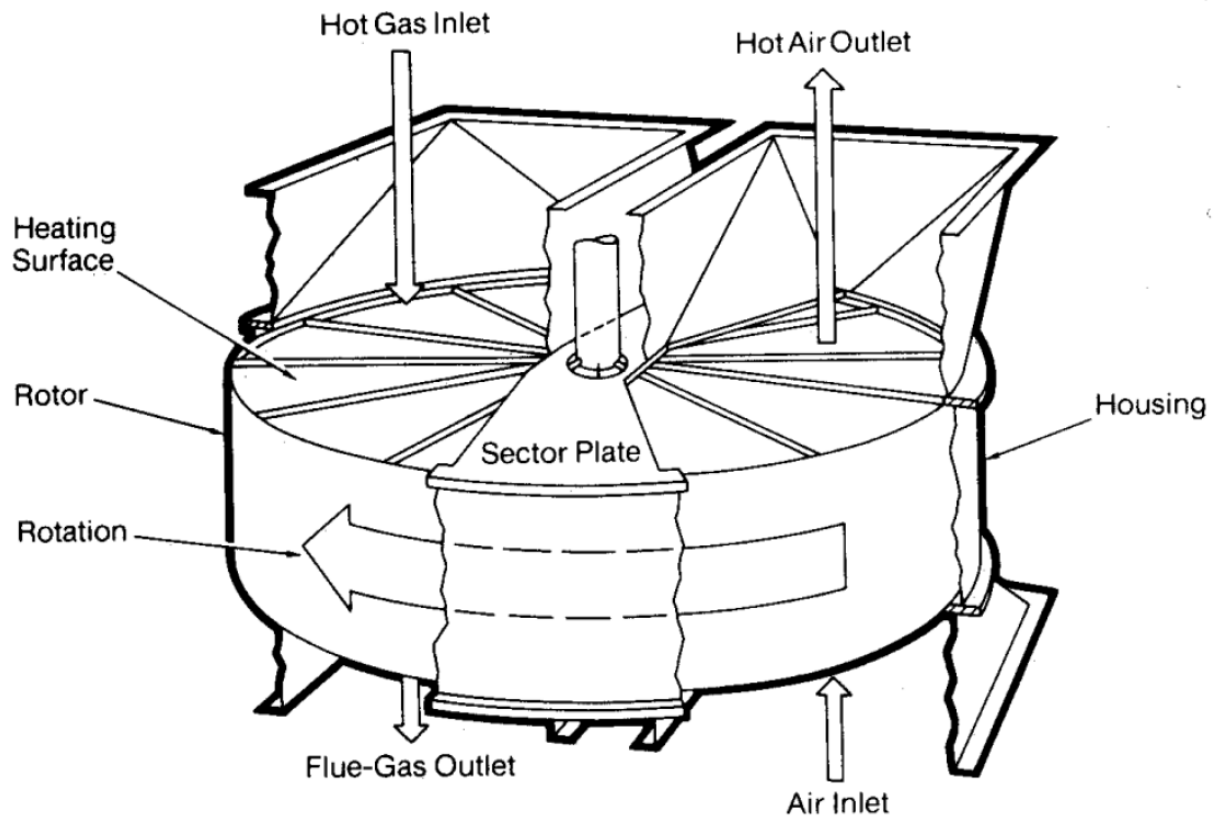


Figure 9: Air heater schematic[33]

The leakages in the system are primarily a consequence of two factors. The first is of the rotating matrix and the streams and the second is through the direct leakage between the high-pressure clean air stream and the low-pressure flue gas stream. The seals on the air heater are used to minimize the direct leakages, this however does not eliminate the leakage and typically operate with a 7 % leakage due to the practical limitations such as seal clearance. The consequence of the leaks is a higher fan power requirement for a given air outlet flow rate.[34]

The impact of air ingress in the air heaters was also studied by Bhatt as the issues is linked to the previous anomaly, air ingress into the boiler. He noted that large capacity restraints (a loss of about 20%) can be seen at a certain level of air ingress and operation with the anomaly is quite difficult.[31]

### 2.6.5 Feed water heaters out-of-service

Feedwater heaters (FWH) are heat exchangers that preheat the feedwater before it enters the boiler. It does this by drawing a portion of the steam from turbine. The effect is that the average temperature of the feedwater is increased and in term this increases the cycle efficiency. Typically, modern power plants have between six to eight FWH within the feedwater heating train [35]. Figure 10 depicts the impact of number of FWHs on the steam cycle efficiency.

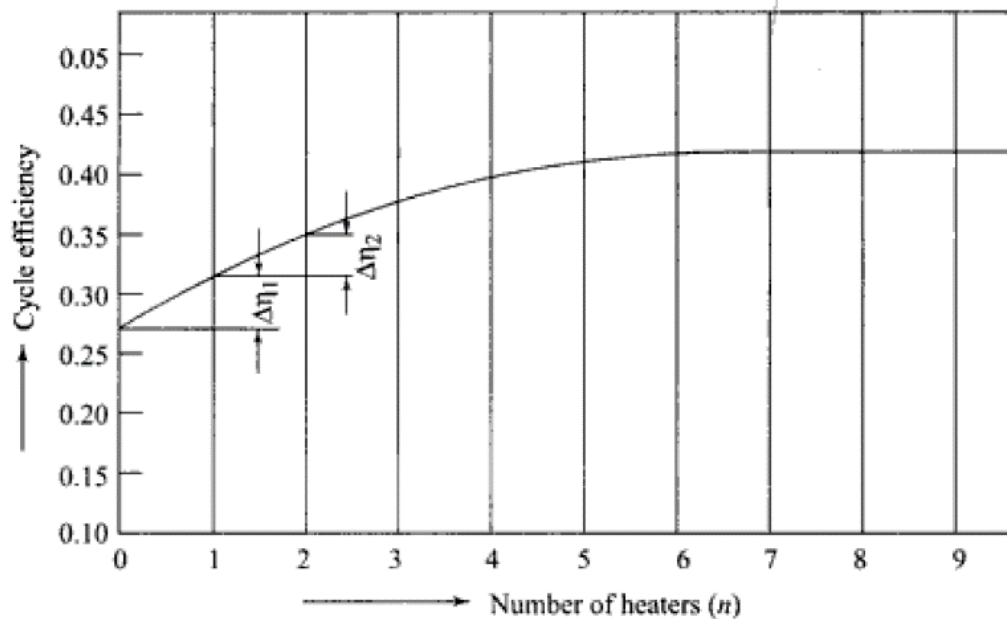


Figure 10: Impact of number of feedwater heaters on the steam cycle efficiency [7]

As a number of heaters are taken out of service a major impact can be seen on the cycle[7]. FWH are put out of service if there are issues with the condensate level control. Improper level control is the accumulation of condensate in the FWH. This is often caused by tube leaks and/or other external factors. High condensate in the FWH may result in thermal shock in the bled steam tubes, and eventually quenching of the turbine.

In some power stations the final feedwaters are configured to have parallel flows. Each leg will be referred to as a bank. Figure 11 illustrates this as the top leg referred to as Bank A and the lower leg referred to as Bank B.

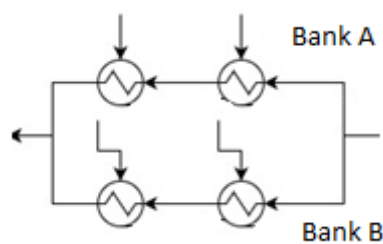


Figure 11: Feedwater heater banks

The removal of a FWH from the feedwater train results in a lower final feedwater temperature. For the same power output level, the heat input into the boiler is expected to increase in order to compensate for the drop in the final feedwater temperature. This increased boiler heat input increases the fuel and air mass flow requirement, which in turn increases the flue gas flow across the ID fan. This increases the load on the ID fan.

Other components will also be affected with varying outcomes to their life span. For instance, the turbine will have more flow through it as the steam usually being diverted will now continue through the turbines flow path. After longer periods, this above normal flow can increase the blade erosion rate as more stress is experienced.[36]

## 2.6.6 Condenser backpressure degradation

The condenser has two main objectives on a steam power plant. One reason is to recover the high-quality feedwater to feed back into the system without having to go through all the treatment processing again. The other reason is to reduce the exhaust pressure of the low-pressure turbine. This can be achieved if the cooling water within the condenser is low enough to create a vacuum for the turbine. Since the work done by the turbine is much greater at the lower pressure end, the condenser can increase plant efficiency.[7]

In the situation where the condenser is underperforming, the system will need to compensate for it by putting more energy into the system in the form of more fuel being burnt thus increase the ID fan's load.



### 3. Model development

The model is developed in three parts. The Rankine cycle in Virtual Plant (VP), draught group in FlownexSE (FNX) and a BMEB tool. An overview of the full model is given in Figure 12. The main blocks (solid sections with one open side) are the inputs/outputs that feed into each section. The red dotted blocks indicate where each anomaly will be implemented.

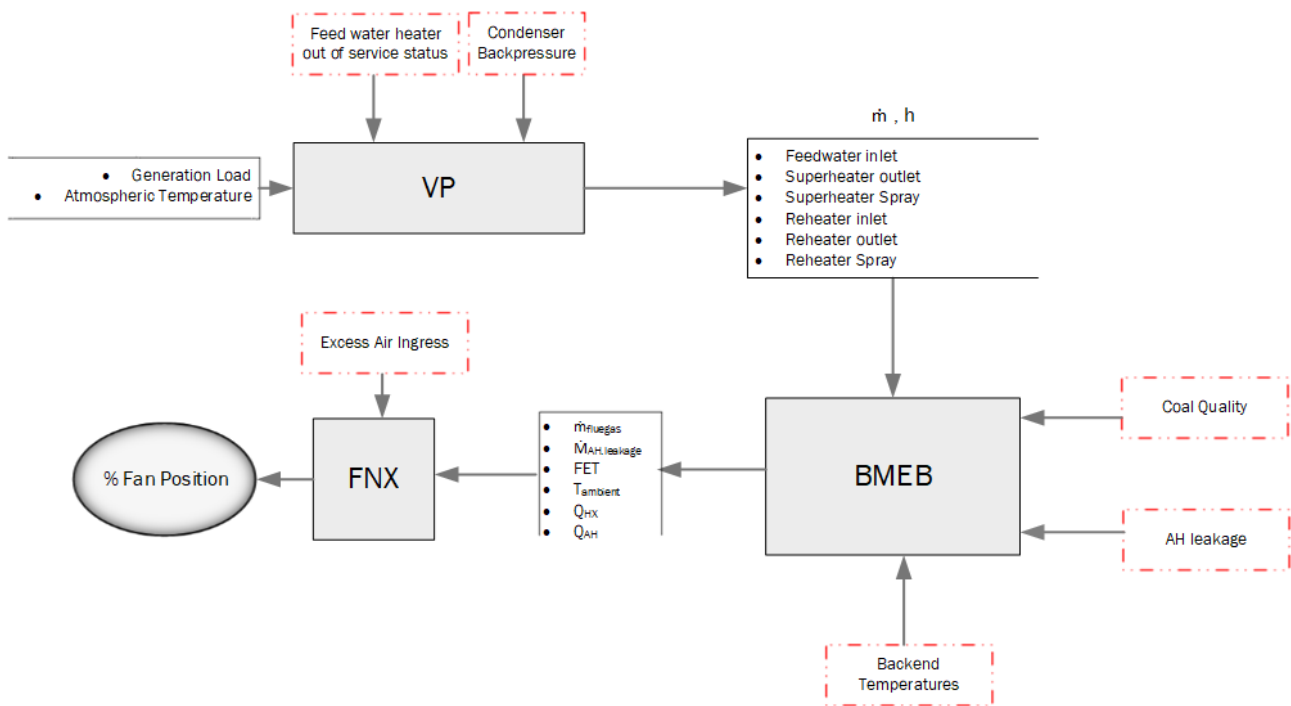


Figure 12: Full Model Flowchart

Each model would need to be validated at full load and part load conditions. The approach taken during development of each sub model is to thoroughly verify them individually before putting it all together. Validation of power plant data is often challenging as the environment does not allow for controlled measurements. Therefore, the validation study will rely on baseline information of the power plant. Secondly, heat balance diagrams and performance test data can also be used to validate these models.

## 3.1 Rankine cycle model

### 3.1.1 Overview of steam cycle

Power plants are designed using the Rankine cycle as a template. In the simplest example, the cycle comprises of the turbines, condenser, pumps and the boiler. One addition to the cycle is to redirect exhaust steam of the first turbine back to the boiler for reheating to increase the heat extraction and thus increasing the cycle efficiency. Multiple stages of feedwater heating further increases efficiency using inter-stage turbine extractions.

The coal fired power plant being modelled, Plant A, is a 600MWe class single reheat drum type unit. It operates with a main steam pressure of 17MPa and a final steam temperature at 540°C. The Intermediate Pressure (IP) turbine has a double flow configuration and the Low Pressure (LP) turbine is split into two double flow turbines. The attached condensers are of the dual-pressure, single pass, surface type. The condenser operates with a steam-jet air ejector and a water-jet air ejector. The dual pressure zones of the condenser are dubbed the hot condenser and cold condenser. This is due to the fact that the cooling water travels consecutively through one side of the condenser to the other. This means that the second zone, the hot condenser, runs warmer than the first because the cooling water has already extracted energy from the first zone. There is a total of seven feed water heaters. They are the LP heater, a deaerator and HP feedwater heaters. The HP feedwater heaters have two banks that work in parallel.[37]

The Steam cycle model will have the generation load percentage and atmospheric temperature as inputs, run its simulation and output the mass flows and enthalpies of various water/steam flows from the steam cycle focused around the boiler. Figure 13 depicts the inputs and outputs going around the model.

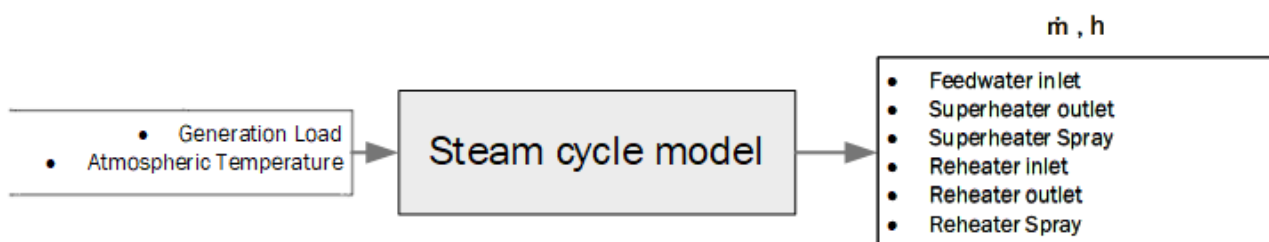


Figure 13: Steam cycle model inputs and outputs

### 3.1.2 Steam cycle modelling

Steam cycle models see their benefits in power plants when they are used either for Condition Monitoring (CM) or Performance Monitoring (PM). Typically, a performance monitoring tool is a model built from thermodynamic first principles and a condition monitoring tool is empirical and data driven. Tools that integrate both PM and CM create the possibility to identify and diagnose root causes of system abnormalities while also quantifying their impact on plant availability [38]. The EtaPRO - VP combination is one such tool.

VP is a specialized thermodynamic modelling software focused around conventional fossil steam power plants, combined cycle power plants, and nuclear power plants [39]. It takes a first principle thermodynamic approach while discretizing the power plant into interconnected components. The EtaPRO platform allows users to easily view plant data. It also performs calculations in the background to determine unmeasured parameters. This is done using calculation templates and VP models. Each operating plant has a VP model configured based on its design data. The EtaPRO tool relays boundary conditions for the VP model from running plant data, allows it to solve for the expected cycle performance. The results can be compared to actual values measured on site. While deviations from expected measurements can be used to diagnose plant faults. The program utilises a computationally inexpensive method for calculating cycle performance parameters. The VP model is run to validate process data to predict performance at specific operating conditions. This is done through GP Strategies' on-line EtaPRO system. The offline mode is primarily used to run studies to evaluate the impact of off-design scenarios on the system.

The interface with the draught group is the boiler where the quantity of heat extracted by the cycle from the boiler is needed. Therefore, for the purposes of this study the VP model would need to accurately predict the heat transferred to the steam cycle under various operating conditions, with or without anomalies.

The results from the Virtual Plant simulations at 100 %, 80 % and 60 % of the boiler maximum continuous rating (BMCR) were compared to that of the heat balance diagrams (HBD). The plant's design data also includes a case where one bank and both banks of HP heaters are out of service. The boiler was neglected since a mass and energy calculation on the boiler is done in the BMEB tool. The relative difference between the inputs and outputs for energy ( $\Delta$  Energy) and mass flows ( $\Delta$  Mass) are shown for each component. The residuals between the model and the HBD were calculated and displayed as a percentage.



### a) Boiler

The fossil boiler component in VirtualPlant is shown in Figure 14. In its simple form, it is responsible for calculating the heat required having set the configuration data for the following properties:

- Superheat steam temperature
- Reheat steam temperature
- Superheater outlet steam flow
- Superheat spray flow

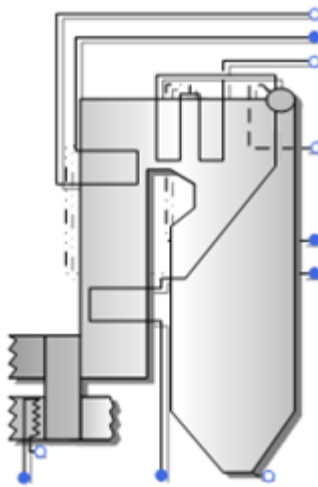


Figure 14: Fossil Boiler as in VirtualPlant

There is a Simple Boiler mode and a more advanced Heat Transfer Model.

In more advanced calculation modes, the boiler can be tuned using more detailed plant data to fully simulate the convective pass within the boiler and as far as the air heater. This is all used to then calculate the superheater steam flows, steam conditions and flue gas temperatures using the  $\epsilon$ -NTU method.

The modelling of the boiler was done using the simple boiler calculations with spray water flows at standard conditions inputted. This was done because the model need only produce the heat load for the cycle.

## b) Turbine

The HP turbine is graphically represented in VP as shown in Figure 15. VP calculates the HP turbines efficiency using a widely used standard published by ASME.[40]

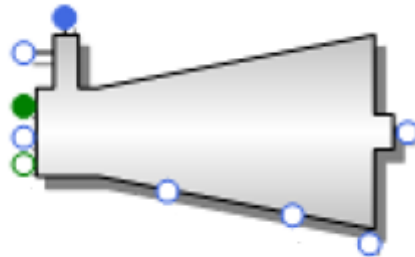


Figure 15: High-pressure turbine as in VirtualPlant

The HP turbine has steam from the superheater entering it and it exits by way of bled steam at the first stage leak-off and the exhaust port leaving towards the reheater. Energy leaves the turbine in the form of rotational energy on the shaft.

Figure 16 is a diagram of the energy and mass input of the HP turbine.

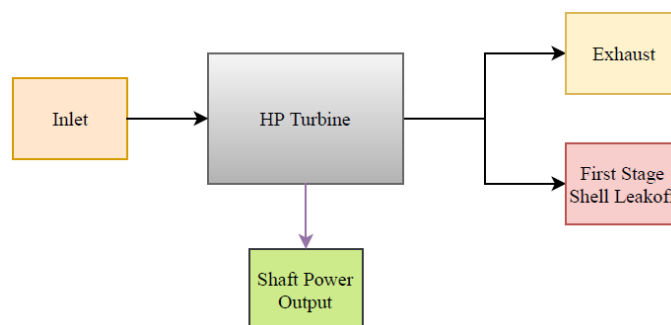


Figure 16: HP Turbine Inputs and Outputs

Table 3 below depicts the results for the mass and energy balance done on the HP turbine. Mass balance residuals shown to be much better than energy balance, however the energy balance is still within tolerance.

Table 3: HP Turbine Mass and Energy Balance Results

| HP Turbine           |                         |                         |                          |
|----------------------|-------------------------|-------------------------|--------------------------|
|                      | 100 %                   | 80 %                    | 60 %                     |
| $\Delta$ Mass (kg/s) | 0 %                     | 0 %                     | $1.36 \times 10^{-14}$ % |
| $\Delta$ Energy (kW) | $1.34 \times 10^{-5}$ % | $1.06 \times 10^{-5}$ % | $7.01 \times 10^{-6}$ %  |

The IP/LP turbine component is represented in Figure 17 below. The description on methodology on how the IP/LP turbine works is similar to the HP turbine. The components connected to the

turbine extraction points drive the flow out of the turbine and similarly the exhaust pressure is determined by the condenser it is connected to.

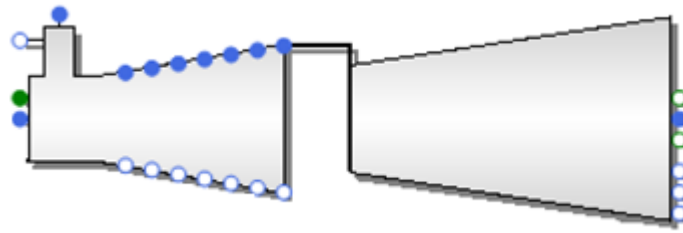


Figure 17: IP/LP turbine as in VirtualPlant

There are four possible sets of data configuration pages to be completed when modelling the IP/LP turbine. These pages are: IP-LP Design Data, Extractions, Efficiency Curve (if selected), and Turbine Exhaust. The efficiency curve selection is to input data that the solver must use for the efficiency of turbine.

The IP/LP turbine has rotational energy entering it since its shaft is connected to the HP turbine, and the shaft is then connected to the generator. The steam flow entering the IP/LP turbine comes from the boiler reheater and a small amount from the gland steam sealing system. The steam exit of the turbine has five major extractions and the final exhaust into the hot and cold side of the condenser. All these inputs and outputs can be seen in Figure 18 below with the horizontal components depicting steam flows and vertical components mechanical energy.

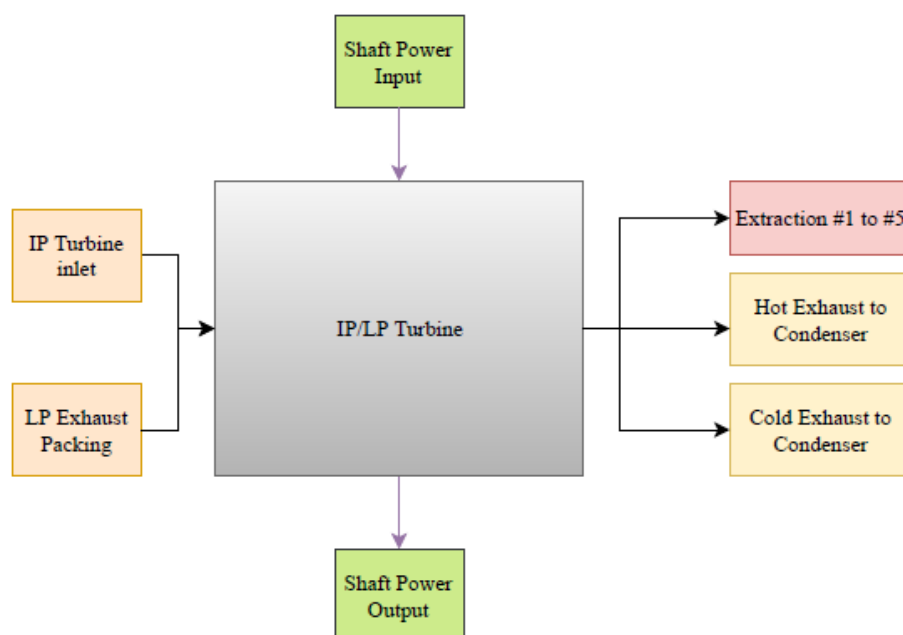


Figure 18: IP/LP Turbine Inputs and Outputs

Table 4 shows the results of the mass and energy balance. Low residuals with the mass balance are shown within the IP/LP turbine

**Table 4: IP/LP Turbine Mass and Energy Balance Results**

| IP/LP Turbine        |                           |                           |                           |
|----------------------|---------------------------|---------------------------|---------------------------|
|                      | 100 %                     | 80 %                      | 60 %                      |
| <b>Δ Mass (kg/s)</b> | $1.21 \times 10^{-14} \%$ | $1.57 \times 10^{-14} \%$ | $2.13 \times 10^{-14} \%$ |
| <b>Δ Energy (kW)</b> | $4.32 \times 10^{-6} \%$  | $4.31 \times 10^{-6} \%$  | $4.31 \times 10^{-6} \%$  |

### c) Condenser

The VirtualPlant condenser model (excluding the air cooled condenser), depicted in Figure 19, is based on the Heat Exchange Institute (HEI) Guideline [41]. The component can have a total of three zones and the user can deactivate the unnecessary zones which changes the component diagram. Plant A has a two-zone condenser and was modelled as such.

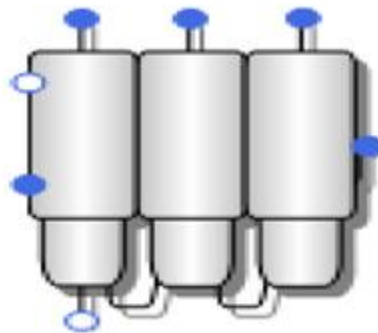


*Figure 19: Main Condenser as in VirtualPlant*

The condenser component can also connect to a cooling tower component with the tower's performance curves inputted.

The condenser has two stream flows, the circulating water and the exhaust steam/feedwater stream. The circulating water takes up the heat from the exhaust steam and the two flows can be seen in Figure 20 below.

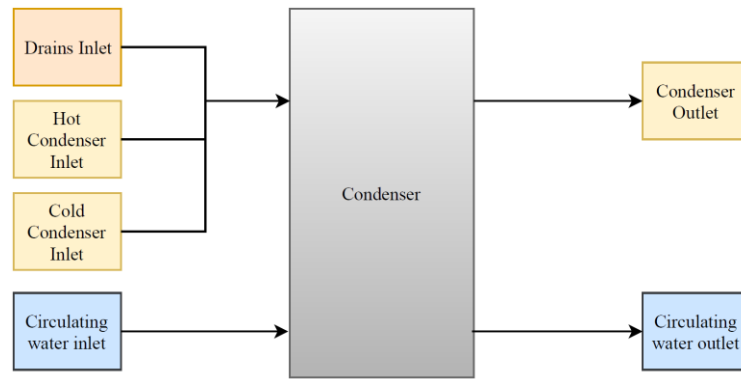


Figure 20: Condenser Inputs and Outputs

The results for the mass and energy balance are showed in Table 5 and showed practically no residual difference with respect to this mass balance and low residuals on the energy balance side.

Table 5: Condenser Mass and Energy Balance Results

| Condenser            |                         |                         |                          |
|----------------------|-------------------------|-------------------------|--------------------------|
|                      | 100 %                   | 80 %                    | 60 %                     |
| $\Delta$ Mass (kg/s) | 0 %                     | 0 %                     | $1.36 \times 10^{-14}$ % |
| $\Delta$ Energy (kW) | $1.34 \times 10^{-5}$ % | $1.06 \times 10^{-5}$ % | $7.01 \times 10^{-6}$ %  |

#### d) Feedwater Heater

There is no difference in the component used for the LP and HP feedwater heaters. The feedwater heaters are responsible for raising the feedwater temperatures via steam bled from the turbine. Open feedwater heaters are designed to also remove dissolved gases within the feedwater through the mixing of the steam and feedwater. Plant A has four HP FWH and four LP FWH with an open FWH (and deaerator) in between. The closed and open feedwater heaters are shown in Figure 21 as they are depicted in VP.

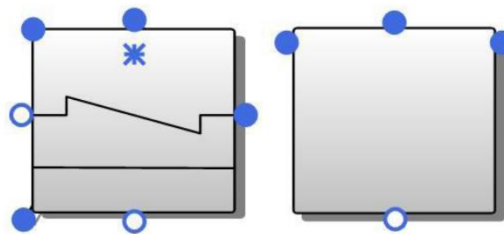


Figure 21: Closed (left) and Open (right) feedwater heater as in VirtualPlant

The last HP FWH is split into two streams, bank A and bank B. Figure 22 depicts the feedwater flow rate entering and exiting the FWH in the horizontal plane with the heating bled steam from the HP turbine entering the FWH and leaving out the FWH drains.

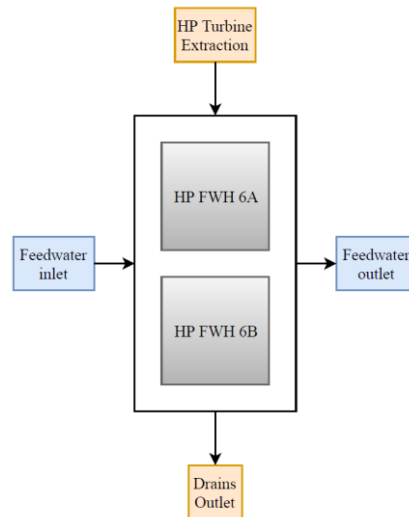


Figure 22: HP FWH Inputs and Outputs

In Table 6 below, the results for the error analysis of the mass and energy balance for the HP FWH showed practically negligible residuals on both the mass and energy balance for this component.

Table 6: HP FWH Mass and Energy Balance Results

| HP FWH               |       |                          |                          |
|----------------------|-------|--------------------------|--------------------------|
|                      | 100 % | 80 %                     | 60 %                     |
| $\Delta$ Mass (kg/s) | 0 %   | 0 %                      | 0 %                      |
| $\Delta$ Energy (kW) | 0 %   | $1.38 \times 10^{-14}$ % | $2.03 \times 10^{-14}$ % |

#### e) Discussion

In conclusion, the steam model was run at multiple loads with successful verification. The mass and energy residuals in the model are acceptable with values well below 1 %.

### 3.1.3 Validation of model

The validation of the steam model was done by comparing the total turbine power and HP turbine inlet steam flow to that of the formal HBD. The load cases compared are the 100 %, 80 % and 60 % of the BMCR and their results are depicted in Figure 23 and Figure 24. The reference data comes from Plant A's heat balance diagrams.

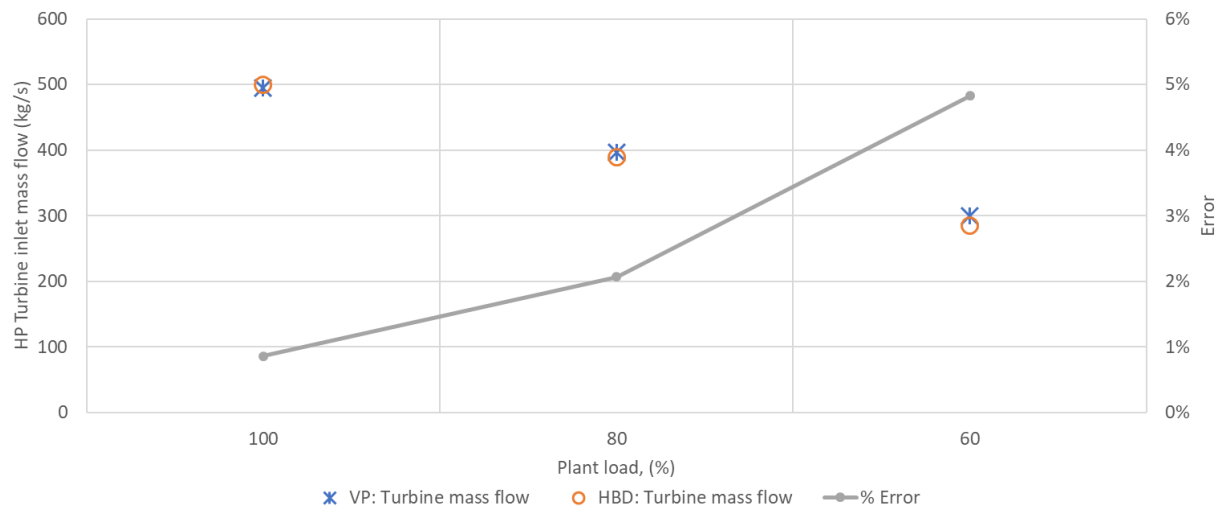


Figure 23: HP inlet steam mass flow vs Plant load

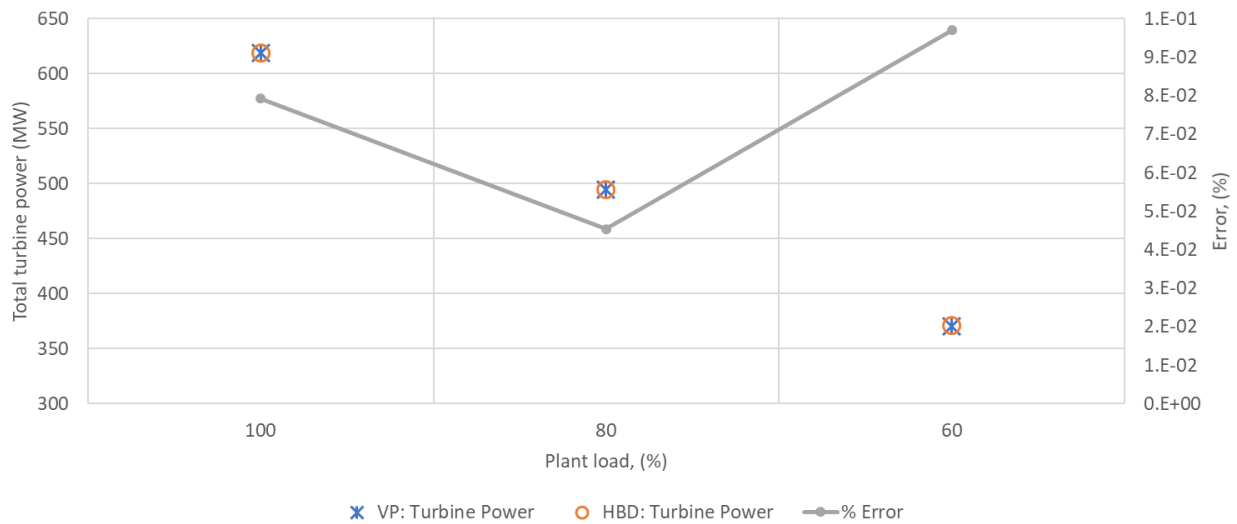


Figure 24: Total turbine power vs Plant load

The average error for the mass flow was 2.6 % while the turbine power was correct within 0.074 %. These values are acceptable differences and the model can be deemed valid for cases between 100 % and 60 % with errors increasing towards the lower end.

## 3.2 Boiler mass and energy balance tool

### 3.2.1 Literature

Setting up a draught group model required an appropriate identification of the boundary. Once the boundary is decided on, discretising the components within the boundary can move the modelling process forward. A suitable boundary for the draught group can start at the furnace exit and ending at the chimney exit. The flue gas composition, temperature and flow rate at the furnace exit, are difficult to measure and complex to calculate [30]. The FET is specifically complex to calculate due to the estimation of energy transferred to a portion of the furnace walls.

The complexity of calculating the FET has been studied to varying degrees of success. The usual way is done by performing a radiation heat transfer calculation from the adiabatic flame to the evaporator walls. An advanced numerical model solving this is the zone (or zonal) method described by Hottel and Cohen in 1958 [42]. In recent years, Monnaemang [43] developed a radiation heat transfer network solution based on the zonal method. The solution evaluated direct exchange areas using discrete numerical integration after which a least square technique using Lagrange multipliers was implemented for two scenarios[43]. There is also complexity due to the gas medium being filled with particulate matter. In conclusion, the complexity in setting up an adequate zonal method and calibrating the gas medium is not necessary for this study and a simplified solution is required.

Other methods to avoid estimating radiation is by performing calculations upstream from the furnace exit. A method described by Chandok et. al. [44] was focused on developing a neural network model that estimated the FET. The neural network used an analytical solution based on the Map Entered Variable (MEV) technique that was completely independent of heat transfer theory. An indirect estimation was required as the method created multiple boundaries starting at the economiser outlet working backwards to the FET over each heat exchanger that also covered a portion of the evaporator wall. Measuring the water temperature is not an indicator of energy transfer in the evaporator wall since all sections in the wall are in a saturation state. Chandok et al did not consider this aspect, but their approach showed comparable results.

Govindsamy [45] followed a similar approach to Chandok et. al.[44] in the calculation of the FET. However, he estimated the total energy provided to the water wall to be distributed by some factor between the furnace section of the evaporator walls and that of the convective heat exchanger pass[45]. This, though an improvement, introduced a separate uncertainty of verifying the evaporator wall energy transfer contribution in different stations. A less uncertain boundary for the model would be the adiabatic flame temperature as well as ensure the total fire wall and convective heat exchanger pass is initially lumped into a single component.



This larger boundary for the draught group benefits the creation of the methodology. The more inclusive boundary removes the uncertainty related with lower furnace evaporator wall energy distribution. All the energy can be accounted for without any assumptions on its amount. The boundary also coincides with those of the American standard ASME PTC 4 [46] and the European standard EN 12952-15 [47]. Both standards can be used to calculate the coal, air and flue gas flow rate. The flue gas flow rate is a vital input to the draught group model as a boundary condition.

The direct measurement of the air, coal and flue gas flow rates on a power plant is such a challenging task, with not much reward, that plant owners do not install the required equipment. The coal flow rate is measured by the coal feeder. However, most coal feeders in Eskom are of a volumetric type[48]. This means the volumetric flow of coal is controlled without consideration of the bulk density (which includes the air) or coal moisture content. The air and flue gas flow rates that are calculated with reference to the OEM can be inaccurate. As found by Godre[9], there may have been changes in performance of installed fans over time altering the perceived performance of the fan based off of the OEM fan curves.

### 3.2.2 Overview

The BMEB developed for this study is a set of calculations that will be used to determine the fluid properties at the boundaries of the boiler given some constants and plant data. One notable reading required depends on whether the air heater is included in the initial BMEB or not.

As can be seen in Figure 25, the decision was taken to exclude the air heater from the BMEB. The benefit of its inclusion would have been a small increase in the accuracy. However, if this methodology is to be easily rolled out to multiple power stations, it would need some drastic alterations as the required outlet oxygen measurement of the flue gas of the air heater is often not found on some power stations. This alteration to the calculation method requires a separate mass and energy balance calculation to be done solely on the air heater. Since it is also a mass and energy balance, it will be implemented as a section within the BMEB [48].

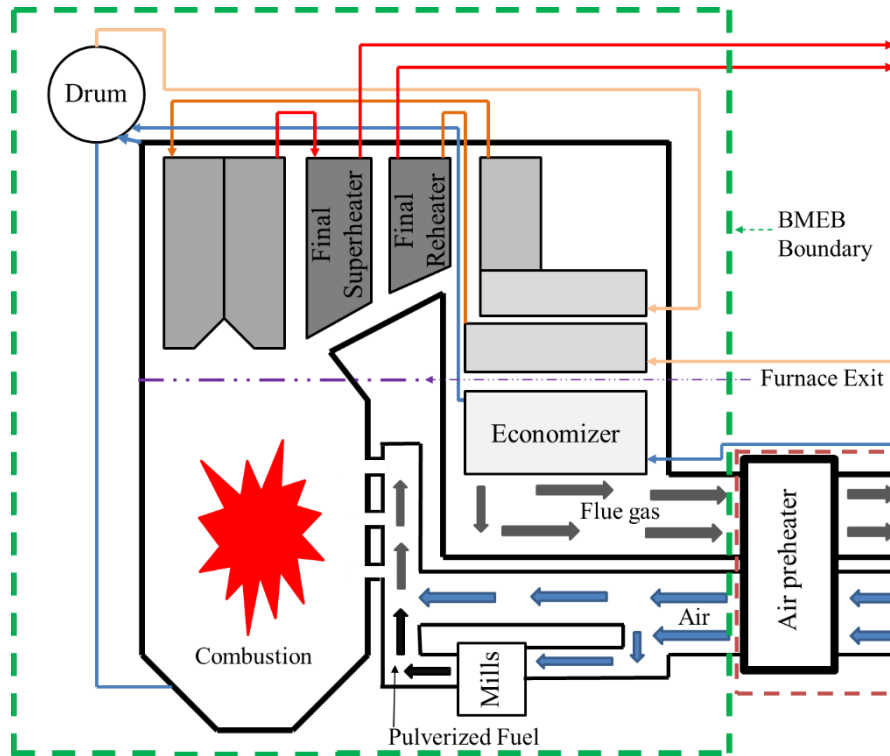


Figure 25: BMEB Boundary

The BMEB, in simple terms, will show the relationship between: coal flow rate, combustion air flow rate, flue gas flow rate, ash flow rate, and heat transfer and losses. The air heater MEB will show the relationship between the flue gas flow rate, the total air flow rate, and the ingress air flow rate. A schematic of the BMEB and air heater can both be seen in Figure 26 and Figure 27 respectively.

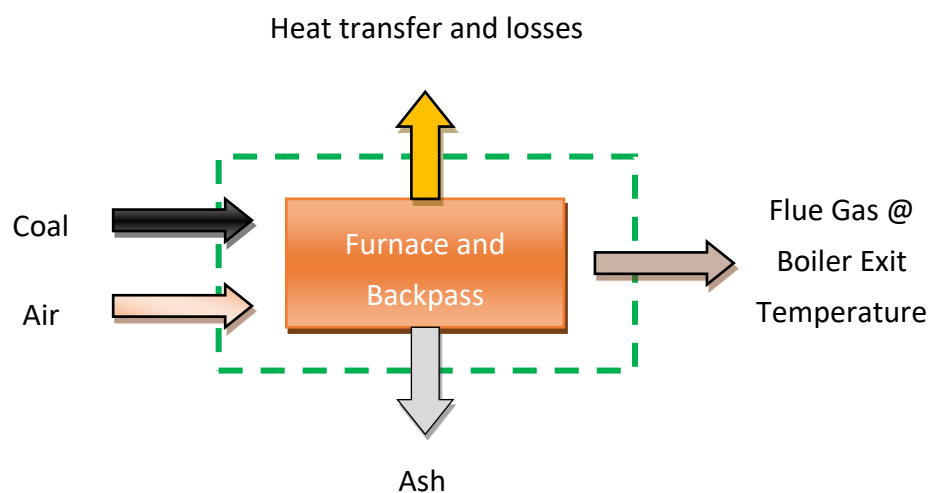


Figure 26: High level schematic of BMEB

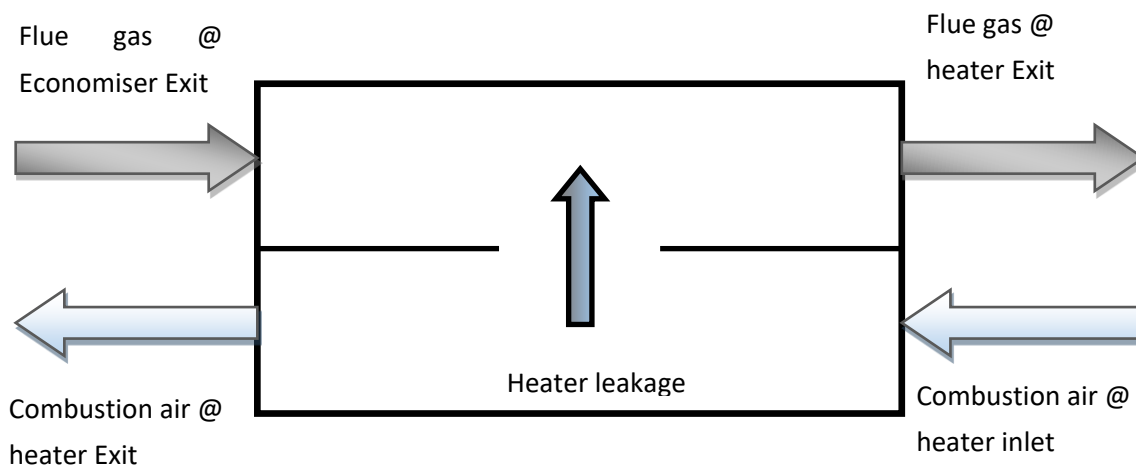


Figure 27: Air heater schematic

The set of calculations for the BMEB and air heater is derived, and further improved upon, from the work done by Tootla and Jestin [48]. The calculation set was initially developed in MathCAD (See Appendix B for full set). Once the calculation set was finalised it was ported into a C# script to be used within FlownexSE. The calculation flow is visualised in Figure 28. The block “Br” is the calculated burn rate of the boiler.

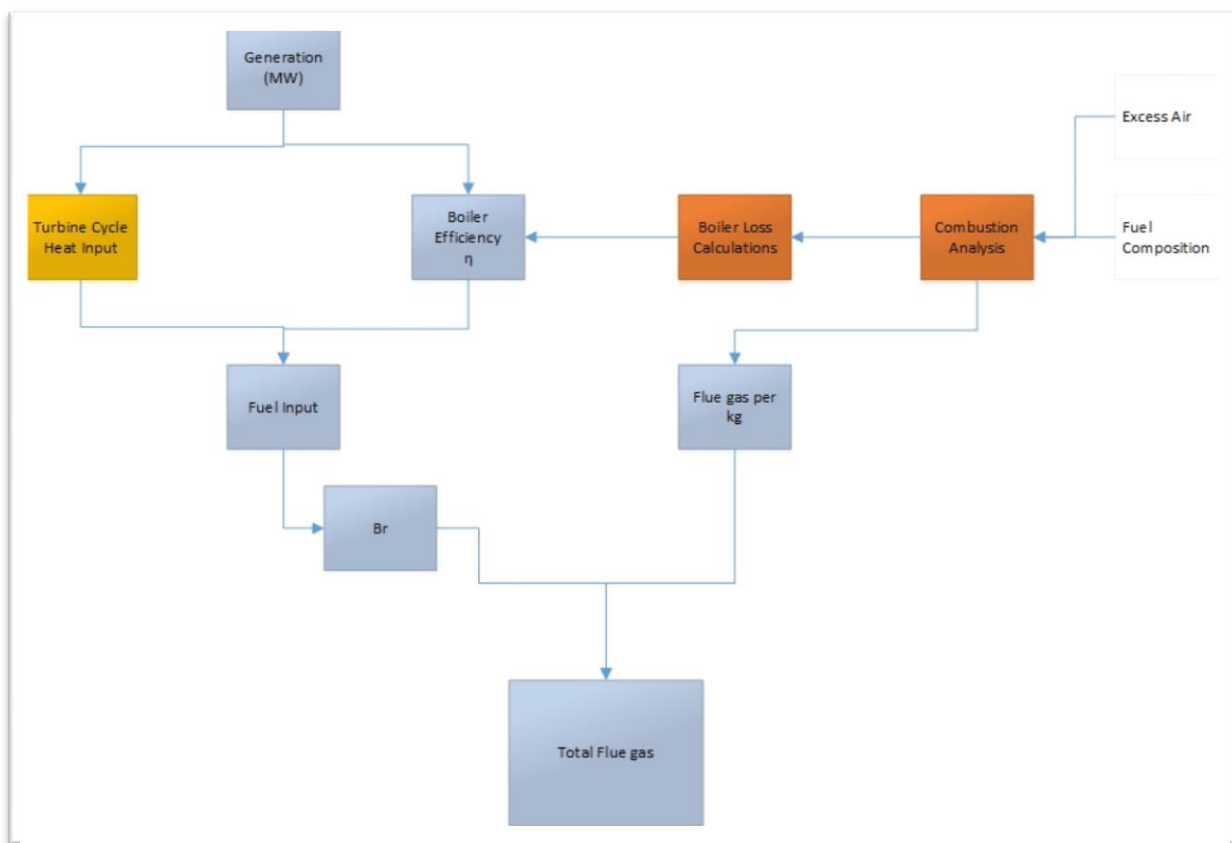


Figure 28: BMEB high level calculation flow

The inputs and outputs, with specific reference to information being shared between the three sub models, to the BMEB tool can be summarised in Figure 29. The inputs are the water/steam mass flows and enthalpies calculated from the Rankine cycle model. The outputs are the mass flows of flue gas and air heater inleakage, furnace exit temperature (FET), the energy extracted by the heat exchangers in the boiler, and the heat extracted by the air heater.



Figure 29: BMEB tool inputs and outputs

The comparison between BMEB and the baseline information can be seen in Table 7 below. Low residuals were obtained which boded well for some of the input parameter assumptions made.

Table 7: Residuals between BMEB and baseline information

| % Load Generation (%BMCT) | 68.6 | 97    | 100   |
|---------------------------|------|-------|-------|
| Coal mass flow            | 0.7% | -0.1% | -0.1% |
| Flue gas                  | 3.5% | 4.1%  | 4.1%  |

### 3.2.3 Noteworthy calculations adjustments

The MEB was created from the ground up, using the work done by Tootla and Jestin[48] as a framework. The following additions to the calculation sequence were made to decrease the number of valid assumptions being made as more site-specific data was available.

#### a) Air composition

The combustion air composition excluded argon. The argon properties were added to process of calculating the flue gas enthalpy as well as taking a portion of the mass fraction. The composition of air on a mass, molar and volume basis were all added as inputs for conversion purposes.

#### b) Air heater boundary temperatures

To determine off design operating loads, design data for the flue gas inlet, flue gas outlet, and air inlet temperatures around the air heater are now stored. A function, based on a linear interpolation, is used to calculate the above boundary air heater temperatures at percentage generation loads of 68.6% to 100%.

**c) Moist air enthalpy calculation**

To account for the moist air enthalpy, the ASHRAE handbook was used to approximate this value [49]. Relative humidity and atmospheric pressure are inputted into the model. This is used to calculate the specific humidity of the incoming air. ASHRAE calculation uses the specific humidity and dry bulb temperature to calculate the moist air enthalpy that are valid for temperatures up to 1000°C as long as water content does not result in condensate.

**d) Elemental enthalpies**

Polynomial fits were created to calculate the enthalpy of various gases between temperatures of 0°C and 2000°C. The curves were obtained from the NIST database [23]. Another change was done to the fly ash enthalpy which was initially assumed equal to the coal. This has been corrected and now uses the data presented by Bentz et al [50].

**e) Excess air calculation**

The excess air calculation was redone to verify the theory behind it. The full derivation can be seen in Appendix A.2 – Excess air calculation. The main difference was that the excess air calculation done by Tootla and Jestin[48] included a subtraction of the ash mass fraction within the calculation whereas my formulation deals with that in the initial stages.

**f) Flue gas composition:  $\text{NO}_x$** 

During combustion of, Nitrogen Oxides ( $\text{NO}_x$ ) are formed. After consultation with system engineers and my industrial mentor it was noted that during combustion nitric oxide (NO) is more likely to be formed during combustion rather than the previously set nitrogen dioxide ( $\text{NO}_2$ ) [23]. Furthermore, the formation of  $\text{NO}_2$  is formed when NO is oxidised [30].

This change is seen in the calculation of the flue gas ratio and the enthalpy calculation of flue gas. The flue gas ratio is the ratio of how much flue gas is formed per kg of coal. The enthalpy calculation of flue gas is the summation of the enthalpies of the flue gas constituent each multiplied by their mass fraction.

**g) Flue gas mass flow rate**

The total flue gas mass flow rate was calculated as the sum of the constituents and can be seen in the complete BMEB in Appendix A.1 - Complete BMEB.

**h) Air Heater calculations**

An air heater MEB was created on the side to calculate the air leakage based on the oxygen measurements. Including the air heater into the boundary of the BMEB is only possible if there is a  $\text{O}_2$  measurement on the air heater outlet. The separation of the air heater to the model allows for a more generic approach that is easily reproducible at different stations.

### 3.3 Draught group model

#### 3.3.1 Overview of draught group

The draught group comprises of all the components associated with the functioning of the coal/flue gas stream, mentioned in Chapter 1. The structure of the draught group may vary depending on the system, but a typical draught group can be seen in Figure 30 below.

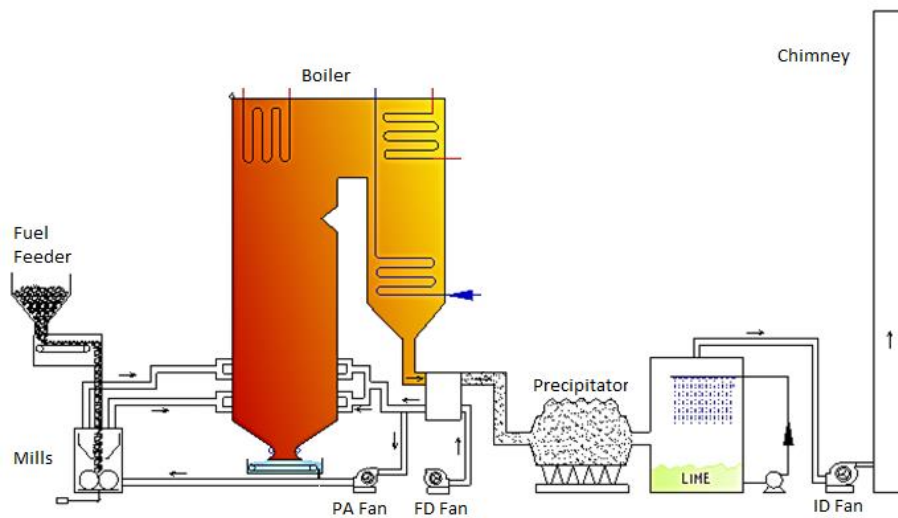


Figure 30: Draught group diagram

The draught group is an open system with its operating fluid changing in properties as reactants are added to the stream, chemical reaction occurs, products are removed from the stream and the rest is expelled into the atmosphere. The power plant typically has duplicates of fans and precipitators, multiple mills and feeders. These are referred to as the left and right-hand side of the boiler with symmetry seen in that axis.

Plant A is designed to be a balanced draught plant where a forced draught (FD) fan supplies air to the boiler, the primary air (PA) fan is used to pneumatically transport coal to the mills and the ID fan is used to maintain pressure in the furnace [7]. Plant A's fans are driven by fixed speed motors with radial vanes limiting the volume flow. The formal fan performance curves have each curve corresponding to a vane angle opening

Draught group components can be categorised into three sections: the pre-combustion section, combustion section, and the post combustion section. The pre-combustion section comprises of the FD and PA fan, mills, fuel feeders, and the air side of the air heater. The combustion section comprises of the burners and the area in the boiler known as the furnace. The post combustion section is the remainder of the boiler, the flue gas side of the air heater, the precipitator, id fan, and the chimney.

The inputs and outputs, with specific reference to information being shared between the three sub models, to the draught group model can be summarised in Figure 31. The inputs are the mass flows of flue gas and air heater inleakage, furnace exit temperature (FET), the energy extracted by the heat exchangers in the boiler, and the heat extracted by the air heater. The draught group model will use those inputs as boundary conditions. Once the model has converged it will output the fan position.

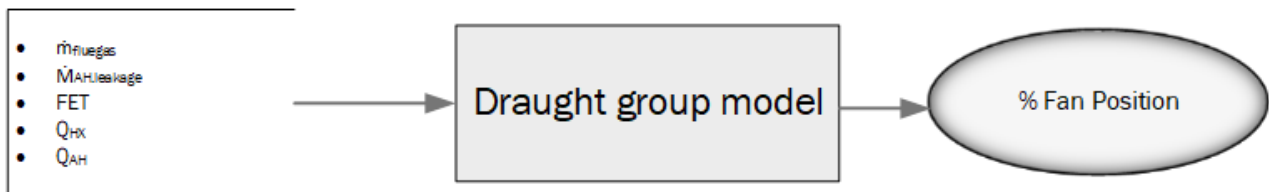


Figure 31: Draught group model inputs and output

### 3.3.2 Draught group modelling

As the objective of this project was to look at the impact of anomalies on the ID fan, it was identified that it would be appropriate to set the boundary of the model to start at the burners and end at the chimney exit. Power plant A is also symmetric between the left- and right-hand side. This symmetry allowed for half a draught group to be modelled. Modelling the plant this way would be sufficient for the purposes of this study as no pre-combustion anomalies are being investigated and validation (using plant data) would be clear. The boundary of the system was thus set, and a representative diagram of Plant A's draught group can be seen in Figure 32 below.

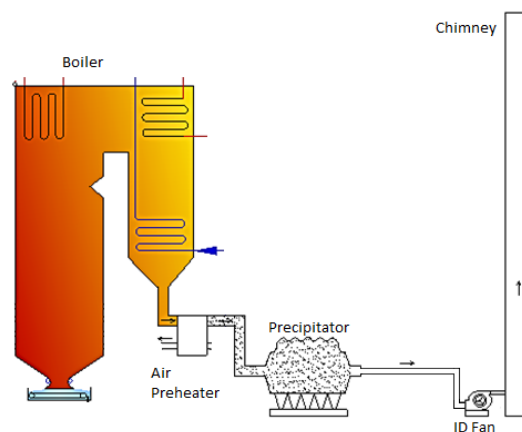








Figure 32: Draught group representative boundary

#### a) Key FlownexSE components

Table 8 includes the component description and icons all FlownexSE components used in the development of the draught group model.

Table 8: FlownexSE component icons.

| Description   | Component icon  |
|---|---|
| <b>Variable Speed Fan:</b><br>Functions as a pump when a gas is used as a fluid in the system and a pump when a liquid is used. Simulates a variable speed pump/fan based on the specific pump/fan charts provided. The inputs to the component are the Pressure rise vs. Flow, and Efficiency vs. Flow charts. | <br><i>Figure 33: Variable Speed Fan</i>             |
| <b>Flow Resistance:</b><br>Used when specific process conditions are known to simulate pressure drops through a component. Geometry is not required. Flow admittance is the minimum requirement.  | <br><i>Figure 34: Flow resistance</i>                |
| <b>General Empirical Relationship:</b><br>Similar to the Flow Resistance, however the minimum requirements are the pressure drop constants: $\alpha$ , $\beta$ , $c_k$ . The constants are used in Equation (14)  | <br><i>Figure 35: General empirical relationship</i> |
| <b>Script:</b><br>The Flownex Script component is an environment to write full Microsoft C# code. A pre-made Script used in the project is the Steady state controller.   | <br><i>Figure 36: Script</i>                       |
| <b>Boundary Condition:</b><br>Specifies the condition properties and fluid composition on the inlet or outlet of any component/system. It can also specify known conditions along the flow path of the fluid.   | <br><i>Figure 37: Boundary Condition</i>           |
| <b>Node:</b><br>A point to connect components to each other. It can be given a volume, in which case it resembles a container.  | <br><i>Figure 38: Node</i>                         |



### Variable speed fan: use and theory

Plant A utilises a fixed speed fan with a variable inlet vane to control the volume flow and effect pressure rise of the flow through the ID fan. The acceptance test data depicts the ID fan's performance as various curves at different vane opening angles. To simulate this behaviour, a variable speed fan component was used. With the input of a digitized performance curves, the speed selector of the fan in FlownexSE was used to select the different vane opening angles with 1 rpm correlating to 1°. This was found to work exceptionally well as Flownex does not take the actual speed into account when performance curves are provided.

Flownex also interpolates between the different vane angles using the following methodology firstly illustrated with Figure 39.

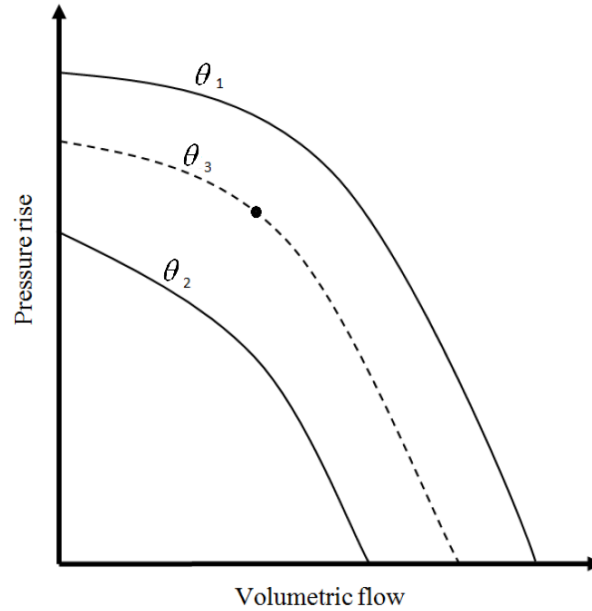


Figure 39: Illustration of fan chart with two vane angle curves

The two closest fan curves are used to calculate two possible points on the fan chart with:

$$\frac{Q_3}{Q_1} = \frac{\theta_3}{\theta_1} \quad (5)$$

$$\frac{H_3}{H_1} = \left( \frac{\theta_3}{\theta_1} \right)^2 \quad (6)$$

and

$$\frac{Q_3}{Q_2} = \frac{\theta_3}{\theta_2} \quad (7)$$

$$\frac{H_3}{H_2} = \left( \frac{\theta_3}{\theta_2} \right)^2 \quad (8)$$

Where:

|          |   |                         |
|----------|---|-------------------------|
| Q        | = | Volume flow             |
| H        | = | Pressure rise           |
| $\theta$ | = | Vane opening percentage |

Linear interpolation is then used between the resulting values to obtain the pump operating values at vane angle  $\theta_3$ .

### Flow resistance: use and theory

When considering the boiler; air heater; precipitators; and chimney; it was seen that in terms of their effect on the draught group as seen from the ID fan they have the same functionality. That was to remove heat energy from the fluid stream and cause a pressure drop. To limit the required information to complete the model, these two aspects informed the decision to model the rest of the components as a flow resistance element.

Characterising the pressure drop of each component required inlet and outlet fluid properties, and mass flows. The total pressure drop of a component without secondary losses can be given by:

$$\Delta p_0 = \left( \frac{fL}{D} \right) \frac{1}{2} \rho V |V| + \rho g \Delta z \quad (9)$$

Where

|   |   |  |
|---|---|--|
| $f$   | = | friction factor  |
| L   | = | Length [m] of the pipe                                 |
| D   | = | inside diameter [m] of the pipe                        |
| $\rho$  | = | fluid density [kg/m <sup>3</sup> ]                     |
| V   | = | mean fluid velocity [m/s]                              |
| g   | = | gravitational acceleration constant                    |
| $\Delta z = z_{\text{exit}} - z_{\text{inlet}}$ | = | the height difference [m] between the inlet and outlet |

This can however be simplified to have one variable comprising the various dimensional characteristics. Since the following is true:

$$\dot{m} = \rho VA \quad (10)$$

Where

|           |   |                             |
|-----------|---|-----------------------------|
| $\dot{m}$ | = | fluid mass flow [kg/s]      |
| A         | = | flow area [m <sup>2</sup> ] |

Equation (10) can be rearranged to the following:

$$V = \frac{\dot{m}}{\rho A} \quad (11)$$

Thus (9) becomes:

$$\Delta p_0 = \frac{|\dot{m}| \dot{m}}{\rho A_f} + \rho g \Delta z \quad (12)$$

The constant terms in this can be simplified to define the flow admittance:

$$\frac{1}{A_f} = \left( \frac{fL}{D} \right) \frac{1}{2A^2} \quad (13)$$

Where

$A_f$  = flow admittance

For a given operating point, the design data is used to determine the flow admittance for a component. This is expected to remain the same for all operating conditions unless the component has moving parts forcing a change in the pressure profile across it.

The heat removal for the boiler and air heaters are calculated in the BMEB tool and can be connected to the flow resistance component to specify the required rate of energy extraction required.

#### **General empirical relationship: use and theory**

Leaks were added as boundary conditions, however, FlownexSE requires that a component exists between the boundary condition and a node thus necessitating the need for another element. The general empirical component was used.

The general empirical component calculates pressure loss using the following relation:

$$\Delta p_0 = C_k \rho^\beta Q^\alpha \quad (14)$$

Where

$C_k, \beta$  and  $\alpha$  = pressure drop constants

$\rho$  = mean density [kg/m<sup>3</sup>]

$Q$  = volume flow rate [m<sup>3</sup>/s]

The pressure drop constants are  $\beta = 1$ ,  $\alpha = 2$ , and  $C_k$  is calculated per leakage for the pressure to move from atmospheric to flue gas stream pressure at leakage site. The  $C_k$  value is calculated with the aid of a steady-state controller.

#### **Script (Steady state controller): use and theory**

The operating point of the fan is determined using a steady state controller. As mentioned above, the variable speed fan is used to simulate the ID fan with adjustable vane. To specify the current vane condition, the steady state controller is used to adjust the vane angle to satisfy the condition that the outlet pressure of the chimney must be at atmospheric conditions. The controller will iterate changing the vane angle until the output gets within a specified tolerance. The flow of the calculations can be seen in Appendix C -1 Steady state controller flowchart.

### b) Model prototype

A systematic approach was followed in the development of the model. Each component was initially modelled separately with boundaries across them to ensure validity of the component properties. The properties are the flow admittance and the heat input. To ensure model validity, acceptance test data was used to set the boundary conditions across each component and thus used as the tuning data. Figure 40 below shows the initial development path of the air heater, with included air heater leakage into the flue gas stream.

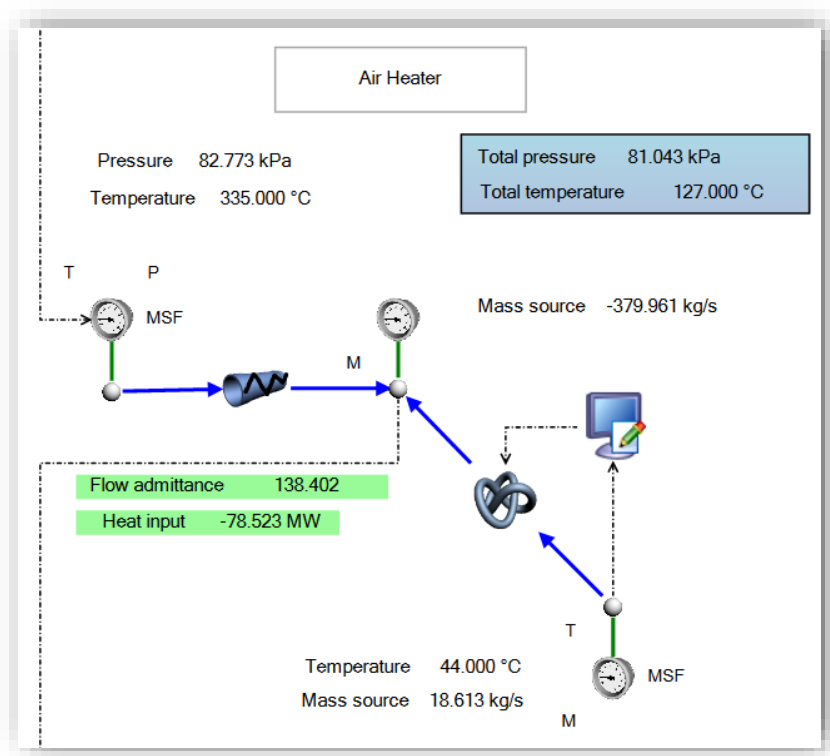


Figure 40: Prototype air heater (with leakage)

The connecting lines coming into and out of Figure 40's frame are data transfer links, linking the previous sections end boundary node to the beginning of the current sections boundary condition component.

The process of collecting the flow admittances and heat inputs for the four sections was carried out three times at different load cases (100 %, 97 % and 68.6 %).

### c) Final Model

The final draught group model is a connection of each sub model of the four sections created with the added ID fan with OEM fan curves inputted. Figure 41 shows the full model from the furnace entrance to the chimney exit of one side of the boiler at 100 % load.

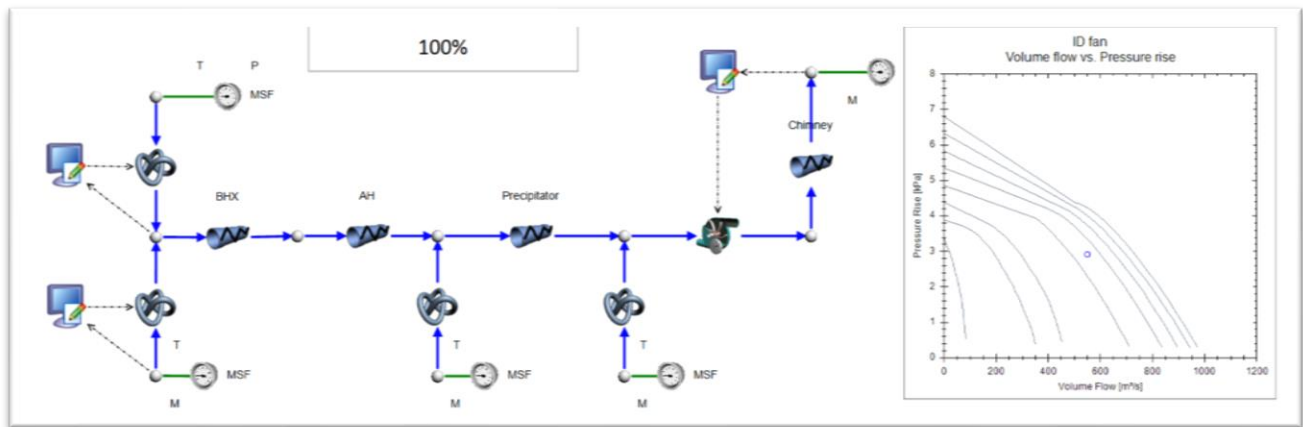


Figure 41: Full draught group model

The two general empirical relationship components on the far left of Figure 41 are the inlet stream of the flue gas (top) and the boiler air leakage (bottom). Modelling the boiler air leakage at the root is done as the worst-case scenario where a larger mass flow through the boiler is seen causing larger pressure drops throughout the system. The air heater leakage on the other hand is modelled after the component. This is justified due to the largest pressure difference between the incoming clean combustion air and the outgoing flue gas is at the flue gas stream exit and is thus more likely to occur there.

The values for the admittance at each section changed and as such the integrated model linearly extrapolates for loads from 97 % down to 80 % using the 100 % and 97 % design load case values. This was not an expected occurrence, but for the purpose of this study it was decided that this was acceptable.

### 3.4 Model integration methodology

C# script has been developed that accesses the VP Application Programming Interface (API) to send data to the FlownexSE model. The following process has been identified as the calculations needed to yield viable information to input into the Flownex model.

The use of the VP model is to have a means of calculating the required heat input for the system. This is then sent to the BMEB script to calculate the amount of flue gas going through the system as well as setting the leakages throughout. The structure of the completed model, as seen in Flownex, can be seen in Figure 42.

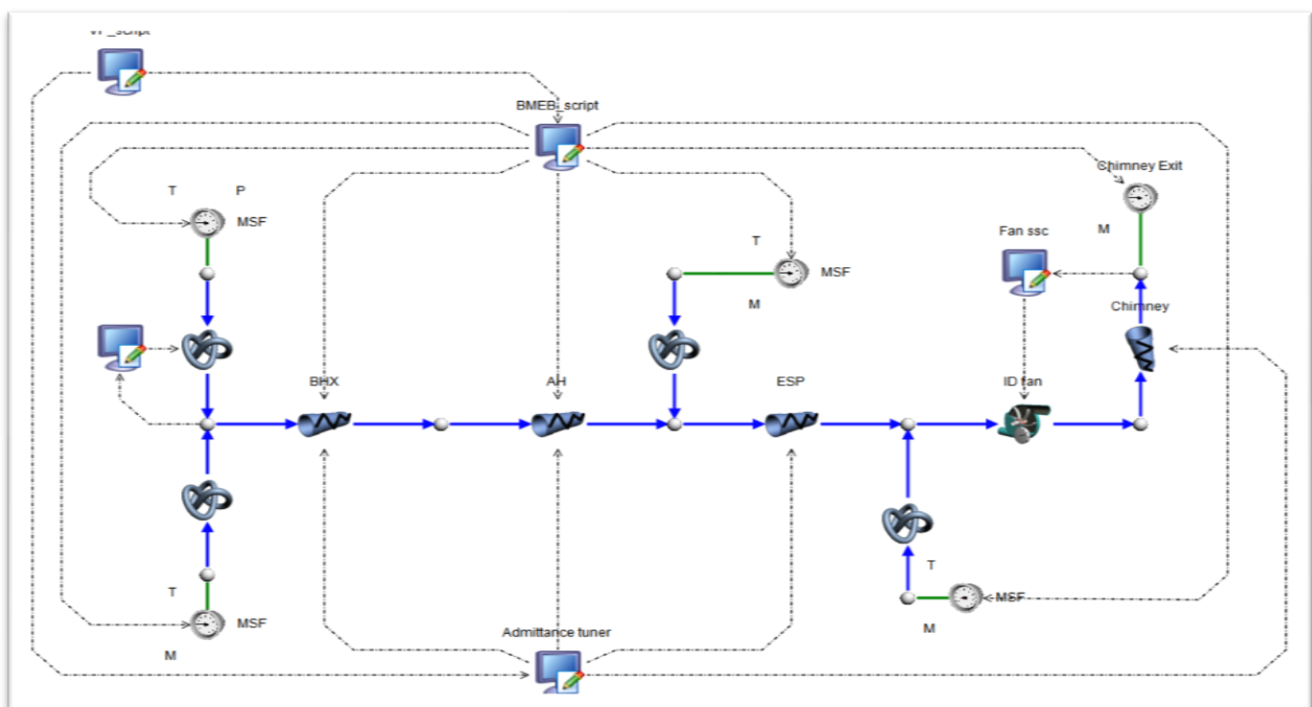


Figure 42: Final connected model

For multiple runs, Flownex has an Excel plugin that runs the model multiple times in succession if it is set up correctly. To test the limitations of this mode, a verification test was run with plant data of 500 snapshots for Plant A running at close to design plant health. Figure 43 is a screen shot of the setup within Excel to run the model remotely. As stated in CHAPTER 3.1.1 Overview of steam cycle, the condenser of Plant A is a two zone condenser. The inputs to the model were the gross generation and the condenser pressure in the high-pressure and low-pressure zones. Data for the steam and coal mass flow rates was compared to that calculated by the model. An average deviation of 5% was calculated for the steam flow and 6 % for the coal flow.

|           |                          |          |          |          |          |          |          |          |          |
|-----------|--------------------------|----------|----------|----------|----------|----------|----------|----------|----------|
| File Name | Masters_Model_V7_BP.proj |          |          |          |          |          |          |          |          |
| Visibe    | 1                        |          |          |          |          |          |          |          |          |
|           |                          |          |          |          |          |          |          |          |          |
|           | Conditions               | 1        | 2        | 3        | 4        | 5        | 6        | 7        | 8        |
| Input     | MW_in                    | 617.606  | 618.722  | 620      | 616.305  | 618.009  | 616.064  | 619.678  | 616.943  |
|           | HP_Condenser             | 4.199    | 4.339    | 4.395    | 4.633    | 4.541    | 4.639    | 4.59     | 4.59     |
|           | LP_Condenser             | 3.369    | 3.467    | 3.467    | 3.512    | 3.516    | 3.516    | 3.516    | 3.516    |
|           | -                        |          |          |          |          |          |          |          |          |
| Outputs   | mfg                      | 769.0949 | 770.538  | 772.1723 | 767.4384 | 769.6248 | 767.1319 | 771.766  | 768.2567 |
|           | coal                     | 94.81278 | 94.99587 | 95.19736 | 94.60105 | 94.88044 | 94.56188 | 95.14726 | 94.70561 |
|           | mair                     | 354.323  | 355.0072 | 355.7602 | 353.5318 | 354.5758 | 353.3854 | 355.573  | 353.9225 |
|           | --                       |          |          |          |          |          |          |          |          |
|           | DeltaP                   | 2.954193 | 2.964624 | 2.980263 | 2.94336  | 2.957641 | 2.94134  | 2.976275 | 2.948674 |
|           | Volume Flow              | 323.551  | 324.1586 | 324.8462 | 322.8533 | 323.7741 | 322.7243 | 324.6752 | 323.198  |
|           | RPM                      | 57.14885 | 57.45354 | 57.85787 | 56.82503 | 57.25357 | 56.76591 | 57.75438 | 56.98314 |
|           | Density                  | 0.690381 | 0.690212 | 0.69009  | 0.690596 | 0.690315 | 0.690635 | 0.690121 | 0.690491 |
|           | ---                      |          |          |          |          |          |          |          |          |
|           | Efficiency (Direct)      | 89.75377 | 89.75023 | 89.75018 | 89.7589  | 89.75218 | 89.75985 | 89.75019 | 89.75638 |
|           | Efficiency (HHV)         | 85.81291 | 85.81123 | 85.81116 | 85.81533 | 85.81216 | 85.81578 | 85.81118 | 85.81415 |
|           | mass flow                | 498.4424 | 499.5333 | 500.8247 | 497.2075 | 498.8387 | 496.9778 | 500.5036 | 497.817  |

Figure 43: Excel model setup

## 4. Application case studies

The anomalies that are considered for these case studies can be split into two categories, air/flue gas side anomalies and steam side anomalies. On the air/flue gas side, the effect of coal quality; increased boiler exit flue gas temperature; boiler air ingress and; air heater inleakage to flue gas stream are investigated. While on the steam side, the effects of feed water heaters out-of-service and condenser backpressure degradation are considered. The anomalies are those discussed in Chapter 2.6 ID fan anomalies and their locations can be seen in Figure 44 below.

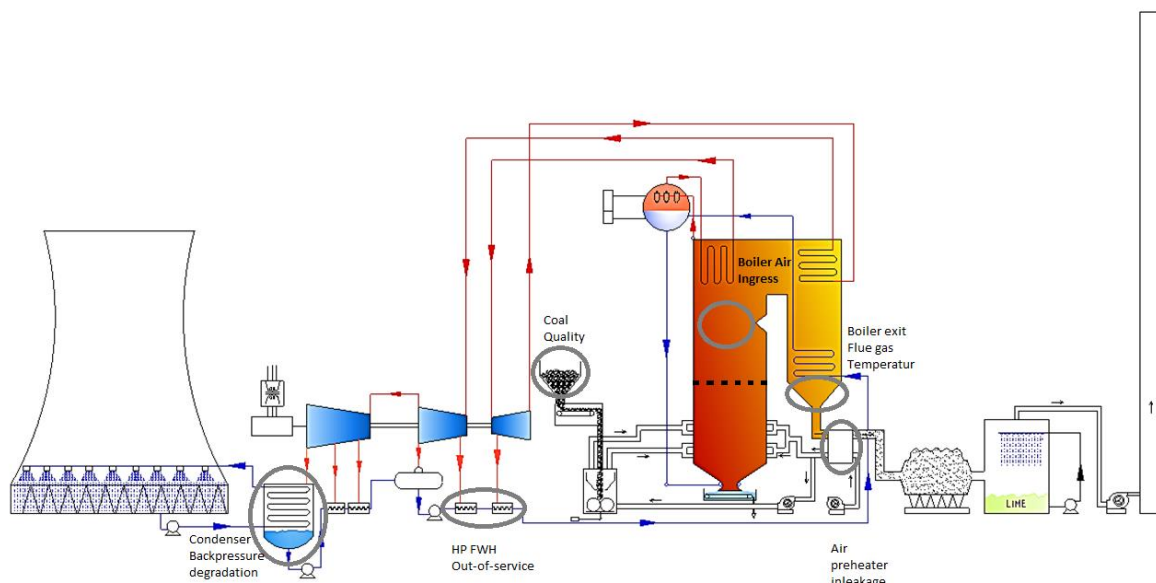


Figure 44: Anomaly locations

Each anomaly was run at eight different boiler heat load cases. Validation data was only available for 100 %, 97 % and 68.6 %.

The operating point produced by the model is the static pressure head across the fan plotted against the volume flow through the fan. This point is where the system requirements (pressure loss and mass flow requirement) correspond to that of a certain point on the fan's curve.

Although the method of representing the fan performance using the performance curve is standard, it does not give a good representation of where the fan is with respect to its limits. A method of calculating the fan's normalised remaining capacity was thus formulated. The method is described below and was derived by work done by Godre.[9]



### Normalised Capacity loss derivation

The ID fan capacity loss ( $\delta_{capacity}$ ) is defined as the ratio of capacity lost at abnormal operation  $\Delta I_{ab}$  to the capacity available at normal operation  $\Delta I_{ref}$ . The capacity lost at abnormal operation is the difference in the abnormal operational current  $I_{abnormal}$  and that of the reference current  $I_{ref}$  at a given load. The capacity available at normal operation is the difference in the reference current  $I_{ref}$  and that of the limiting ID fan current  $I_{limit}$ . The calculation of  $\delta_{capacity}$  can be seen in Equation (15) below (which was derived from work done by Godre [9]).

$$\delta_{capacity} = \frac{\Delta I_{ab}}{\Delta I_{ref}} = \frac{I_{abnormal} - I_{ref}}{I_{ref} - I_{limit}} \quad (15)$$

The ID fan capacity loss was evaluated for each anomaly across various boiler load points. In Figure 45 it is shown how the reference current decreases as the boiler load decreases. The decrease in boiler load shows an increase in ID fan capacity as can be seen in the change from  $\Delta I_{ref2}$  to  $\Delta I_{ref3}$ .

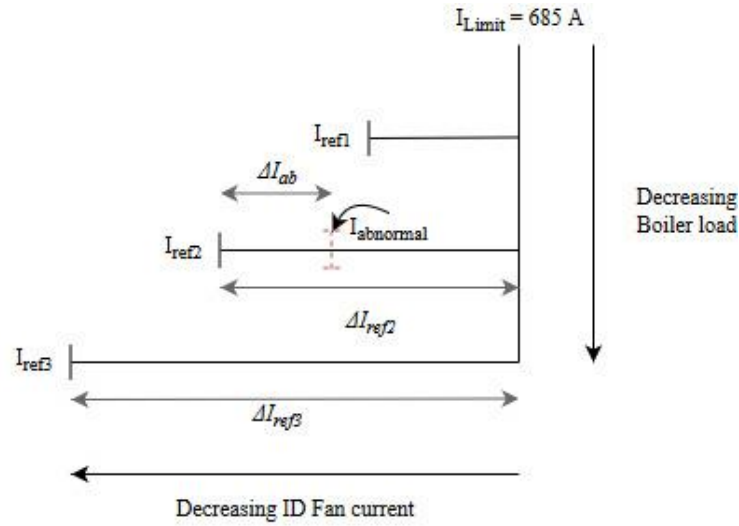


Figure 45: ID fan capacity loss at varying loads schematic

Where the result of an anomaly shows a negative loss in capacity, it would imply that the impact of the anomaly is actually positive on the capacity limitations on the ID fan.

## 4.1 Coal quality effects

Three representative coal compositions were used to study the effects of the coal quality on the ID fan's capacity. All three coal composition values were taken from the ultimate analysis, that is done monthly, between 2003 and 2016. The typical coal was chosen as one that was a comparative replacement to that found in Plant A's baseline information [8]. For high- and low-quality coal, samples were chosen representing a higher and lower carbon content value.

**Table 9: The composition of the coals examined**

|  | Low Quality<br>(Type 1) | Typical coal | High Quality<br>(Type 3) |
|--|-------------------------|--------------|--------------------------|
|  | Mass Fraction (%)       |              |                          |
| Carbon                                   | 37.09                   | 42.15        | 53.15                    |
| Hydrogen                                 | 1.73                    | 2.47         | 2.47                     |
| Oxygen                                   | 11                      | 8.45         | 5.15                     |
| Nitrogen                                 | 0.85                    | 1.08         | 1.34                     |
| Sulphur                                  | 0.74                    | 1.0          | 0.7                      |
| Moisture content                         | 4.7                     | 5.0          | 4.4                      |
| Ash Content                              | 42.6                    | 38.82        | 30.4                     |
| CV Calculated using equation (4) (MJ/kg) | 14,30                   | 17,49        | 20,46                    |
| CV Measured (MJ/kg)                      | 13,64                   | 16,28        | 19,24                    |
| % Difference from measured               | 4.8                     | 7.4          | 6.3                      |

Figure 46 and Figure 47 depict the results of the normalised capacity lost by the ID fan due to coal quality variations. Figure 46 is that when the program uses the measured CV values found on the monthly reports while Figure 47 utilises the calculated CV values.

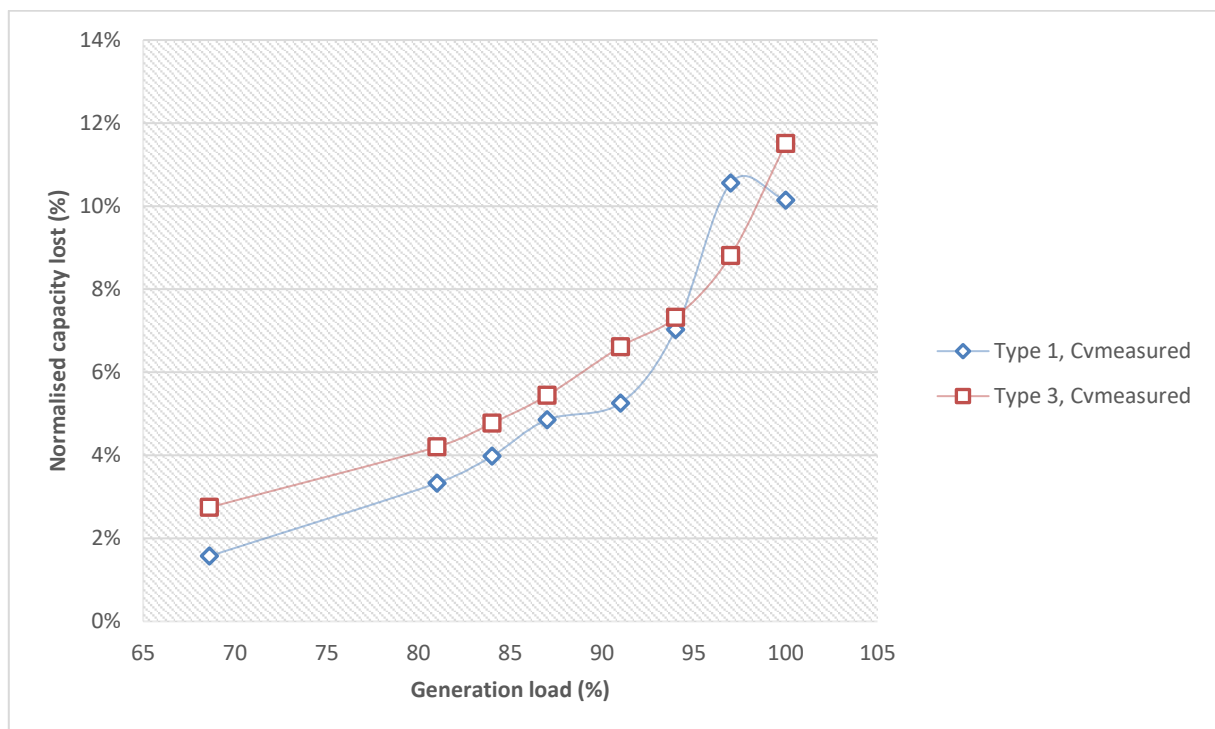


Figure 46: Normalised capacity lost due to coal quality (CV Measured)

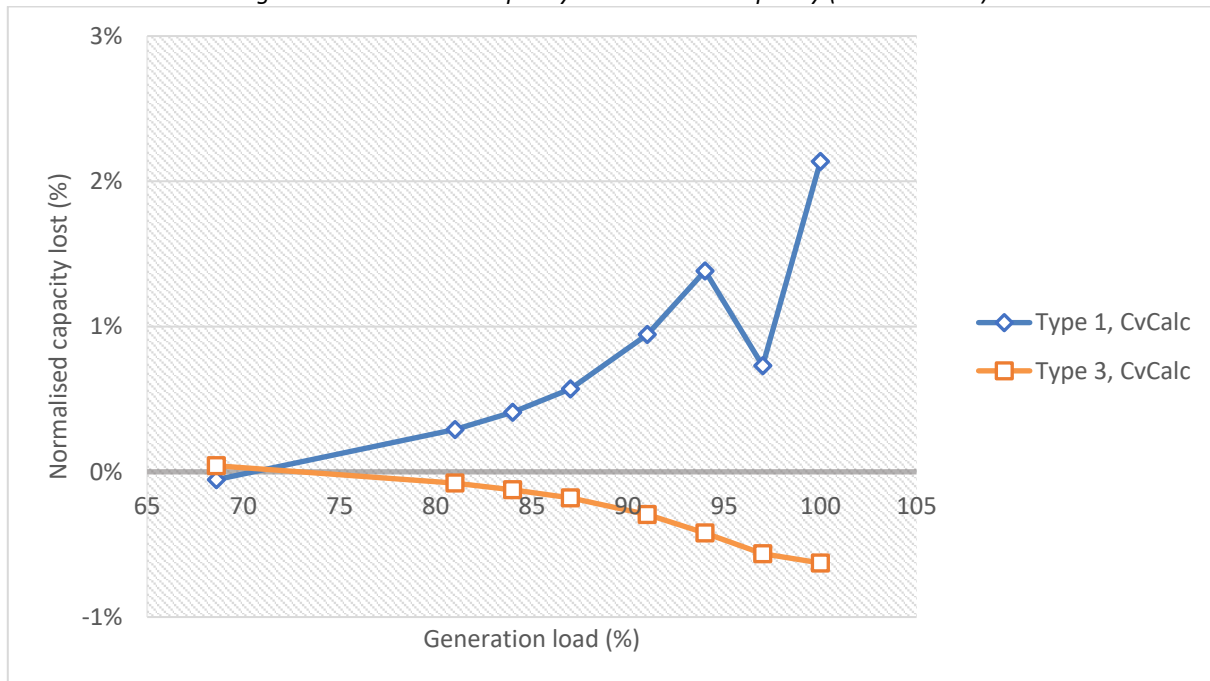


Figure 47: Normalised capacity lost due to coal quality (CV Calculated)

The results shown in Figure 46 are peculiar since both the high content carbon and low content carbon coals appear to perform worse than the reference coal. The model uses the coal composition to calculate the flue gas to coal burnt ratio. The CV on the other hand is used to calculate the amount of coal that is required to burn at a required output. Logically, a higher CV value would result in less coal required for burning. Less coal burnt, translates to a lower flue gas mass flow which in turn results in a reduced fan capacity required. In Table 9, the measured CVs were approximately 6% lower than the calculated CVs. Using the calculated CVs, Figure 47 was produced showing a better correlation between the different types of coal.

The magnitude difference in coal CV value affecting the simulation so drastically is a point that can be further investigated. One anomaly with the model not converging resulted in the erroneous point in Figure 44 (97% gen load on type 1 coal).

The worst case for Type 1 coal saw a 2.1% loss in ID fan capacity while the Type 3 coal allowed the plant to perform marginally better with 0.6%

## 4.2 Increased boiler flue gas exit temperatures

The nominal backend temperature was increased by 15°C, 30°C, 45°C, 60°C, and 75°C. The study was limited to investigating the impact of having higher backend temperatures with respect to the fluid properties and not the other implications that can arise over prolonged operation at these temperatures. A notable impact would be the formation of sulphuric acid in the flue gas stream which would greatly impact the air heaters' performance leading to larger leakages. Figure 48 depicts the results from their comparison to design values.

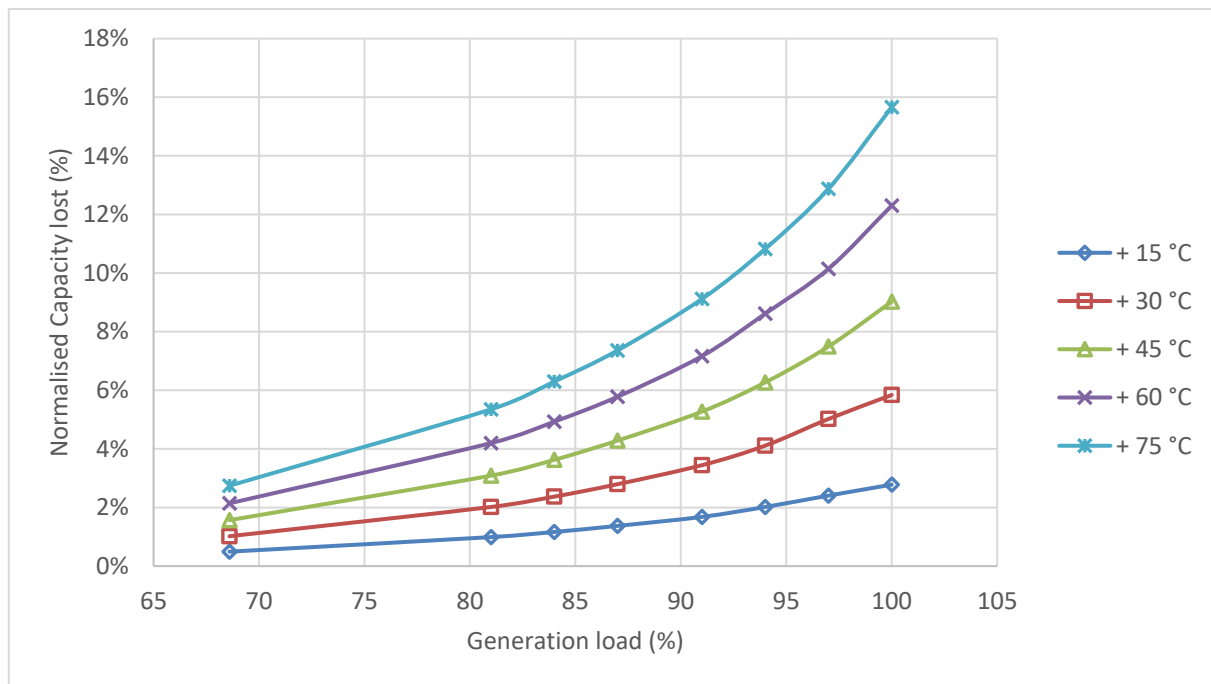


Figure 48: Normalised capacity lost by boiler flue gas exit temperature

This study showed a general trend of increasing consumption of ID fan capacity as both the load and the boiler flue gas exit temperature increased maxing out at a 15.7 % loss in ID fan capacity.

### 4.3 Air ingress into the boiler

The air ingress in the boiler is calculated in the BMEB tool. The actual flow rate is then transferred to the boiler air leakage general empirical relationship component in the draught group model to simulate its influence. This value is a percentage of the mass of the air ingress over the mass of the flue gas at the furnace exit. Plant A was designed with the expectation that air could leak into the boiler at around 2.2% of the total flue gas flowing through it. With that in mind, multiple runs attributing to larger air inleakages were done to a maximum of 15%. Figure 49 shows the results obtained by the model on the impact of boiler air ingress on the ID fan's capacity.

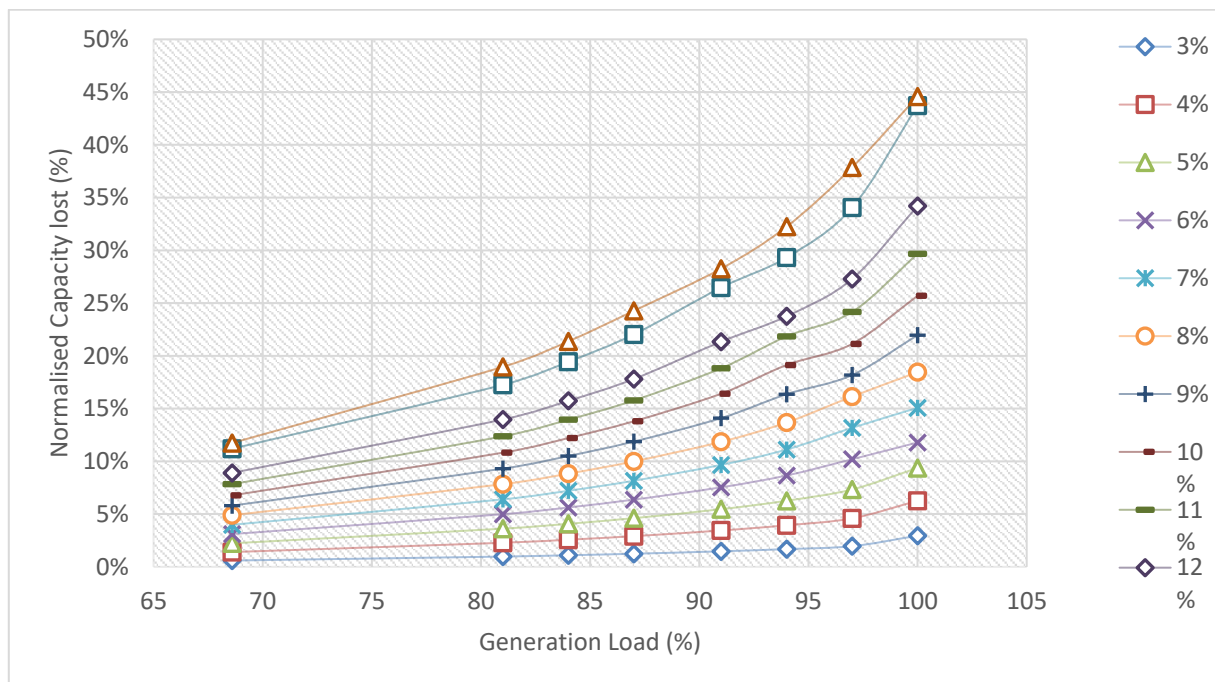


Figure 49: Normalised capacity lost by air ingress into the boiler

As can be seen, at a boiler air ingress of 15%, the lost capacity on the ID fan is 44.6%. This impact is due to an additional 165 kg/s of air flowing through the whole draught group that the ID fan must compensate for. There is a general trend that more boiler air ingress creates a larger loss in ID fan capacity. It is also seen that at high loads, the impact increases in a non-linear fashion.

## 4.4 Air heater inleakage to flue gas stream

The air heater (AH) air inleakage is calculated in the BMEB tool. This value is a percentage of ingress air over flue gas at the boiler exit. Plant A was designed with a leeway of 5.3% expected AH leakage due to mechanical limitations of the sealing ring and general wear and tear of the environment the AH works in. This study ran multiple runs increasing the total AH air ingress from 6% to 26% in increments of 2%. The AH has the high differential pressure between the heat exchanging streams and as such a small leak can amount to a large amount of flow between them. Figure 50 shows the results of these increases with respect to the ID fan's capacity.

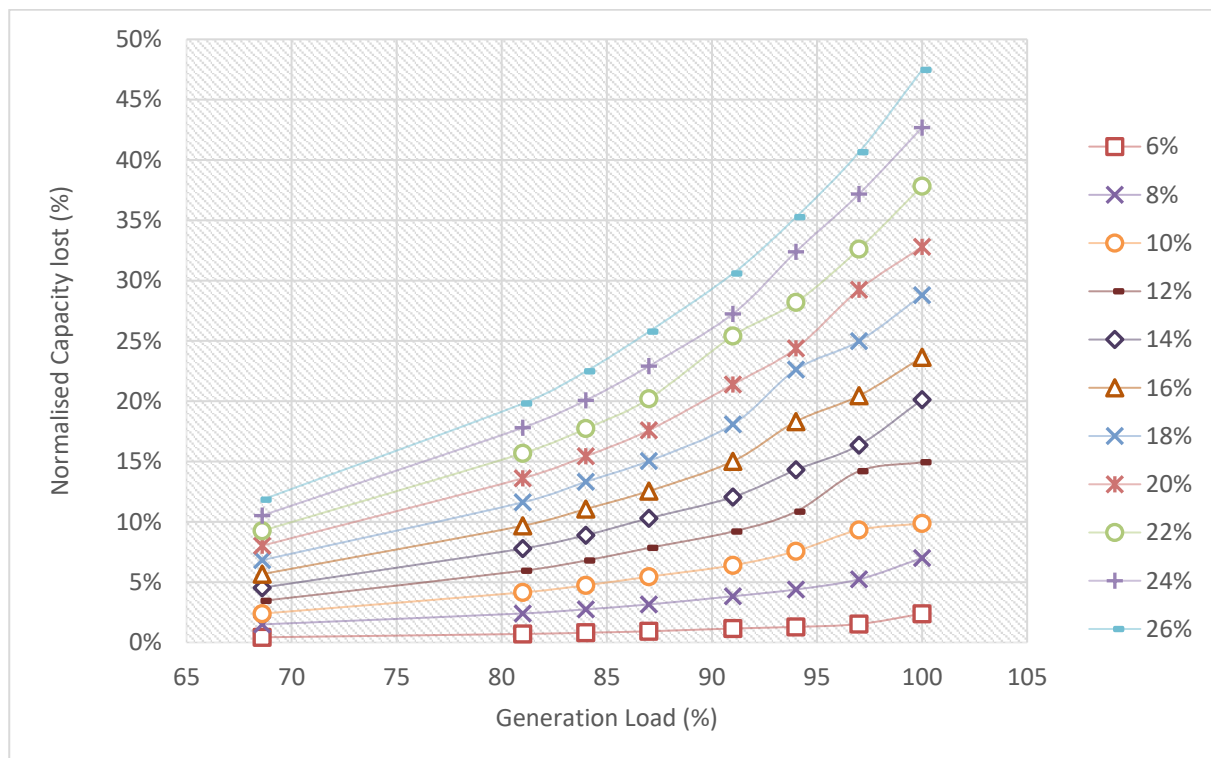


Figure 50: Normalised capacity lost by air leakage into the flue gas stream of air heater

The general trend of increased load increases the fan's lost capacity as well as the increase in AH leakage. With the highest leakage of 26 %, the capacity lost was 47.5 %. This is due to an additional 216 kg/s of air that the ID fan must compensate for.

## 4.5 Feed water heaters out-of-service

A schematic of the feedwater heater train of Plant A is shown in Figure 51. There are three low pressure FWHs (1 to 3), a deaerator, and two HP FWHs (5 and 6). Plant A has two parallel banks of HP FWH with two FWHs in each bank. The first bank (bank A) is made up of FWH 5A and 6A, while second (bank B) contains FWH 5B and 6B.

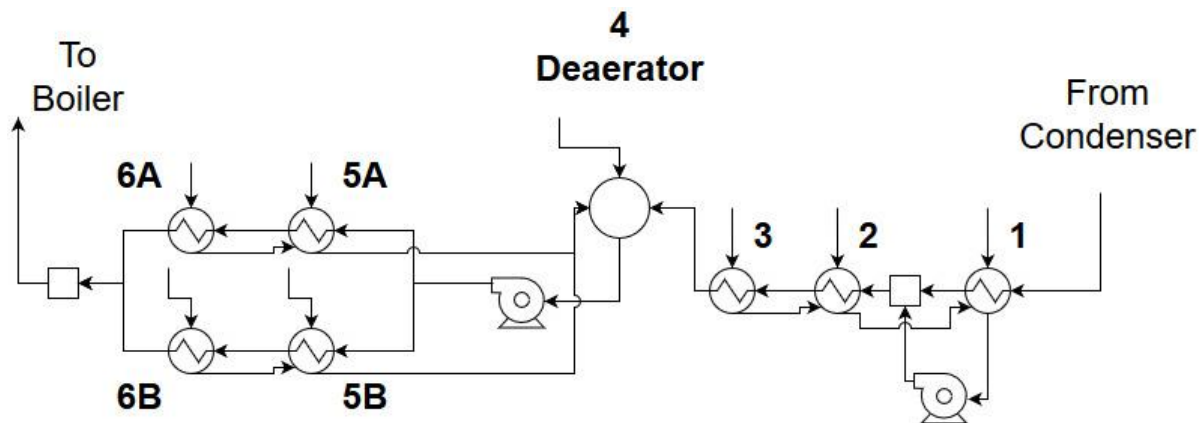


Figure 51: Feedwater heater train of Plant A

The case study investigated in this section looks at the effect of taking FWH out of service. This was limited to the HP FWH. Table 10 gives an overview of all the runs carried out with reference to which HP FWH were taken out of service during each run. Plant A does not have the capability to remove only one FWH from the cycle, as such the possible scenarios are limited to: Bank A (i.e. FWH 5A and 6A out of service), Bank B (i.e. FWH 5B and 6B out of service), and Both Banks (all FWH out of service).

Table 10: Runs carried out for out of service HP FWHs

| Heater | Runs      |            |        |        |
|--------|-----------|------------|--------|--------|
|        | Reference | Both Banks | Bank A | Bank B |
| 5A     |           | X          | X      |        |
| 5B     |           | X          |        | X      |
| 6A     |           | X          | X      |        |
| 6B     |           | X          |        | X      |

Figure 52 shows the normalised ID fan capacity loss of the various runs. At full load (100 %), it can be seen that both banks being out has the highest loss in ID fan capacity with 16.2 % at 100 % generation load. This is to be expected since switching off all 4 HP FWHs would result in the largest additional heat requirement from the boiler. It is also to be expected that taken out Bank A or Bank B should yield the same normalised ID fan capacity loss. The similarity in the run pairs is attributed to the fact that the same feed water temperature rise is experienced for the FWHs in each of the combined FWHs. The next significant normalized ID fan capacity loss of 8.5 % is seen in Runs 6 and 7 where a bank of FWHs is taken out of service.

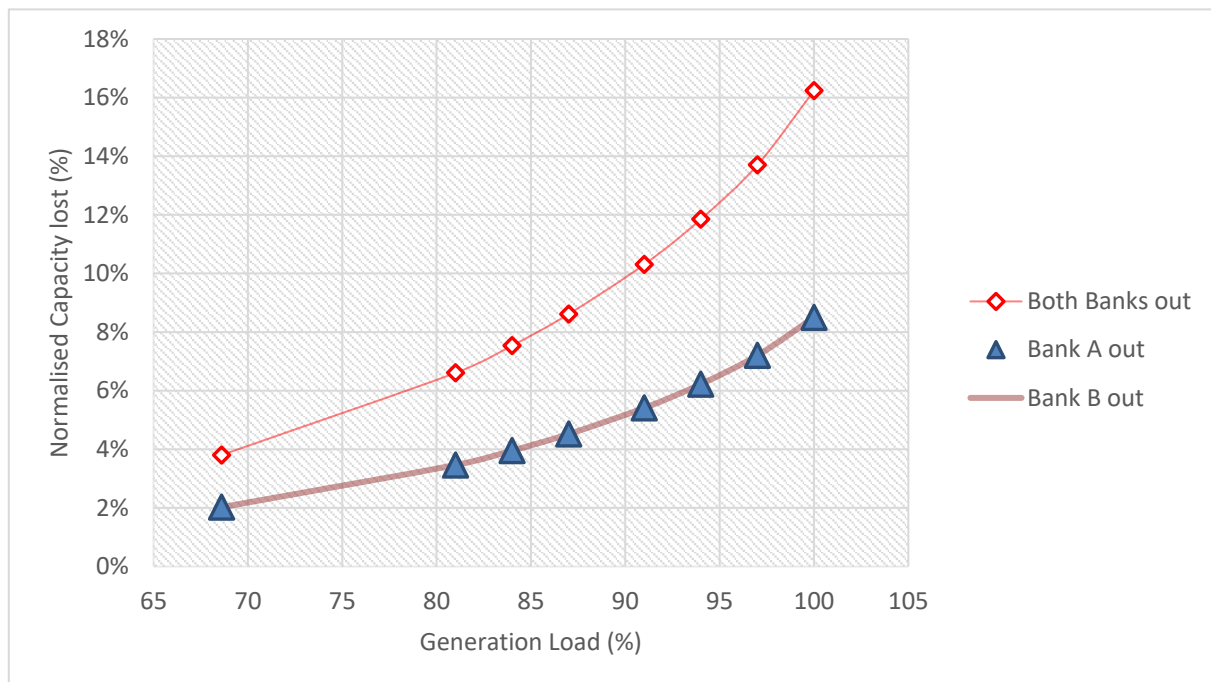


Figure 52: Normalised capacity lost by out of service HP FWH at various boiler loads

The effect of taking out the LP FWH was not considered in this study. The methodology for setting up the model does allow for the simulation of runs that describes situations where LP FWHs are put out of service. Similar normalised ID fan capacity losses, like those seen in Figure 52, are likely to be seen if the feedwater temperature rise in those LP FWHs are of the same magnitude as those in the HP FWHs.



## 4.6 Condenser backpressure degradation

The case study investigated in this section is that of the degradation of the condenser in the steam cycle. Degradation of the condenser backpressure refers to the pressure rising effecting multiple things such as the LP turbine exhaust steam properties. At BMCR, the reference average condenser backpressure was set to 5.4 kPa as per the official heat balance diagrams. As the load decreased, there was a constant difference between the two condenser zones with a decrease in both pressures. A linear relationship was found and used in this case study.

This study was conducted at three average pressures (7 kPa, 9 kPa and 12 kPa) correlating to 100 % with the same linear relationship found in the heat balance diagrams. They were then compared to the 5.3 kPa average to calculate the normalised capacity lost by the ID fan. The results can be seen in Figure 53 below.

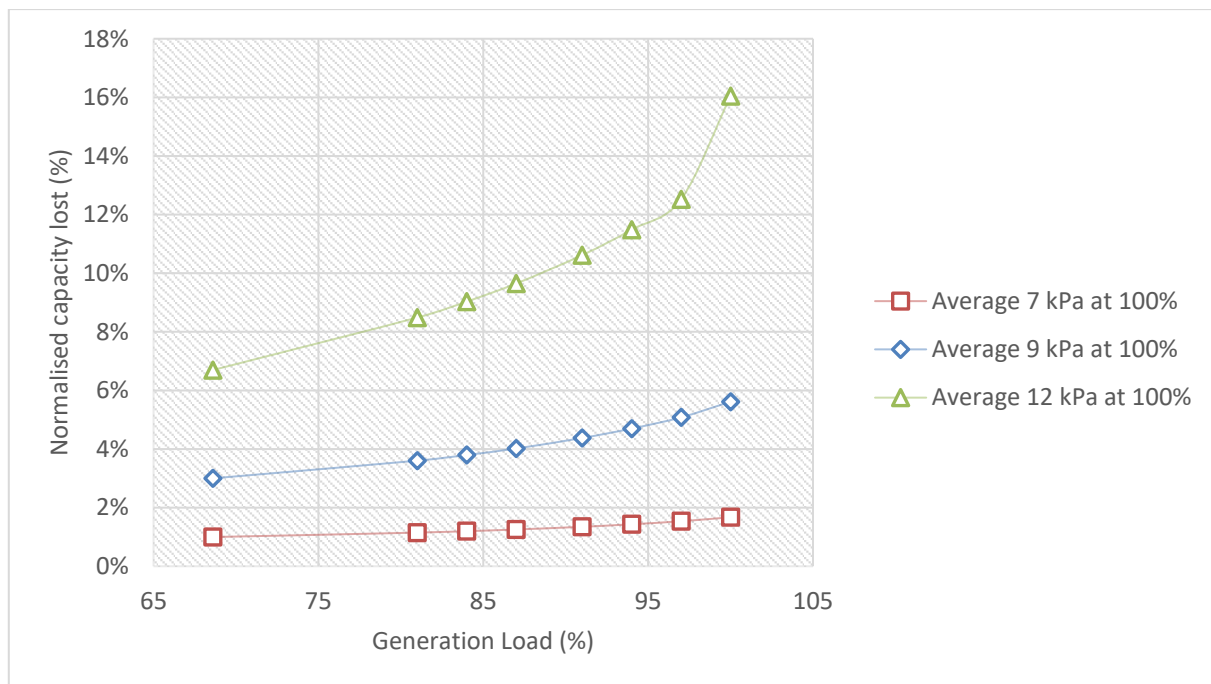


Figure 53: Normalised capacity lost by condenser backpressure degradation

From the figure it is seen that as the load increase the capacity lost on the fan increases. On top of that, with higher average condenser backpressures the issue is exasperated as the trend seems to have a steeper curve closer to 100 % generation load.

The full load operation of the plant with 12 kPa, 9 kPa and 7 kPa average condenser backpressure correlate to a loss in ID fan capacity of 16 %, 5.6 % and 1.7 % respectively.

## 5. Conclusions and recommendations

### 5.1 Conclusions

The primary objective of this project was to develop a modelling methodology that can be used to conduct a systematic study of the impact of various anomalies, within the power plant, on the ID fan. The methodology outlined within this report was used to successfully create a model. The success of this model was based on the two tests. The first being its ability to accurately calculate the vane position of the ID fan using baseline information. The second test used plant data from a stable month of Plant A's operation.

The BMEB was a substantial part to getting the full model working. The inclusion of which allowed for the simulation of various boiler related performance metrics. Its use in this study established the connection between the draught group and Rankine cycle, thus becoming the enabling factor of the study.

The systematic study of the six anomalies showed varying degrees of impact on the ID fan. The studies had similarities in the fact that the same anomaly at higher loads had a greater impact on the fan than at lower ones. The trend was also nonlinear in all six cases per anomaly severity.

The lowest impact came from the changes in coal quality. This was surprising due to the general consensus that the composition of the flue gas should affect not only the flow but also its quantity. The highest impact tested came from the AH leakage. The large amount of air flow into the flue gas stream was slightly more impactful than the boiler air ingress that happens upstream

In conclusion setting up the model is possible and practical results can be achieved in this way.

## 5.2 Recommendations

As the aim of the study to start a framework in the form of a practical methodology to further study the use of a tool to calculate ID fan capacity limitations, it was not possible to delve into minute details on many sections. One point that could supplement the study is to create/use other Rankine cycle modelling software for a comparison on the speed of the calculations. This could in turn bring the project to the point where it could sync up with an online plant data server to calculate the losses in the system in-situ.

The current state of the BMEB is generic and can easily be recreated for different power plant setups. But more could still be done if more data in specific areas could be obtained. The constants implemented give adequate accuracy to give out results; however, this can still be improved for a higher standard.

The issue of the difference in coal CV value effecting the simulation so drastically is a point that can be further investigated. One anomaly with the model not converging resulted in the erroneous point in Figure 47 (97% gen load on type 1 coal).

The lack of Plant A data resulted in a lot of assumptions between the main generation points to be made. Having a more detailed set of data to construct the model would result in a reduced use of interpolations to create the simulated data.

The draught group model can be created in greater detail to further investigate the effects of AH and boiler leakages in varying position along the draught group plant. This could further feed into a robust fault-finding system that gives an idea of the type of leaks a system engineer should look for across the draught group.

Finally, the model was geared for individual anomalies to be tested one at a time. The addition of choosing different anomalies to test their connected influence on the draught group can be done to increase the knowledge base on the ID fans capacity.

## 6. List of references

- [1] J. Roy-aikins, "Challenges in meeting the electricity needs of South Africa," in *ASME Power and Energy Conference*, 2016, pp. 1–11.
- [2] L. S. Jeffrey, "Characterization of the coal resources of South Africa," *J. South African Inst. Min. Metall.*, vol. 105, no. 2, pp. 95–102, 2005.
- [3] J. Radebe, "Integrated Resource Plan (Final Draft)," Pretoria, 2018.
- [4] A. Stodola and L. C. Loewenstein, *Steam Turbines with an appendic on gas turbines and the future of heat engines*, Revised. Рипол Классик, 1905.
- [5] D. Glorian and P. R. Spiegelberg, "Thermal Generating Plant (100 MW+) Availability and unavailability factors 1998," vol. 1998, no. September, 1998.
- [6] "ppcm IUP Strategy Statement." 2015.
- [7] P. K. Nag, *Power Plant Engineering*, Third ed. McGraw-Hill, 2008.
- [8] Undisclosed, "Power Plant A Baseline Information," 1986.
- [9] A. Godre, D. H. Kessler, D. C. McLaughlin, and J. R. Nasal, "Overcoming and predicting induced draft fan capacity limitations using a real-time induced draft-fan capacity monitor," in *EPRI Heat Rate Improvement Conference*, 2015, pp. 1–8.
- [10] H. Kim, M. G. Na, and G. Heo, "Application of monitoring, diagnosis, and prognosis in thermal performance analysis for nuclear power plants," *Nucl. Eng. Technol.*, vol. 46, no. 6, pp. 737–752, 2014.
- [11] H. Kazempour-Liacy, M. Mehdizadeh, M. Akbari-Garakani, and S. Abouali, "Corrosion and fatigue failure analysis of a forced draft fan blade," *Eng. Fail. Anal.*, vol. 18, no. 4, pp. 1193–1202, 2011.
- [12] J. H. Bulloch and A. G. Callagy, "An in situ wear-corrosion study on a series of protective coatings in large induced draft fans," *Wear*, vol. 233–235, pp. 284–292, 1999.
- [13] G. A. C. Ramos, "Mathematics modeling of the behavior in operation of induced draft fans for 350-MW Fossil Power Units to predict its optimum maintenance time," *Electr. Power Syst. Res.*, vol. 70, no. 2, pp. 109–113, 2004.
- [14] D. Anson *et al.*, "Root-cause failure analysis - FFPP Draft Fans," Electric Power Research Institute (EPRI), Palo Alto, California, USA, 1983.
- [15] A. E. Tome Jr., D. E. Leaver, and R. G. Brown, "Heat Rate Improvement Guidelines for Existing Fossil Plants," Electric Power Research Institute (EPRI), Palo Alto, California, USA, 1986.
- [16] G. Liu and M. Liu, "Development of simplified in-situ fan curve measurement method using the manufacturers fan curve," *Build. Environ.*, vol. 48, no. 1, pp. 77–83, 2012.
- [17] A. Hauschke and R. Leithner, "Dynamic Simulation of Fouling and Optimization of Sootblowing Intervals in a Hard Coal Fired Power Plant," in *5th international conference on energy environment ecosystems development and landscape architecture (EEESD'09)*, 2009, pp. 301–305.

- [18] J. Keir and I. P. Potgieter, "Basic Boiler Optimisation," Eskom Report, 1991.
- [19] F. Alobaid, N. Mertens, R. Starkloff, T. Lanz, C. Heinze, and B. Epple, "Progress in dynamic simulation of thermal power plants," *Prog. Energy Combust. Sci.*, vol. 59, no. 59, pp. 79–162, 2016.
- [20] A. Afram and F. Janabi-Sharifi, "Review of modeling methods for HVAC systems," *Appl. Therm. Eng.*, vol. 67, no. 1, pp. 507–519, 2014.
- [21] A. Eberhard, "The future of South African coal: Market, investment, and policy challenges," *Progr. Energy Sustain. Dev.*, no. January, p. 20,21,30, 2011.
- [22] R. Falcon and A. J. Ham, "Characteristics of Southern African Coals.," *J. South African Inst. Min. Metall.*, vol. 88, no. 5, pp. 145–161, 1988.
- [23] P. G. Rousseau and W. Fuls, *Power Plant Systems Analysis Course Notes MEC4116Z*. Cape Town: University of Cape Town, 2017.
- [24] R. M. S. Falcon, "Coal resources of south africa and their unique qualities," in *Independent Power Generation One-Day Conference*, 2016, no. March, p. 42.
- [25] M. S. Bhatt, "Effect of Ash in Coal on the Performance of Coal Fired Thermal Power Plants . Part I : Primary Energy Effects Effect of Ash in Coal on the Performance of Coal Fired Thermal Power Plants . Part I : Primary Energy Effects," vol. 7036, 2006.
- [26] EPRI, "Effects of Coal Quality on Power Plant Performance and Costs Volume 4 : Review of Coal Science Fundamentals," Irvine, California, 1986.
- [27] M. N. Skorupska, *Coal Specifications - Impact on Power Station Performance*. 1993.
- [28] P. Rousseau and R. Laubscher, "Analysis of the impact of coal quality on the heat transfer distribution in a high-ash pulverized coal boiler using co-simulation," in *ICCHMT Rome*, 2019.
- [29] C. Yin, L. Rosendahl, and T. J. Condra, "Further study of the gas temperature deviation in large-scale tangentially coal-fired boilers," *Fuel*, vol. 82, no. 9, pp. 1127–1137, 2003.
- [30] J. B. Kitto and S. C. Stultz, *Steam: Its generation and use*, 41st ed. Ohio: Babcock and Wilcox Company, 2005.
- [31] M. Siddhartha Bhatt, "Effect of air ingress on the energy performance of coal fired thermal power plants," *Energy Convers. Manag.*, vol. 48, no. 7, pp. 2150–2160, 2007.
- [32] T. S. Khan, Y. Dai, M. S. Alshehhi, and L. Khezzar, "Experimental flow characterization of sand particles for pneumatic transport in horizontal circular pipes," *Powder Technol.*, vol. 292, pp. 158–168, 2016.
- [33] T. Elliott, *Standard Handbook of Powerplant Engineering*. United States of America: McGraw-Hill, 1989.
- [34] T. J. Sheer, G. B. D. E. Klerk, and H. H. Jawurek, "A Versatile Computer Simulation Model for Rotary Regenerative Heat Exchangers," *Heat Transf. Eng.*, vol. 27, no. 5, pp. 68–79, 2008.
- [35] P. U. Akpan and W. F. Fuls, "Generic approach for estimating final feed water temperature and extraction pressures in pulverised coal power plants," *Appl. Therm. Eng.*, vol. 141, no. December 2017, pp. 257–268, 2018.
- [36] L. L. Dziuba and R. J. Stakenborghs, "Thermal cycle evaluation for feedwater heater out of

- service condition,” in *Proceedings of the 16th International Conference on Nuclear Engineering ICONE16*, 2008, no. 500 V, pp. 1–13.
- [37] Escom, “XXXXX - Technical Information.” Johannesburg, p. 17, 1985.
  - [38] K. S. Raj, “Performance/Condition Monitoring & Optimization for Fossil Power Plants,” in *ASME 2014 Power Conference*, 2014, p. 7.
  - [39] General Physics Corporation, “EtaPRO: VirtualPlant Editor User Guide.” New York, 2016.
  - [40] R. Spencer, K. Cotton, and C. Cannon, *A method for predicting the performance of steam turbine generators 16 500 kW and larger*. New York: American Society of Mechanical Engineers, 1974.
  - [41] Heat Exchange Institute, *HEI 9th edition (HEI 2622)*, 9th ed. 2015.
  - [42] H. Hottel and E. Cohen, “Radiant heat exchange in a gas-filled enclosure: Allowance for nonuniformity of gas temperature,” *AIChE J.*, vol. 4, no. 1, pp. 3–14, 1958.
  - [43] W. O. Monnaemang, “A zonal model for radiation heat transfer in coal-fired boiler furnaces,” MSc dissertatoin, Univeristy of Cape Town, Cape Town, 2015.
  - [44] J. S. Chandok, I. N. Kar, and S. Tuli, “Estimation of furnace exit gas temperature (FEGT) using optimized radial basis and back-propagation nueral networks,” *Energy Convers. Manag.*, vol. 49, no. 8, pp. 1989–1998, 2008.
  - [45] R. Govindsamy, “Thermal Performance Evaluation of Heat Exchangers in Pulverised Coal Boilers,” MSc Engineering, University of Witwatersrand, Johannesburg, 2014.
  - [46] *Fired Steam Generators*, ASME PTC 4. 2013.
  - [47] *Water tube boilers and auxiliary installations - Part 15: Acceptance test*, DIN EN 12952-15. 2004.
  - [48] N. E. Tootla and L. Jestin, “Investigation into methods for the calculation and measurement of pulverised coal boiler flue gas furnace exit temperature,” MSc Engineering, University of Cape Town, Cape Town, 2016.
  - [49] ASHRAE, *ASHRAE Handbook Fundamentals*. 2005.
  - [50] D. Bentz, M. Peltz, A. Durán-Herrera, P. Valdez, and C. Juárez, “Thermal properties of high-volume fly ash mortars and concretes,” *J. Build. Phys.*, vol. 34, no. 3, pp. 263–275, 2011.

# Appendix A. Mathematical derivation

## A.1 – Complete BMEB

### Auxilliary Inputs

Atmospheric Temperature:

$$T_{atm} := 19$$

Generation Load

$$T_{atm} := T_{atm} \text{ } ^\circ\text{C}$$

$$MW_{Gen} := 618.5$$

### Econimiser

#### Inlet

Temperature:

$$tEcon_{in} := 249 \text{ } ^\circ\text{C}$$

Pressure:

$$pEcon_{in} := 19.44\text{MPa}$$

Mass :

$$mEcon_{in} := 487.841 \frac{\text{kg}}{\text{s}}$$

Enthalpy:

$$hEcon_{in} := h_{steam}(pEcon_{in}, tEcon_{in}, "", "", "") = 1081.828 \cdot \frac{\text{kJ}}{\text{kg}}$$

#### Outlet

Temperature:

$$tEcon_{out} := 282 \text{ } ^\circ\text{C}$$

Pressure:

$$pEcon_{out} := 19.01\text{MPa}$$

Mass:

$$mEcon_{out} := 487.841 \frac{\text{kg}}{\text{s}}$$

Enthalpy:

$$hEcon_{out} := h_{steam}(pEcon_{out}, tEcon_{out}, "", "", "") = 1241.595 \cdot \frac{\text{kJ}}{\text{kg}}$$

### Evapourator (and Drum)

#### Inlet

Temperature:

$$tEvap_{in} := 282 \text{ } ^\circ\text{C}$$

Pressure:

$$pEvap_{in} := 19.01\text{MPa}$$

Mass:

$$mEvap_{in} := 487.841 \frac{\text{kg}}{\text{s}}$$

Enthalpy:

$$hEvap_{in} := h_{steam}(pEvap_{in}, tEvap_{in}, "", "", "") = 1241.595 \cdot \frac{\text{kJ}}{\text{kg}}$$

#### At Saturation

Temperature:

$$tEvap_{out} := 361 \text{ } ^\circ\text{C}$$

Pressure:

$$pEvap_{out} := 19.01\text{MPa}$$

Mass:

$$mEvap_{out} := 487.841 \frac{\text{kg}}{\text{s}}$$

Enthalpy:

$$hEvap_{out} := h_{steam}(pEvap_{out}, tEvap_{out}, "", "", "") = 1769.222 \cdot \frac{\text{kJ}}{\text{kg}}$$

### Superheater Primary Inlet

Temperature:

$$t_{PrimSH_{in}} := 362 \text{ }^{\circ}\text{C}$$

Pressure:

$$p_{PrimSH_{in}} := 18.98 \text{ MPa}$$

Mass:

$$m_{PrimSH_{in}} := 487.841 \frac{\text{kg}}{\text{s}}$$

Enthalpy:

$$h_{PrimSH_{in}} := h_{\text{steam}}(p_{PrimSH_{in}}, t_{PrimSH_{in}}, \text{""}, \text{""}, \text{""}) = 2483.85 \cdot \frac{\text{kJ}}{\text{kg}}$$

### Primary Outlet

Temperature:

$$t_{PrimSH_{out}} := 399 \text{ }^{\circ}\text{C}$$

Pressure:

$$p_{PrimSH_{out}} := 18.41 \text{ MPa}$$

Mass:

$$m_{PrimSH_{out}} := 487.841 \frac{\text{kg}}{\text{s}}$$

Enthalpy:

$$h_{PrimSH_{out}} := h_{\text{steam}}(p_{PrimSH_{out}}, t_{PrimSH_{out}}, \text{""}, \text{""}, \text{""}) = 2867.33 \cdot \frac{\text{kJ}}{\text{kg}}$$

### Platensuperheater Inlet

Temperature:

$$t_{PlatSH_{in}} := 386 \text{ }^{\circ}\text{C}$$

Pressure:

$$p_{PlatSH_{in}} := 18.41 \text{ MPa}$$

Mass:

$$m_{PlatSH_{in}} := 504.667 \frac{\text{kg}}{\text{s}}$$

Enthalpy:

$$h_{PlatSH_{in}} := h_{\text{steam}}(p_{PlatSH_{in}}, t_{PlatSH_{in}}, \text{""}, \text{""}, \text{""}) = 2788.43 \cdot \frac{\text{kJ}}{\text{kg}}$$

### Platensuperheater Outlet

Temperature:

$$t_{PlatSH_{out}} := 480 \text{ }^{\circ}\text{C}$$

Pressure:

$$p_{PlatSH_{out}} := 17.88 \text{ MPa}$$

Mass:

$$m_{PlatSH_{out}} := 504.667 \frac{\text{kg}}{\text{s}}$$

Enthalpy:

$$h_{PlatSH_{out}} := h_{\text{steam}}(p_{PlatSH_{out}}, t_{PlatSH_{out}}, \text{""}, \text{""}, \text{""}) = 3207.58 \cdot \frac{\text{kJ}}{\text{kg}}$$

### Final Inlet

Temperature:

$$t_{FSH_{in}} := 473 \text{ }^{\circ}\text{C}$$

Pressure:

$$p_{FSH_{in}} := 17.88 \text{ MPa}$$

Mass:

$$m_{FSH_{in}} := 509.763 \frac{\text{kg}}{\text{s}}$$

Enthalpy:

$$h_{FSH_{in}} := h_{\text{steam}}(p_{FSH_{in}}, t_{FSH_{in}}, \text{""}, \text{""}, \text{""}) = 3184.38 \cdot \frac{\text{kJ}}{\text{kg}}$$



**Final Outlet**

Temperature:

$$t_{FSH_{out}} := 540 \text{ }^{\circ}\text{C}$$

Pressure:

$$p_{FSH_{out}} := 17.35 \text{ MPa}$$

Mass:

$$m_{FSH_{out}} := 509.763 \frac{\text{kg}}{\text{s}}$$

Enthalpy:

$$h_{FSH_{out}} := h_{\text{steam}}(p_{FSH_{out}}, t_{FSH_{out}}, \text{""}, \text{""}, \text{""}) = 3396.93 \frac{\text{kJ}}{\text{kg}}$$

**First Attenuator Spray**

Mass:

$$m_{PlatSpray} := 16.826 \frac{\text{kg}}{\text{s}}$$

Enthalpy:

$$h_{PlatSpray} := \frac{m_{PlatSH_{in}} \cdot h_{PlatSH_{in}} - m_{PrimSH_{out}} \cdot h_{PrimSH_{out}}}{m_{PlatSpray}} = 500.794 \frac{\text{kJ}}{\text{kg}}$$

**Second Attenuator Spray**

Mass:

$$m_{FinalSpray} := 5.096 \frac{\text{kg}}{\text{s}}$$

Enthalpy:

$$h_{FinalSpray} := \frac{m_{FSH_{in}} \cdot h_{FSH_{in}} - m_{PlatSH_{out}} \cdot h_{PlatSH_{out}}}{m_{FinalSpray}} = 887.119 \frac{\text{kJ}}{\text{kg}}$$

**Reheater****First Heater Input**

Temperature:

$$t_{RH1_{in}} := 329 \text{ }^{\circ}\text{C}$$

Pressure:

$$p_{RH1_{in}} := 4.178 \text{ MPa}$$

Mass:

$$m_{RH1_{in}} := 467.995 \frac{\text{kg}}{\text{s}}$$

Enthalpy:

$$h_{RH1_{in}} := h_{\text{steam}}(p_{RH1_{in}}, t_{RH1_{in}}, \text{""}, \text{""}, \text{""}) = 3035.06 \frac{\text{kJ}}{\text{kg}}$$

**First Heater Output**

Temperature:

$$t_{RH1_{out}} := 405 \text{ }^{\circ}\text{C}$$

Pressure:

$$p_{RH1_{out}} := 4.127 \text{ MPa}$$

Mass:

$$m_{RH1_{out}} := 467.995 \frac{\text{kg}}{\text{s}}$$

Enthalpy:

$$h_{RH1_{out}} := h_{\text{steam}}(p_{RH1_{out}}, t_{RH1_{out}}, \text{""}, \text{""}, \text{""}) = 3224.01 \frac{\text{kJ}}{\text{kg}}$$

## Second Heater Input

Temperature:

$$t_{RH2_{in}} := 381 \text{ }^{\circ}\text{C}$$

Pressure:

$$p_{RH2_{in}} := 4.127 \text{ MPa}$$

Mass:

$$m_{RH2_{in}} := 478.685 \frac{\text{kg}}{\text{s}}$$

Enthalpy:

$$h_{RH2_{in}} := h_{\text{steam}}(p_{RH2_{in}}, t_{RH2_{in}}, \text{""}, \text{""}, \text{""}) = 3166.65 \frac{\text{kJ}}{\text{kg}}$$

## Second Heater Output

Temperature:

$$t_{RH2_{out}} := 540 \text{ }^{\circ}\text{C}$$

Pressure:

$$p_{RH2_{out}} := 3.986 \text{ MPa}$$

Mass:

$$m_{RH2_{out}} := 478.685 \frac{\text{kg}}{\text{s}}$$

Enthalpy:

$$h_{RH2_{out}} := h_{\text{steam}}(p_{RH2_{out}}, t_{RH2_{out}}, \text{""}, \text{""}, \text{""}) = 3537.48 \frac{\text{kJ}}{\text{kg}}$$

---

## Third Attenuator Spray

Mass:

$$m_{RHS} := 10.69 \frac{\text{kg}}{\text{s}}$$

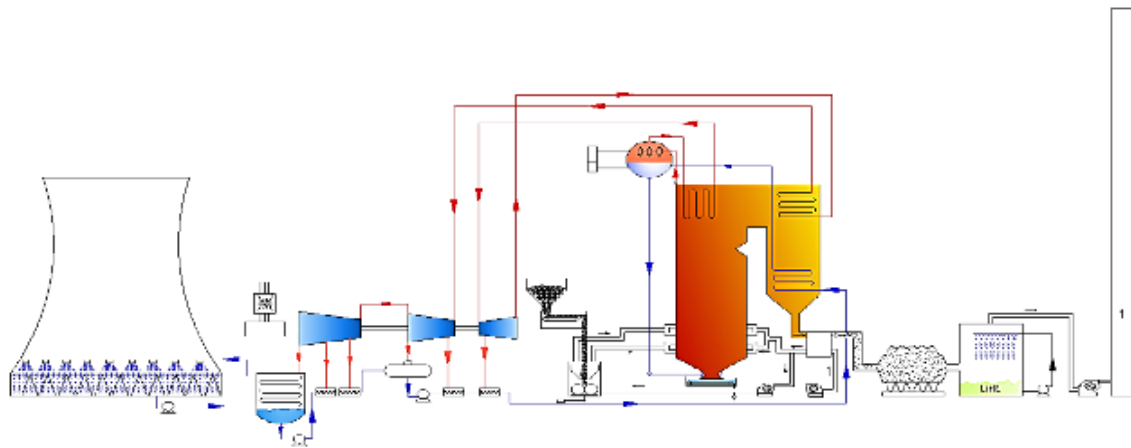
Enthalpy:

$$h_{RHS} := \frac{m_{RH2_{in}} \cdot h_{RH2_{in}} - m_{RH1_{out}} \cdot h_{RH1_{out}}}{m_{RHS}} = 655.671 \frac{\text{kJ}}{\text{kg}}$$

Steam Inputs (C-sched)

Boundary

## Boundary



**Metrological Inputs**

Atmospheric Pressure:

$$P_{atm} := 83.5 \text{ kPa} \quad (\text{Approximation from Vaal altitude})$$

Metrological reports state the Relative Humidity of air.

Relative Humidity of air (m/m):

$$RH := 10\%$$

**Air Concentration** ([http://www.engineeringtoolbox.com/air-composition-d\\_212.html](http://www.engineeringtoolbox.com/air-composition-d_212.html))

|            |                         |                        |                          |
|------------|-------------------------|------------------------|--------------------------|
| %Nitrogen: | $\%N_{2,ww} := 78.12\%$ | $\%N_{2,mm} := 75.5\%$ | $\%N_{2,mb} := 78.119\%$ |
| %Oxygen:   | $\%O_{2,ww} := 20.96\%$ | $\%O_{2,mm} := 23.2\%$ | $\%O_{2,mb} := 20.947\%$ |
| %Argon:    | $\%Ar_{ww} := 0.92\%$   | $\%Ar_{mm} := 1.28\%$  | $\%Ar_{mb} := 0.934\%$   |

**Molar Masses**

$$\text{Molar Mass of Carbon:} \quad M_C := 12.01 \frac{\text{gm}}{\text{mol}}$$

$$\text{Molar Mass of Hydrogen:} \quad M_H := 1.00795 \frac{\text{gm}}{\text{mol}}$$

$$\text{Molar Mass of Oxygen:} \quad M_O := 15.9995 \frac{\text{gm}}{\text{mol}}$$

$$\text{Molar Mass of Nitrogen:} \quad M_N := 14.0065 \frac{\text{gm}}{\text{mol}}$$

$$\text{Molar Mass of Sulphur:} \quad M_S := 32.07 \frac{\text{gm}}{\text{mol}}$$

**Molar masses of Flue Gas constituents**Air

$$\text{Molar mass of } O_2: \quad M_{O2} := 2 \cdot M_O = 31.999 \frac{\text{gm}}{\text{mol}}$$

$$\text{Molar mass of } N_2: \quad M_{N2} := 2 \cdot M_N = 28.013 \frac{\text{gm}}{\text{mol}}$$

$$\text{Molar mass of Ar:} \quad M_{Ar} := 39.95 \frac{\text{gm}}{\text{mol}}$$

Molar mass of Air:

$$M_{dry,air} := \%N_{2,mb} \cdot M_{N2} + \%O_{2,mb} \cdot M_{O2} + \%Ar_{mb} \cdot M_{Ar} = 28.959 \frac{\text{gm}}{\text{mol}}$$

Combustion

$$\text{Molar mass of CO}_2: M_{CO2} := M_C + 2 \cdot M_O = 44.009 \cdot \frac{\text{kg}}{\text{kmol}}$$

$$\text{Molar mass of NO: } M_{NO} := M_N + M_O = 30.006 \cdot \frac{\text{kg}}{\text{kmol}}$$

$$\text{Molar Mass of SO}_2: M_{SO2} := M_S + 2 \cdot M_O = 64.069 \cdot \frac{\text{kg}}{\text{kmol}}$$

$$\text{Molar mass of Water: } M_{H2O} := 2 \cdot M_H + M_O = 18.015 \cdot \frac{\text{kg}}{\text{kmol}}$$

**Other Constants**

$$\text{Enthalpy of Water Vaporization: } h_{H2O.vap} := 2441.7 \frac{\text{kJ}}{\text{kg}}$$

$$\text{Oxygen Flue Gas Density Ratio: } \rho_{ratio} := \frac{M_{O2}}{30.262 \cdot \frac{\text{gm}}{\text{mol}}} = 1.0573987$$

**Humidity of Air**

Specific humidity is needed for the rest of the calculations. conversion is below

$$\text{Ideal Gas Constant of Dry air: } R_d := 287.05 \frac{\text{J}}{\text{kg} \cdot \text{K}}$$

Vapour Pressure of water:

$$\text{Polynomial coefficients } a := (6.108 \quad 0.444 \quad 0.014 \quad 2.65 \times 10^{-4} \quad 3.03 \times 10^{-6} \quad 2.03 \times 10^{-8} \quad 6.14 \times 10^{-11})^T$$

$$e_{vap}(T) := [a_0 + T/^{\circ}\text{C} \cdot [a_1 + T/^{\circ}\text{C} \cdot [a_2 + T/^{\circ}\text{C} \cdot [a_3 + T/^{\circ}\text{C} \cdot [a_4 + T/^{\circ}\text{C} \cdot (a_5 + T/^{\circ}\text{C} \cdot a_6)]]]] \cdot 100 \cdot \text{Pa}$$

$$\text{Partial pressure of water: } P_{H2O} := RH \cdot e_{vap}(T_{atm}) = 0.219 \cdot \text{kPa}$$

$$\text{Comparison to textbook calc: } P_{H2O.therm} := RH \cdot psat\_T(T_{atm}) = 0.22 \cdot \text{kPa}$$

$$\text{Volume mixing ratio of water: } x_{H2O} := \frac{P_{H2O}}{P_{atm}} = 0.262\%$$

Specific Humidity

$$\omega := \frac{x_{H2O} \cdot M_{H2O}}{x_{H2O} \cdot M_{H2O} + (1 - x_{H2O}) \cdot M_{dry.air}} = 0.16305\%$$

Humid air density equation from ([http://wahiduddin.net/calc/density\\_altitude.htm](http://wahiduddin.net/calc/density_altitude.htm))

$$\text{Humid Air Density: } \rho_{air}(T) := \frac{P_{atm}}{R_d \cdot T} \cdot \left( 1 - \frac{0.378 \cdot P_{H2O}}{P_{atm}} \right)$$

**Air/Flue Gas Inputs**

Boiler house temperature (air suction and air ingress temperature)  
(Approx. temperature inside boiler house from P&T TAF Report)

Ambient Air Temperature:

$$T_{amb} := 44 \text{ }^{\circ}\text{C}$$

Oxygen Concentration at Furnace Entrance (v/v):

$$\%O_{2.Furn.inlet} := 2.85\%$$

Oxygen Concentration at A/H inlet (v/v):

$$\%O_{2.A/H.fg.inlet} := 3.16\%$$

Oxygen Concentration at A/H outlet (v/v):

$$\%O_{2.A/H.fg.outlet} := 4.08\%$$

Disclaimer: For simply use for now the temperatures are connected to the C-schedule values and a linear interpolation between the values is taken for a rough estimate. True Temperatures are found at (618.5, 599.945 and 424.291 MW)

Temperature profiles:

$$TT_{fgi} := \begin{pmatrix} \text{FG @ A/H inlet} \\ 424.291 & 305 \\ 599.945 & 331 \\ 618.5 & 334 \end{pmatrix} \quad TT_{fgo} := \begin{pmatrix} \text{FG @ A/H outlet} \\ 424.291 & 113 \\ 599.945 & 126 \\ 618.5 & 127 \end{pmatrix} \quad TT_a := \begin{pmatrix} \text{Air @ A/H outlet} \\ 424.291 & 268 \\ 599.945 & 286 \\ 618.5 & 288 \end{pmatrix}$$

$$Tfgahi(MW\_gen) := \begin{cases} \text{interp}(TT_{fgi}^{(0)}, TT_{fgi}^{(1)}, MW\_gen) & \text{if } 424.291 \leq MW\_gen \leq 618.5 \\ (305) & \text{if } MW\_gen < 424.291 \\ (334) & \text{otherwise} \end{cases}$$

$$Tfgaho(MW\_gen) := \begin{cases} \text{interp}(TT_{fgo}^{(0)}, TT_{fgo}^{(1)}, MW\_gen) & \text{if } 424.291 \leq MW\_gen \leq 618.5 \\ (TT_{fgo_{0,1}}) & \text{if } MW\_gen < 424.291 \\ (TT_{fgo_{2,1}}) & \text{otherwise} \end{cases}$$

$$Taah(MW\_gen) := \begin{cases} \text{interp}(TT_a^{(0)}, TT_a^{(1)}, MW\_gen) & \text{if } 424.291 \leq MW\_gen \leq 618.5 \\ (TT_{a_{0,1}}) & \text{if } MW\_gen < 424.291 \\ (TT_{a_{2,1}}) & \text{otherwise} \end{cases}$$

(Boiler Exit Temperature)

FG Temp at A/H inlet:

$$T_{fg.A/H.inlet} := Tfgahi(MW\_Gen) \text{ }^{\circ}\text{C} = 334 \text{ }^{\circ}\text{C}$$

FG Temp at A/H outlet:

$$T_{fg.A/H.outlet} := Tfgaho(MW\_Gen) \text{ }^{\circ}\text{C} = 127 \text{ }^{\circ}\text{C}$$

Air Temp at A/H outlet:

$$T_{air.A/H.outlet} := Taah(MW\_Gen) \text{ }^{\circ}\text{C} = 288 \text{ }^{\circ}\text{C}$$

**Ash Analysis**

|   |   |
|---|---|
| Concentration of Carbon in Fly Ash (m/m):   | $\%C_{fa} := 1\%$   |
| Concentration of Carbon in Bottom Ash (m/m) | $\%C_{ba} := 1\%$   |
| Fraction of Fly Ash:                        | $\%FA := 90\%$  |
| Fraction of Bottom Ash:                     | $\%BA := 10\%$  |
| Bottom Ash Exit Temperature:                | $T_{BA.exit} := 800\text{ }^{\circ}\text{C}$  |
| Enthalpy of Ash:                            | $h_{ash}(T) := 0.73 \cdot (T - 0\text{ }^{\circ}\text{C}) \cdot \frac{\text{kJ}}{\text{kg} \cdot \text{K}}$ |

**Energy Losses**

|                                |                           |
|--------------------------------|---------------------------|
| Boiler Insulation Heat Losses: | $Q_{insul.loss} := 0.8\%$ |
|--------------------------------|---------------------------|

**Credits**

Energy added to the fluid stream inside the control volume must be accounted for. Some of these energy sources can be considered as credits. The energy contribution from these components are quantified below using values from the Operating Technical Specification Boiler Plant Document (Assume: (i) Power factor = 1, (ii) Electrical efficiency = 95%):

**Mills**

Using the rated power of the mills the total power added to the fluid stream in the mills is as follows:

|                       |  |
|-----------------------|--|
| Mills active at load: | $No_{Mills.FL} := 5$   |
| Mill motor rating:    | $P_{Mill.Motor} := 1550\text{ kW}$   |
| Motor Efficiency:     | $\eta_{Mill.Motor} := 96.45\%$   |
| Mill Power:           | $P_{mills} := \eta_{Mill.Motor} \cdot No_{Mills.FL} \cdot P_{Mill.Motor} = 7474.9\text{ kW}$ |

**Seal air fans (SA fans)**

|                                |  |
|--------------------------------|--|
| Fans Active at load:           | $No_{SA.fans.FL} := 2$   |
| Fan motor rating:              | $P_{SA.fan.Motor} := 75\text{ kW}$   |
| Fan motor efficiency           | $\eta_{SA.fan.Motor} := 79.9\%$  |
| Fan Power:                     | $P_{SA.fans} := \eta_{SA.fan.Motor} \cdot No_{SA.fans.FL} \cdot P_{SA.fan.Motor} = 119.85\text{ kW}$ |
| Volumetric flowrate (One fan): | $V'_{seal.air.one} := 2.65 \frac{\text{m}^3}{\text{s}}$  |
| Total volumetric flowrate:     | $V'_{seal.air} := V'_{seal.air.one} \cdot No_{SA.fans.FL} = 5.3 \frac{\text{m}^3}{\text{s}}$         |
| Mass flowrate:                 | $\dot{m}_{seal.air} := \rho_{air}(T_{amb}) \cdot V'_{seal.air} = 4.856 \frac{\text{kg}}{\text{s}}$   |

**Other Unlisted Auxiliaries**

This is just to account for any other small auxiliary devices that may fall within the boundary that need be accounted for when increasing the MEB's complexity

$$P_{other} := 0\text{ kW}$$

**Primary air fans (PA fans)**

|                      |  |
|----------------------|--|
| Fans Active at load: | $No_{PA.fans.FL} := 2$   |
| Fan motor rating:    | $P_{PA.fan.Motor} := 1850\text{ kW}$   |
| Fan motor efficiency | $\eta_{PA.fan.Motor} := 75.4\%$  |
| Fan Power:           | $P_{PA.fans} := \eta_{PA.fan.Motor} \cdot No_{PA.fans.FL} \cdot P_{PA.fan.Motor} = 2789.8\text{ kW}$ |

**Forced Draft fans (FD fans)**

|                       |  |
|-----------------------|--|
| Fans Active at Load:  | $No_{FD.fans.FL} := 2$   |
| Fan motor rating:     | $P_{FD.fan.Motor} := 2386\text{ kW}$   |
| Fan motor efficiency: | $\eta_{FD.fan.Motor} := 65.8\%$  |
| Fan Power:            | $P_{FD.fans} := \eta_{FD.fan.Motor} \cdot No_{FD.fans.FL} \cdot P_{FD.fan.Motor} = 3139.976\text{ kW}$ |

**Coal Properties**

CV of Coal as Recieved from the Lab:

$$CV_{measured} := 16410 \frac{kJ}{kg}$$

NOx fraction during combustion:

$$f_{NOx} := 70\%$$

| Element  | Mass Fraction          | Calorific Value                   | Stoichiometric Coefficient          |
|----------|------------------------|-----------------------------------|-------------------------------------|
| Carbon   | $mf_C := 43.94\%$      | $CV_C := 32778.15 \frac{kJ}{kg}$  | $St_C := 1$                         |
| Hydrogen | $mf_H := 2.5\%$        | $CV_H := 119931.72 \frac{kJ}{kg}$ | $St_H := \frac{1}{4}$               |
| Oxygen   | $mf_O := 9.61\%$       | $CV_O := 0 \frac{kJ}{kg}$         | $St_O := -\frac{1}{2}$              |
| Nitrogen | $mf_N := 1.11\%$       | $CV_N := 0 \frac{kJ}{kg}$         | $St_N := f_{NOx} \cdot \frac{1}{2}$ |
| Sulphur  | $mf_S := 1\%$          | $CV_S := 9257.524 \frac{kJ}{kg}$  | $St_S := 1.0$                       |
| Water    | $mf_{H_2O} := 10.51\%$ | $CV_{H_2O} := 0 \frac{kJ}{kg}$    | $St_{H_2O} := 0$                    |
| Ash      | $mf_{ash} := 31.33\%$  | $CV_{ash} := 0 \frac{kJ}{kg}$     | $St_{ash} := 0$                     |

Confirming mass fractions  $mf_C + mf_O + mf_H + mf_N + mf_S + mf_{H_2O} + mf_{ash} = 1$

Net Calorific Value of the Coal (LHV):

$$CV_{Coal} := mf_C \cdot CV_C + mf_O \cdot CV_O + mf_H \cdot CV_H + mf_N \cdot CV_N + mf_S \cdot CV_S + mf_{H_2O} \cdot CV_{H_2O} + mf_{ash} \cdot CV_{ash} = 17493.59 \frac{kJ}{kg}$$

Net CV (HHV):

$$CV_{Coal.HHV} := CV_{Coal} + mf_{H_2O} \cdot h_{H_2O.vap} = 17750.21 \frac{kJ}{kg}$$

Difference in Measured and calculated CV values:  $CV_{diff} := CV_{measured} - CV_{Coal.HHV} = -1.34 \frac{MJ}{kg}$

**Elements**

Heat capacities

$$c_{UC} := 0.710 \cdot \frac{kJ}{kg \cdot K}$$

$$c_{FA} := 0.730 \cdot \frac{kJ}{kg \cdot K}$$

$$c_{coal} := 1.380 \cdot \frac{kJ}{kg \cdot K}$$

Constants

$$T_{ref} := 0.01 \text{ } ^\circ\text{C}$$

$$Constants_h := \begin{pmatrix} 9.816 \cdot 10^{-1} & 8.974 \cdot 10^{-1} & 1.015 & 5.205 \cdot 10^{-1} & 8.437 \cdot 10^{-1} & 8.861 \cdot 10^{-1} & 6.426 \cdot 10^{-1} \\ 1.245 \cdot 10^{-4} & 1.994 \cdot 10^{-4} & 1.037 \cdot 10^{-4} & 0 & 4.258 \cdot 10^{-4} & 3.263 \cdot 10^{-4} & 1.850 \cdot 10^{-4} \\ -1.308 \cdot 10^{-12} & -7.432 \cdot 10^{-8} & 5.452 \cdot 10^{-9} & 0 & -1.705 \cdot 10^{-7} & 0 & 0 \\ -2.154 \cdot 10^{-12} & 1.255 \cdot 10^{-11} & -6.693 \cdot 10^{-12} & 0 & 2.819 \cdot 10^{-11} & 0 & 0 \end{pmatrix}$$

$$\begin{pmatrix} Air \\ O_2 \\ N_2 \\ Argon \\ CO_2 \\ NO \\ SO_2 \end{pmatrix} := \begin{pmatrix} 0 \\ 1 \\ 2 \\ 3 \\ 4 \\ 5 \\ 6 \end{pmatrix}$$

$$h(C, Element, T) := \sum_{i=0}^3 \left[ (C_{i, Element}) \cdot \left( \frac{T - T_{ref}}{K} \right)^{(i+1)} \right] \cdot \frac{kJ}{kg}$$

Water Enthalpy

$$h_{water}(T) := \left[ 2501 + 1.86 \cdot \frac{(T - 0 \text{ } ^\circ\text{C})}{K} \right] \cdot \frac{kJ}{kg}$$

UBC enthalpy

$$h_{UBC}(T) := c_{UC} \cdot (T - T_{ref})$$

FA enthalpy

$$h_{FlyAsh}(T) := c_{FA} \cdot (T - T_{ref})$$

Enthalpy of Coal

$$h_{coal}(T) := c_{coal} \cdot (T - T_{ref})$$

Moist Air Enthalpy:

$$h_{ASHRAE}(T, \omega) := \left[ 1.006 \cdot \left( \frac{T - 0 \text{ } ^\circ\text{C}}{K} \right) + \omega \cdot \left[ 2501 + 1.86 \cdot \left( \frac{T - 0 \text{ } ^\circ\text{C}}{K} \right) \right] \right] \cdot \frac{kJ}{kg}$$

$$h_{moist, air}(T, \omega) := h_{ASHRAE}(T, \omega)$$

Air Enthalpy:

$$h_{air}(T) := h(Constants_h, Air, T)$$

Oxygen (O<sub>2</sub>) Enthalpy:

$$h_{O_2}(T) := h(Constants_h, O_2, T)$$

Nitrogen (N<sub>2</sub>) Enthalpy:

$$h_{N_2}(T) := h(Constants_h, N_2, T)$$

Argon (Ar) Enthalpy:

$$h_{Ar}(T) := h(Constants_h, Argon, T)$$

Carbon Dioxide (CO<sub>2</sub>) Enthalpy:

$$h_{CO_2}(T) := h(Constants_h, CO_2, T)$$

Nitrogen Monoxide (NO) Enthalpy:

$$h_{NO}(T) := h(Constants_h, NO, T)$$

Sulphur Dioxide (SO<sub>2</sub>) Enthalpy:

$$h_{SO_2}(T) := h(Constants_h, SO_2, T)$$



## Boiler Mass Balance

### Unburnt Carbon

Mass of UBCarbon per kg of Coal:  $C' := mf_{ash} \cdot [(\%C_{fa} \cdot \%FA) + (\%C_{ba} \cdot \%BA)] = 0.313 \cdot \%$

Mass of UBCarbon per kg of Cabon:  $C'' := \frac{C'}{mf_C} = 0.713 \cdot \%$

Energy loss of UBCarbon per kJ of Energy input:  $C''' := \frac{CV_C \cdot C'}{CV_{measured}} = 0.626 \cdot \%$

### Air Ratios

Theoretical Air/Fuel Ratio:

$$TAR := \frac{M_{dry,air}}{\%O_{2,mb}} \cdot \left[ St_C \cdot \frac{(mf_C - C')}{M_C} + St_O \cdot \frac{mf_O}{M_O} + St_H \cdot \frac{mf_H}{M_H} + St_N \cdot \frac{mf_N}{M_N} + St_S \cdot \frac{mf_S}{M_S} \right] = 5.54552$$

Air ingress into the boiler, tramp air, needs to be accounted for in the flue gas calculation. This is to account for the additional energy loss due to it being lost to the heating up of the additional air. The total "Excess Air" is thus calculated using the oxygen concentration at the air heater flue gas inlet and atmospheric oxygen concentration values.

Calculation of excess air:  $EA_{AH,fg.inlet} := \frac{\%O_{2,A/H,fg.inlet}}{\frac{\%O_{2,vv}}{p_{ratio}} - \%O_{2,A/H,fg.inlet}} = 18.965 \cdot \%$

Overwrite feature to eliminate miss calculations due to the above formula. Purely for testing reasons

Excess air overwrite:  $EA_{AH,fg.inlet} := 17.36\%$

Air Ingress:  $\%Air_{ing} := EA_{AH,fg.inlet} \cdot \frac{\%O_{2,Furn.inlet}}{\frac{\%O_{2,vv}}{p_{ratio}} - \%O_{2,Furn.inlet}} = 2.173 \cdot \%$

Dry Air Required at Furnace:  $DAR := TAR \cdot (1 + EA_{AH,fg.inlet}) = 6.597$

Humid Air Ratio:  $HAR := (1 + \omega) \cdot DAR = 6.608$

A "New" carbon mass fraction is calculated to account for the amount of carbon that is not burnt during combustion

New Carbon Mass Fraction:  $mf_{C'} := mf_C - C' = 43.627 \cdot \%$

**Mole Fractions**

Mole fractions of each major coal element relative to 1 mole of carbon

$$\text{Moles of Carbon:} \quad n_C := \frac{mf_{C'} \cdot M_C}{M_C \cdot mf_{C'}} = 1$$

$$\text{Moles of Hydrogen} \quad n_H := \frac{mf_H \cdot M_C}{M_H \cdot mf_{C'}} = 0.683$$

$$\text{Moles of Oxygen:} \quad n_O := \frac{mf_O \cdot M_C}{M_O \cdot mf_{C'}} = 0.165$$

$$\text{Moles of Nitrogen:} \quad n_N := \frac{mf_N \cdot M_C}{M_N \cdot mf_{C'}} = 0.022$$

$$\text{Moles of Sulphur:} \quad n_S := \frac{mf_S \cdot M_C}{M_S \cdot mf_{C'}} = 0.009$$

**Flue gas constituents per kg Coal ( $FR_{const}$ )**

The following section calculates the mass flow of each constituent in the flue gas per kg of coal combusted

$$\text{Mass Flow Rate of CO}_2 \text{ per kg Coal:} \quad FR_{CO2} := n_C \cdot \frac{M_{CO2}}{M_C} \cdot mf_{C'} = 1.599$$

$$\text{Mass Flow Rate of H}_2\text{O per kg Coal:} \quad FR_{H2O} := \frac{1}{2} \cdot n_H \cdot \frac{M_{H2O}}{M_C} \cdot mf_{C'} + DAR \cdot \omega + mf_{H2O} = 0.339$$

$$\text{Mass Flow Rate of O}_2 \text{ per kg Coal:} \quad FR_{O2} := EA_{AH,fg,inlet} \cdot TAR \cdot \%O2_{mb} \cdot \frac{M_{O2}}{M_{dry,air}} = 0.243$$

$$\text{Mass Flow Rate of N}_2 \text{ per kg Coal:} \quad FR_{N2} := \frac{1}{2} \cdot (1 - f_{NOx}) \cdot n_N \cdot \frac{M_{N2}}{M_C} \cdot mf_{C'} + DAR \cdot \%N2_{mb} \cdot \frac{M_{N2}}{M_{dry,air}} = 4.989$$

$$\text{Mass Flow Rate of NO per kg Coal:} \quad FR_{NO} := f_{NOx} \cdot n_N \cdot \frac{M_{NO}}{M_C} \cdot mf_{C'} = 0.017$$

$$\text{Mass Flow Rate of SO}_2 \text{ per kg Coal:} \quad FR_{SO2} := n_S \cdot \frac{M_{SO2}}{M_C} \cdot mf_{C'} = 0.02$$

$$\text{Mass Flow Rate of Argon per kg Coal:} \quad FR_{Ar} := DAR \cdot \%Ar_{mb} \cdot \frac{M_{Ar}}{M_{dry,air}} = 0.085$$

$$\text{Mass Flow Rate of Fly Ash per kg Coal:} \quad FR_{FA} := mf_{ash} \cdot \%FA \cdot (1 - \%C_{fa}) = 0.279$$

$$\text{Mass Flow Rate of Unburnt Carbon in Coal:} \quad FR_{UBC} := mf_{ash} \cdot (\%C_{fa} \cdot \%FA) = 0.003$$

$$\text{Mass Flow Rate of Flue Gas per kg Coal:} \quad FGR := FR_{CO2} + FR_{H2O} + FR_{O2} + FR_{N2} + FR_{NO} \dots = 7.574 \\ + FR_{SO2} + FR_{Ar} + FR_{FA} + FR_{UBC}$$

---

**Flue gas constituents per kg Flue Gas ( $mf_{const,fg}$ )**

Mass fraction of CO<sub>2</sub>:  $mf_{CO_2,fg} := \frac{FR_{CO_2}}{FGR} = 21.108\%$

Mass fraction of H<sub>2</sub>O:  $mf_{H_2O,fg} := \frac{FR_{H_2O}}{FGR} = 4.48\%$

Mass fraction of O<sub>2</sub>:  $mf_{O_2,fg} := \frac{FR_{O_2}}{FGR} = 3.214\%$

Conversion of oxygen mass fraction to compare to plant measurement devices

Volume Fraction of O<sub>2</sub>:  $v_{O_2,fg} := \frac{mf_{O_2,fg}}{\rho_{ratio}} = 3.04\%$

Mass fraction of N<sub>2</sub>:  $mf_{N_2,fg} := \frac{FR_{N_2}}{FGR} = 65.869\%$

Mass fraction of NO:  $mf_{NO,fg} := \frac{FR_{NO}}{FGR} = 0.22\%$

Mass fraction of SO<sub>2</sub>:  $mf_{SO_2,fg} := \frac{FR_{SO_2}}{FGR} = 0.264\%$

Mass fraction of Argon:  $mf_{Ar,fg} := \frac{FR_{Ar}}{FGR} = 1.122\%$

Mass fraction of Fly Ash:  $mf_{FA,fg} := \frac{FR_{FA}}{FGR} = 3.686\%$

Mass fraction of UBC:  $mf_{UBC,fg} := \frac{FR_{UBC}}{FGR} = 0.037\%$

**Flue Gas**

$$M_{FG} := mf_{O_2,fg} \cdot M_{O_2} + mf_{CO_2,fg} \cdot M_{CO_2} + mf_{N_2,fg} \cdot M_{N_2} + mf_{Ar,fg} \cdot M_{Ar} + mf_{SO_2,fg} \cdot M_{SO_2} + mf_{H_2O,fg} \cdot M_{H_2O} + mf_{NO,fg} \cdot M_{NO} + mf_{UBC,fg} \cdot M_C = 30.265 \cdot \frac{kg}{kmol}$$

Enthalpy of Flue gas using NIST Data

$$h_{fg}(T) := mf_{O_2,fg} \cdot h(Constants_h, O_2, T) + mf_{CO_2,fg} \cdot h(Constants_h, CO_2, T) + mf_{N_2,fg} \cdot h(Constants_h, N_2, T) + mf_{SO_2,fg} \cdot h(Constants_h, SO_2, T) + mf_{H_2O,fg} \cdot h_{water}(T) + mf_{UBC,fg} \cdot h_{UBC}(T) + mf_{FA,fg} \cdot h_{FlyAsh}(T) + h(Constants_h, NO, T) \cdot mf_{NO,fg} + mf_{Ar,fg} \cdot h(Constants_h, Argon, T)$$

## Global Boiler Energy Balance

The net energy recovered by the steam can be accounted for by considering the enthalpies and flowrates of water/steam entering and leaving the control volume:

Net Energy recieved by Steam:

$$Steam_{out} := mFSH_{out} \cdot hFSH_{out} + mRH2_{out} \cdot hRH2_{out}$$

$$Steam_{in} := mRH1_{in} \cdot hRH1_{in} + mEcon_{in} \cdot hEcon_{in} \dots \\ + mRHS \cdot hRHS + mPlatSpray \cdot hPlatSpray + mFinalSpray \cdot hFinalSpray$$

$$\Delta Q_{steam} := Steam_{out} - Steam_{in} = 1456.86 \cdot MW$$

Energy from Credits:

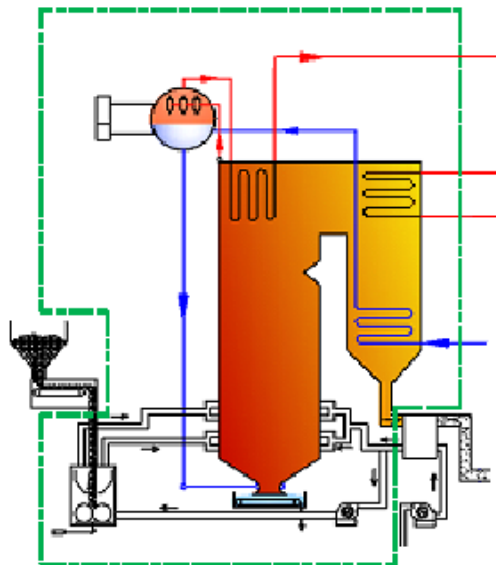
$$Q'_{credits} := P_{mills} + P_{SA.fans} + P_{other} = 7594.725 \cdot kW$$

### Mass flowrate of coal:

Coal mass flowrate is determined by an energy balance over the boiler boundary.

Inputs consist of the energy of the CV of coal, the enthalpy of coal, the energy of the air going to the boiler, energy of water entering the boiler, and the energy of other credits.

The outputs consist of the energy recovered by steam, flue gas losses, radiant losses, unburnt carbon losses, the energy lost in sensible heat in fly ash and bottom ash, and the energy lost due to evaporation of fuel



The Inputs and outputs:

| Inputs  | Outputs  |
|---|--|
| $m_{coal} \cdot CV + m_{coal} \cdot h_{coal}$               | $Q_{steam.out}$  |
| $\dot{m}_{air.A/H.outlet} \cdot h_{moist.air}(AH_{airOut})$ | $\dot{m}_{fg.A/H.inlet} \cdot h_{fg}(AH_{fg.in})$              |
| $m_{seal.air} \cdot h_{moist.air}(T_{amb})$                 | $m_{coal} \cdot m_{fash} \cdot \%BA \cdot h_{BA}(T_{BA.exit})$ |
| $Q_{credits}$   | $m_{coal} \cdot CV_{LHV} \cdot \%Q_{Loss}$                     |
| $Q_{steam.in}$  |  |
| $m_{air.ing} \cdot h_{moist.air}(T_{amb})$                  |  |

Unburnt carbon is incorporate into the formation of Fluegas.

CV is in it's LHV state therefore the heat used to vapourise the inherent water is already accounted for.

note:  $\Delta Q_{steam} = Q_{Steam.out} - Q_{Steam.in}$

Mass flow correlations

$$m_{air.total} = \dot{m}_{air.A/H.outlet} + m_{air.ing} + m_{seal.air}$$

$$m_{air.total} = HAR \cdot m_{coal}$$

$$m_{air.ing} = \%Air_{ing} \cdot m_{air.total}$$

$$\dot{m}_{air.A/H.outlet} = m_{air.total} - (m_{air.ing} + m_{seal.air}) = m_{coal} \cdot HAR \cdot (1 - \%Air_{ing}) - m_{seal.air}$$

$$\dot{m}_{fg.A/H.inlet} = FGR \cdot m_{coal}$$

Energy Balance

$$\sum Energy_{in} = \sum Energy_{out}$$

$$Energy_{in} = m_{coal} \cdot CV + m_{coal} \cdot h_{coal} + \dot{m}_{air.A/H.outlet} \cdot h_{moist.air}(AH_{airOut}) \dots$$

$$+ m_{seal.air} \cdot h_{moist.air}(T_{amb}) + Q_{credits} + Q_{steam.in} \dots$$

$$+ m_{air.ing} \cdot h_{moist.air}(T_{amb})$$

$$Energy_{out} = Q_{steam.out} + \dot{m}_{fg.A/H.inlet} \cdot h_{fg}(AH_{fg.in}) + m_{coal} \cdot m_{fash} \cdot \%BA \cdot h_{BA}(T_{BA.exit}) \dots$$

$$+ m_{coal} \cdot CV \cdot \%Q_{loss}$$

$$\begin{aligned}
 &m_{coal} \cdot CV \dots &= Q_{steam.out} \dots \\
 &+ m_{coal} \cdot h_{coal} \dots &+ \dot{m}_{fg.A/H.inlet} \cdot h_{fg}(AH_{fg.in}) \dots \\
 &+ \dot{m}_{air.A/H.outlet} \cdot h_{moist.air}(AH_{airOut}) \dots &+ m_{coal} \cdot m_{fash} \cdot \%BA \cdot h_{BA}(T_{BA.exit}) \dots \\
 &+ m_{seal.air} \cdot h_{moist.air}(T_{amb}) + Q_{credits} + Q_{steam.in} \dots &+ m_{coal} \cdot CV_{LHV} \cdot \%Q_{loss} \\
 &+ m_{air.ing} \cdot h_{moist.air}(T_{amb})
 \end{aligned}$$

$$\begin{aligned}
& m_{\text{coal}} \cdot CV \dots & = Q_{\text{steam.out}} \dots \\
& + m_{\text{coal}} \cdot h_{\text{coal}} \dots & + (FGR \cdot m_{\text{coal}}) \cdot h_{fg}(AH_{fg.in}) \dots \\
& + [m_{\text{coal}} \cdot HAR \cdot (1 - \%Air_{ing}) - m_{\text{seal.air}}] \cdot h_{\text{moist.air}}(AH_{\text{airOut}}) \dots & + m_{\text{coal}} \cdot m_{\text{fash}} \cdot \%BA \cdot h_{BA}(T_{BA.exit}) \dots \\
& + m_{\text{seal.air}} \cdot h_{\text{moist.air}}(T_{\text{amb}}) + Q_{\text{credits}} + Q_{\text{steam.in}} \dots & + m_{\text{coal}} \cdot CV_{LHV} \cdot \%Q_{\text{loss}} \\
& + (\%Air_{ing} \cdot HAR \cdot m_{\text{coal}}) \cdot h_{\text{moist.air}}(T_{\text{amb}})
\end{aligned}$$

$$m_{\text{coal}} \left[ \begin{aligned} & CV \dots \\ & + h_{\text{coal}} \dots \\ & + HAR \cdot (1 - \%Air_{ing}) \cdot h_{\text{moist.air}}(AH_{\text{airOut}}) \dots \\ & + \%Air_{ing} \cdot HAR \cdot h_{\text{moist.air}}(T_{\text{amb}}) \dots \\ & + -FGR \cdot h_{fg}(AH_{fg.in}) \dots \\ & + -m_{\text{fash}} \cdot \%BA \cdot h_{BA}(T_{BA.exit}) \dots \\ & + -CV_{LHV} \cdot \%Q_{\text{loss}} \end{aligned} \right] = \Delta Q_{\text{steam}} - Q_{\text{credits}} \dots + m_{\text{seal.air}}(h_{\text{moist.air}}(AH_{\text{airOut}}) - h_{\text{moist.air}}(T_{\text{amb}}))$$

$$m_{\text{coal}} \left[ \begin{aligned} & CV(1 - \%Q_{\text{loss}}) \dots \\ & + h_{\text{coal}} \dots \\ & + HAR \cdot (1 - \%Air_{ing}) \cdot h_{\text{moist.air}}(AH_{\text{airOut}}) \dots \\ & + \%Air_{ing} \cdot HAR \cdot h_{\text{moist.air}}(T_{\text{amb}}) \dots \\ & + -FGR \cdot h_{fg}(AH_{fg.in}) \dots \\ & + -m_{\text{fash}} \cdot \%BA \cdot h_{BA}(T_{BA.exit}) \end{aligned} \right] = \Delta Q_{\text{steam}} - Q_{\text{credits}} \dots + m_{\text{seal.air}}(h_{\text{moist.air}}(AH_{\text{airOut}}) - h_{\text{moist.air}}(T_{\text{amb}}))$$

And Finally the coal flow rate is calculated as:

$$m_{\text{coal}} := \frac{\Delta Q_{\text{steam}} - Q'_{\text{credits}} + (h_{\text{moist.air}}(T_{\text{air.A/H.outlet}} \cdot \omega) - h_{\text{moist.air}}(T_{\text{amb}} \cdot \omega)) \cdot \dot{m}_{\text{seal.air}}}{(1 - Q_{\text{insul.loss}}) \cdot CV_{\text{measured}} \dots + h_{\text{coal}}(T_{\text{amb}}) \dots + HAR \cdot \%Air_{ing} \cdot h_{\text{moist.air}}(T_{\text{amb}} \cdot \omega) \dots + HAR \cdot (1 - \%Air_{ing}) \cdot h_{\text{moist.air}}(T_{\text{air.A/H.outlet}} \cdot \omega) \dots + -FGR \cdot h_{fg}(T_{fg.A/H.inlet}) \dots + -m_{\text{fash}} \cdot \%BA \cdot h_{FlyAsh}(T_{BA.exit})} = 98.43 \frac{\text{kg}}{\text{s}}$$

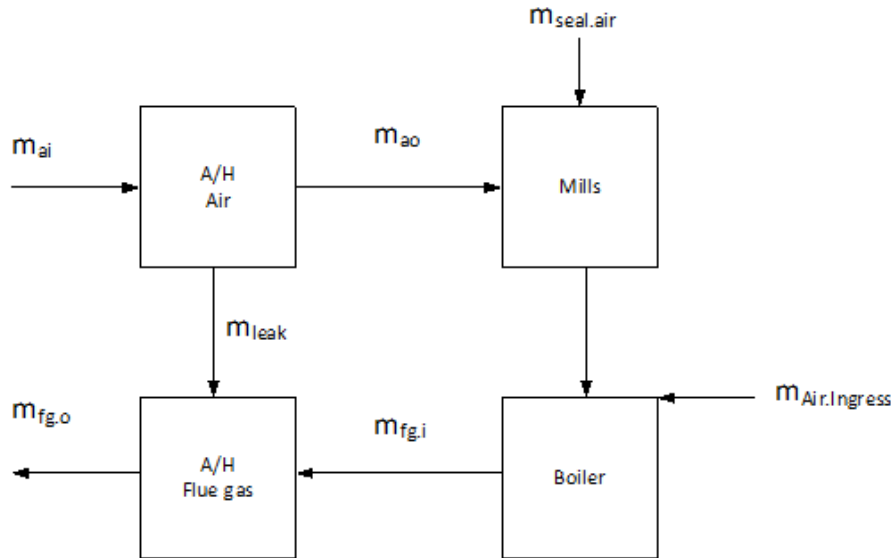
**A/H Mass Balance****Mass Flowrates of Air and Flue Gas Streams:**

Mass Flowrate of Total Air in Control Volume:

$$\dot{m}_{air.total} := HAR \cdot \dot{m}_{coal} = 650.423 \frac{kg}{s}$$

Mass Flowrate of Flue gas at A/H Inlet:

$$\dot{m}_{fg.A/H.inlet} := \dot{m}_{coal} \cdot FGR = 745.461 \frac{kg}{s}$$

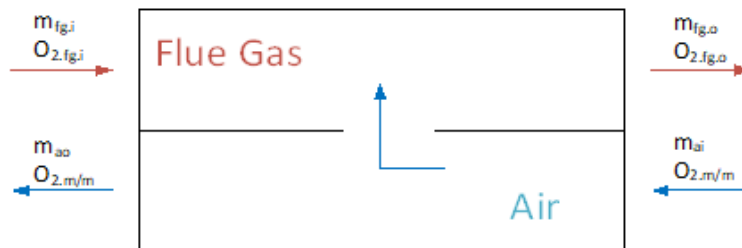
**Air Flow Analysis:**

Ingress Air Flow:

$$\dot{m}_{air.ing} := \dot{m}_{air.total} \cdot \%Air_{ing} = 14.133 \frac{kg}{s}$$

Mass flowrate of Air at A/H Outlet:

$$\dot{m}_{air.A/H.outlet} := \dot{m}_{air.total} - \dot{m}_{air.ing} - \dot{m}_{seal.air} = 631.434 \frac{kg}{s}$$

Control Volume around the A/H can then help determine the A/H leakage by mass balancing the O<sub>2</sub> Concentration

$$\dot{m}_{air.A/H.inlet} = \dot{m}_{air.A/H.outlet} + \dot{m}_{A/H.Leak}$$

$$\dot{m}_{fg.A/H.outlet} = \dot{m}_{fg.A/H.inlet} + \dot{m}_{A/H.Leak}$$

O2 mass balance:

$$\sum (\%O_2 \cdot \text{MassFlow}_{\text{inlet}}) = \sum (\%O_2 \cdot \text{MassFlow}_{\text{outlet}})$$

$$\begin{aligned} \%O_{2.FG.inlet} \cdot \dot{m}_{fg.A/H.inlet} \dots &= \%O_{2.FG.outlet} \cdot \dot{m}_{fg.A/H.outlet} \dots \\ + \%O_{2.mm} \cdot \dot{m}_{Air.A/H.inlet} &+ \%O_{2.mm} \cdot \dot{m}_{Air.Outlet} \end{aligned}$$

$$\begin{aligned} \%O_{2.FG.inlet} \cdot \dot{m}_{fg.A/H.inlet} \dots &= \%O_{2.mm} \cdot \dot{m}_{Air.Outlet} \dots \\ + \%O_{2.mm} \cdot (\dot{m}_{air.A/H.outlet} + \dot{m}_{A/H.Leak}) &+ \%O_{2.FG.outlet} \cdot (\dot{m}_{fg.A/H.inlet} + \dot{m}_{A/H.Leak}) \end{aligned}$$

$$\begin{aligned} \%O_{2.FG.inlet} \cdot \dot{m}_{fg.A/H.inlet} \dots &= \%O_{2.mm} \cdot \dot{m}_{Air.Outlet} \dots \\ + \%O_{2.mm} \cdot \dot{m}_{air.A/H.outlet} \dots &+ \%O_{2.FG.outlet} \cdot \dot{m}_{fg.A/H.inlet} \dots \\ + \%O_{2.mm} \cdot \dot{m}_{A/H.Leak} &+ \%O_{2.FG.outlet} \cdot \dot{m}_{A/H.Leak} \end{aligned}$$

$$\%O_{2.mm} \cdot \dot{m}_{A/H.Leak} - \%O_{2.FG.outlet} \cdot \dot{m}_{A/H.Leak} = \%O_{2.FG.outlet} \cdot \dot{m}_{fg.A/H.inlet} - \%O_{2.FG.inlet} \cdot \dot{m}_{fg.A/H.inlet}$$

$$\dot{m}_{A/H.Leak} \cdot (\%O_{2.mm} - \%O_{2.FG.outlet}) = \dot{m}_{fg.A/H.inlet} \cdot (\%O_{2.FG.outlet} - \%O_{2.FG.inlet})$$

$$\dot{m}_{A/H.Leak} = \dot{m}_{fg.A/H.inlet} \cdot \frac{\%O_{2.FG.outlet} - \%O_{2.FG.inlet}}{\%O_{2.mm} - \%O_{2.FG.outlet}}$$

$$\text{where: } \%O_{2.FG.outlet} = \%O_{2.A/H.fg.outlet} \cdot P_{ratio} \text{ and } \%O_{2.FG.inlet} = \%O_{2.A/H.fg.inlet} \cdot P_{ratio}$$

AH Leakage:

$$\dot{m}_{A/H.Leak} = \dot{m}_{fg.A/H.inlet} \cdot P_{ratio} \cdot \frac{\%O_{2.A/H.fg.outlet} - \%O_{2.A/H.fg.inlet}}{\%O_{2.mm} - \%O_{2.A/H.fg.outlet} \cdot P_{ratio}} = 38.399 \frac{kg}{s}$$

Mass flowrate of Air at A/H inlet:

$$\dot{m}_{air.A/H.inlet} = \dot{m}_{air.A/H.outlet} + \dot{m}_{A/H.Leak} = 669.832 \frac{kg}{s}$$

Mass flowrate of Flue gas at A/H outlet

$$\dot{m}_{fg.A/H.outlet} = \dot{m}_{fg.A/H.inlet} + \dot{m}_{A/H.Leak} = 783.859 \frac{kg}{s}$$



**A/H Energy Balance**

The only energy condition not known is that of the air heater inlet air temperature taken from the top of the boiler house.

$$Q_{fg.inlet} = h_{fg.inlet} \cdot \dot{m}_{fg.A/H.inlet}$$

$$Q_{fg.outlet} = h_{fg.outlet} \cdot \dot{m}_{fg.A/H.outlet}$$

$$Q_{air.inlet} = h_{air.inlet} \cdot \dot{m}_{air.A/H.inlet}$$

$$Q_{air.outlet} = h_{air.outlet} \cdot \dot{m}_{air.A/H.outlet}$$

**Energy Balance**

$$\sum Energy_{in} = \sum Energy_{out}$$

$$Q_{fg.inlet} + Q_{air.inlet} = Q_{fg.outlet} + Q_{air.outlet}$$

$$Q_{air.inlet} = Q_{fg.outlet} + Q_{air.outlet} - Q_{fg.inlet}$$

$$h_{air.inlet} = \frac{Q_{fg.outlet} - Q_{fg.inlet} + Q_{air.outlet}}{\dot{m}_{air.A/H.inlet}}$$

$$h_{air.inlet} := \frac{\dot{m}_{fg.A/H.outlet} \cdot h_{fg}(T_{fg.A/H.outlet}) - \dot{m}_{fg.A/H.inlet} \cdot h_{fg}(T_{fg.A/H.inlet}) \dots + \dot{m}_{air.A/H.outlet} \cdot h_{moist.air}(T_{air.A/H.outlet}, \omega)}{\dot{m}_{air.A/H.inlet}} = 46.004 \frac{kJ}{kg}$$

To calculate the temperature, use the root function to see when the moist air enthalpy equals the above enthalpy

$$T_{initialise} := 30 \text{ } ^\circ\text{C}$$

$$T_{air.A/H.inlet} := \text{root}(h_{air.inlet} - h_{moist.air}(T_{initialise}, \omega), T_{initialise}) = 41.551 \text{ } ^\circ\text{C}$$

**Energy Losses:**

Total Energy Input:  $Q'_{in} := \dot{m}_{coal} \cdot CV_{measured} + Q'_{credits} = 1622.827 \cdot MW$

Unburnt Carbon Energy Loss:  $Q_{loss.UBC} := C''' \cdot (\dot{m}_{coal} \cdot CV_{measured}) = 10.108 \cdot MW$

$$\%Q_{loss.UBC} := \left( \frac{Q_{loss.UBC}}{Q'_{in}} \right) = 0.623 \cdot \%$$

**Heat transfer losses (Convective and radiative losses):**

Radiative Energy Loss:  $Q_{loss.rad} := Q_{insul.loss} \cdot Q'_{in} = 12.983 \cdot MW$

$$\%Q_{loss.rad} := \left( \frac{Q_{loss.rad}}{Q'_{in}} \right) = 0.8 \cdot \%$$

**Flue gas humidity loss:**

Exiting Flue Gas contains water in the vapour phase. If this water were to be condensed additional energy would be released. The loss due to not condensing this water is quantified below:

Flue Gas Humidity Loss:  $Q_{loss.H2O} := \dot{m}_{fg.A/H.inlet} \cdot mf_{H2O.fg} \cdot h_{H2O.vap} = 81.54 \cdot MW$

$$\%Q_{loss.H2O} := \left( \frac{Q_{loss.H2O}}{Q'_{in}} \right) = 5.025 \cdot \%$$

**Sensible heat loss in ash:**

Sensible Heat Loss in Bottom Ash:  $Q_{loss.ba} := \dot{m}_{coal} \cdot (mf_{ash} \cdot \%BA) \cdot h_{ash}(T_{BA.exit}) = 1.801 \cdot MW$

$$\%Q_{loss.ba} := \left( \frac{Q_{loss.ba}}{Q'_{in}} \right) = 0.111 \cdot \%$$

Sensible Heat Loss in Fly Ash:  $Q_{loss.fa} := \dot{m}_{coal} \cdot (mf_{ash} \cdot \%FA) \cdot h_{ash}(T_{fg.A/H.inlet}) = 6.767 \cdot MW$

$$\%Q_{loss.fa} := \left( \frac{Q_{loss.fa}}{Q'_{in}} \right) = 0.417 \cdot \%$$

Total Sensible Heat Loss in Ash:  $Q_{loss.ash} := Q_{loss.ba} + Q_{loss.fa} = 8.568 \cdot MW$

$$\%Q_{loss.ash} := \left( \frac{Q_{loss.ash}}{Q'_{in}} \right) = 0.528 \cdot \%$$

**Flue gas energy loss/ Dry gas loss:**

The Dry Flue Gas Loss is defined as the net Energy Loss in the Flue Gas, i.e. the energy in the fluegas at the exit of the control volume minus the energy in the air and coal as they enter the control volume:

$$Q_{loss,fg} := \dot{m}_{fg,A/H.inlet} \cdot h_{fg}(T_{fg,A/H.inlet}) \dots = 147.66 \cdot MW$$

$$+ -(\dot{m}_{air,total} \cdot h_{air}(T_{air,A/H.outlet}) + \dot{m}_{coal} \cdot h_{coal}(T_{amb}))$$

$$\%Q_{loss,fg} := \frac{Q_{loss,fg}}{Q'_{in}} = 9.099 \cdot \%$$

**Boiler Efficiency****LHV Boiler Efficiency (Direct Method):**

$$\eta_{direct} := \frac{\Delta Q_{steam}}{Q'_{in}} = 89.773 \cdot \%$$

$$Q'_{in} - \Delta Q_{steam} = 165.967 \cdot MW$$

$$Q_{out} := \Delta Q_{steam}$$

**LHV Boiler Efficiency (Input - Losses):**

$$Losses := Q_{loss,fg} + Q_{loss,UBC} + Q_{loss,rad} + 0Q_{loss,evap} + Q_{loss,ash} = 179.319 \cdot MW$$

$$\eta_{LHV} := \frac{(Q'_{in} - Losses)}{Q'_{in}} = 88.95 \cdot \%$$

**HHV Boiler Efficiency:**

$$\eta_{HHV} := \frac{(Q'_{in} - Q_{loss,fg} - Q_{loss,ash} - Q_{loss,rad} - Q_{loss,UBC} - Q_{loss,H2O})}{Q'_{in}} = 83.926 \cdot \%$$

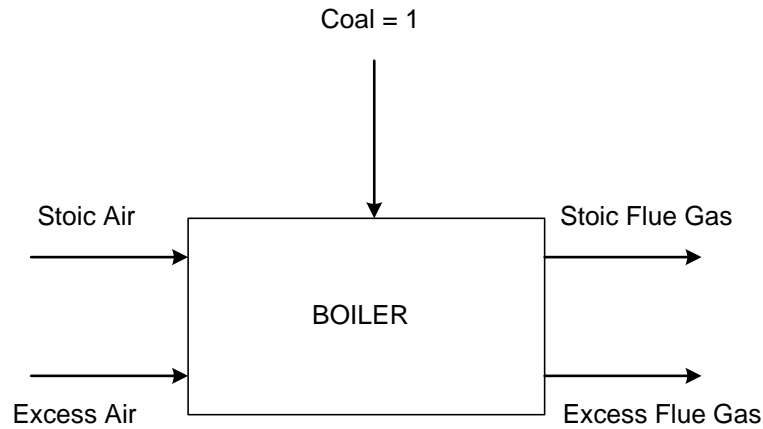
## Energy Balance Results:

|   |                                    |
|---|------------------------------------|
| Total Energy Input:                         | $Q'_{in} = 1622.827 \cdot MW$      |
| Energy Recovered by Steam:                  | $Q_{out} = 1456.86 \cdot MW$       |
| Radiative Energy Loss:                      | $\%Q_{loss.rad} = 0.8 \cdot \%$    |
| Unburnt Carbon Losses:                      | $\%Q_{loss.UBC} = 0.623 \cdot \%$  |
| Sensible Heat Losses in Bottom and Fly Ash: | $\%Q_{loss.ash} = 0.528 \cdot \%$  |
| Dry Flue Gas Losses:                        | $\%Q_{loss.fg} = 9.099 \cdot \%$   |
| Coal Fuel Moisture Loss:                    | $\%Q_{loss.evap} = 1.557 \cdot \%$ |
| Boiler Efficiency (Direct Method):          | $\eta_{direct} = 89.773 \cdot \%$  |
| Boiler Efficiency (Input - Losses):         | $\eta_{LHV} = 88.95 \cdot \%$      |
| HHV Boiler Efficiency:                      | $\eta_{HHV} = 83.926 \cdot \%$     |

## Mass Balance Results:

|   |   |
|---|---|
| Mass Flow Rate of Coal:   | $\dot{m}_{coal} = 98.43 \frac{kg}{s}$             |
| Total Air Flow Rate into Control Volume (incl. Ingress + Seal Air): | $\dot{m}_{air.total} = 650.423 \frac{kg}{s}$      |
| Total Air Flow Rate from A/H outlet:                                | $\dot{m}_{air.A/H.outlet} = 631.434 \frac{kg}{s}$ |
| Total Air Flow Rate at A/H inlet:                                   | $\dot{m}_{air.A/H.inlet} = 669.832 \frac{kg}{s}$  |
| Mass Flow Rate of Flue Gas at A/H outlet:                           | $\dot{m}_{fg.A/H.outlet} = 783.859 \frac{kg}{s}$  |
| Mass Flow Rate of Flue Gas at A/H inlet:                            | $\dot{m}_{fg.A/H.inlet} = 745.461 \frac{kg}{s}$   |

## A.2 – Excess air calculation



Let us assume that the mass units and quantities of the air and flue gas are associated with burning one unit of coal.

The stoichiometric air required is based on the coal coming into the boiler. The oxygen in the air reacts with each component of the coal to form gases that make up the flue gas. For example, oxygen reacts with sulphur to form sulphur dioxide. Therefore, to determine this stoichiometric air we need the coal composition. Consider the hypothetical coal sample below:

| Component        | As Received % |
|------------------|---------------|
| C                | 50            |
| H                | 2             |
| O                | 5             |
| N                | 1             |
| S                | 1             |
| Ash              | 30            |
| H <sub>2</sub> O | 11            |
| Total            | 100           |
| Unburned Carbon  | 2             |

The equation for calculation of stoichiometric air is given as:

$$\frac{1}{0.23} \left[ \frac{32}{12} (C - C') + \frac{32}{32} (S) + \frac{32}{4} (H) - O + 0.3 \frac{32}{14} (N) \right]$$

Therefore:

$$m_{stoic\ AIR} = \frac{1}{0.23} \left[ \frac{32}{12} \frac{(50-4)}{100} + \frac{32}{32} \frac{(1)}{100} + \frac{32}{4} \frac{(2)}{100} - \frac{(5)}{100} + 0.3 \frac{32}{14} \frac{(1)}{100} \right] = 6.18 \text{ kg Air / kg Coal}$$

The total flowrates of flue gas and air are given below:

$$m_{Total\ AIR} = m_{stoic\ AIR} + m_{excess\ AIR}$$

$$m_{Total\ FG} = m_{stoic\ FG} + m_{excess\ FG}$$

The excess air equation is written as:

$$Excess\ Air\ (EA) = \frac{m_{excess\ AIR}}{m_{stoic\ AIR}}$$

Thus, the total air can also be written as:

$$m_{Total\ AIR} = m_{stoic\ AIR} (1 + EA)$$

$$m_{stoic\ FG} = m_{stoic\ AIR} + 1$$

$$m_{O_2\ in\ FG} = m_{O_2\ in\ excess\ FG} = 0.23 \times m_{excess\ AIR} = 0.23 \times EA \times m_{stoic\ AIR} \quad (1)$$

The mass percentage of oxygen in flue gas is:

$$\gamma_{m_{O_2\ FG}} = \frac{m_{O_2\ in\ FG}}{m_{Total\ FG}} = \frac{m_{O_2\ in\ FG}}{m_{stoic\ FG} + m_{excess\ FG}} = \frac{m_{O_2\ in\ FG}}{(m_{stoic\ AIR} + 1) + \left( \frac{m_{O_2\ in\ FG}}{0.23} \right)}$$

Rearranging the equation to make the mass of oxygen in the flue gas the subject of the formula we obtain:

$$m_{O_2 \text{ in FG}} = \frac{\gamma_{m O_2 FG} [m_{stoic AIR} + 1]}{1 - \left( \frac{\gamma_{m O_2 FG}}{0.23} \right)}$$

Combining this with equation (1) we obtain:

$$EA = \frac{\gamma_{m O_2 FG} [m_{stoic AIR} + 1]}{(0.23 \times m_{stoic AIR}) \left[ 1 - \left( \frac{\gamma_{m O_2 FG}}{0.23} \right) \right]}$$

### Simplified Equation for Excess Air

From the ideal gas law

$$\gamma_{v O_2 FG} = \frac{V_{O_2 FG}}{V_{FG}} = \frac{m_{O_2 FG} / \rho_{O_2}}{m_{Total FG} / \rho_{FG}} = \left[ \frac{m_{O_2 FG}}{m_{Total FG}} \right] \times \left[ \frac{\rho_{FG}}{\rho_{O_2}} \right]$$

Therefore since:

$$\gamma_{m O_2 FG} = \frac{m_{O_2 FG}}{m_{Total FG}}$$

We have

$$\gamma_{v O_2 FG} = \gamma_{m O_2 FG} \times \left[ \frac{\rho_{FG}}{\rho_{O_2}} \right] \quad \& \quad \gamma_{m O_2 FG} = \gamma_{v O_2 FG} \times \left[ \frac{\rho_{O_2}}{\rho_{FG}} \right]$$

Therefore, replacing the mass percentages with volume percentages, we obtain:

$$EA = \frac{\left[ \gamma_{vO_2 FG} \times \left[ \frac{\rho_{O_2}}{\rho_{FG}} \right] \right] [m_{stoicAIR} + 1]}{(0.23 \times m_{stoicAIR}) \left[ 1 - \left( \frac{\gamma_{vO_2 FG} \times \left[ \frac{\rho_{O_2}}{\rho_{FG}} \right]}{0.23} \right) \right]}$$

To simplify the notation, let  $m_{stoicAIR} = x$  and  $\gamma_{vO_2 FG} = y$ .

Therefore, with the density ratio  $\frac{\rho_{O_2}}{\rho_{FG}} = 32/30 = 1.07$  we obtain:

$$EA = \frac{[1.07y][x+1]}{(0.23x) \left[ 1 - \left( \frac{1.07y}{0.23} \right) \right]}$$

Next, we separate the terms and we get:

$$EA = [1.07y] \times \frac{[x+1]}{x} \times \frac{1}{(0.23) \left[ 1 - \left( \frac{1.07y}{0.23} \right) \right]}$$

$$EA = [1.07y] \times \frac{[x+1]}{x} \times \frac{1}{0.23 - 1.07y}$$

$$\text{Now: } \frac{x+1}{x} \approx 1 \therefore EA = 1.07y \times \frac{1}{0.23 - 1.07y}$$

$$EA = \frac{y}{1.07^{-1}[0.23 - 1.07y]} = \frac{y}{[0.21 - y]}$$



## Appendix B. Program code

### B.1 - MEB C# script

```
//script using directives
//css_ref IPS.Core.dll;
//css_ref IPS.PluginInterface.dll;
//css_ref IPS.Units.dll;
//css_ref IPS.Utilities.CSharp.dll
using System;
using IPS.Properties;
using IPS.Scripting;

//script must be derived from IComponentScript
public class Script: IPS.Scripting.IComponentScript
{
//-----
    // Inputs
    IPS.Properties.Double _MW_Gen;
    IPS.Properties.Double _AtmTemp;

    IPS.Properties.Double _mfw;
    IPS.Properties.Double _hfw;

    IPS.Properties.Double _msh;
    IPS.Properties.Double _hsh;

    IPS.Properties.Double _mshs;
    IPS.Properties.Double _hshs;

    IPS.Properties.Double _mrhin;
    IPS.Properties.Double _hrhin;

    IPS.Properties.Double _mrhout;
    IPS.Properties.Double _hrhout;

    IPS.Properties.Double _mrhs;
    IPS.Properties.Double _hrhs;

    IPS.Properties.Double _CV_Value;
//-----
    //Outputs
    IPS.Properties.Double _m_fg;
    IPS.Properties.Double _m_fg_leak;
    IPS.Properties.Double _m_air_ing;
    IPS.Properties.Double _mair_id;

    IPS.Properties.Double _Q_bhx;
    IPS.Properties.Double _Q_AH;

    IPS.Properties.Double _Furnace_Temp;
    IPS.Properties.Double _T_amb;
//-----
    //Coal specs
    IPS.Properties.Double _Condition;
    IPS.Properties.Double _CVcalcMode;
```

```

IPS.Properties.Double _CVcorr;
IPS.Properties.Double _CoalFlow;
//-----
IPS.Properties.Double _coal;
IPS.Properties.Double _effD;
IPS.Properties.Double _effHHV;

//do pre simulation initialisation here
public override void Initialise(){
}

//do post simulation cleanup here
public override void Cleanup(){
}

//=====
//-----Important Functions-----
//=====

static public double evap(double Temp)
{
    double[] a = { 6.108, 0.444, 0.014, 2.65e-4, 3.03e-6, 2.03e-8,
6.14e-11 };
    double result;
    result = (a[0] + Temp * (a[1] + Temp * (a[2] + Temp * (a[3] + Temp *
(a[4] + Temp * (a[5] + Temp * a[6]))))) * 100; //PA
    return result;
}

static public double rho_air(double T, double Patm, double Rd, double
pH2O)
{
    double result;
    result = (Patm / (Rd * T)) * (1 - (0.378 * pH2O) / Patm);
    return result;
}

static public double Interpolation(double[] Data, double MW_Gen)
{
    if (MW_Gen < 424.291)
    {
        double result1 = Data[0];
        return result1;
    }
    else if ((424.291 <= MW_Gen) && (MW_Gen < 599.945))
    {
        double deltam_1 = (Data[1] - Data[0]) / (599.945 - 424.291);
        double result2 = deltam_1 * (MW_Gen - 424.291) + Data[0];
        return result2;
    }
    else if ((599.945 <= MW_Gen) && (MW_Gen <= 618.5))
    {
        double deltam_2 = (Data[2] - Data[1]) / (618.5 - 599.945);
        double result3 = deltam_2 * (MW_Gen - 599.945) + Data[1];
        return result3;
    }
    else
    {
        return Data[2];
    }
}

```

```

    }

}

static public double p_h2o(double rh, double Tatm)
{
    double result;
    result = rh * evap(Tatm) / 1000;           //kPA
    return result;
}

//=====
//-----Constituent Enthalpies-----
//=====

// Carbon based Enthalpies
static public double h_coal(double Temp)
{
    double Tref = 0.01;
    double result = 1.38 * (Temp - Tref);
    return result;
}

static public double h_ubc(double Temp)
{
    double Tref = 0.01;
    double result = 0.710 * (Temp - Tref);
    return result;
}

static public double h_FA(double Temp)
{
    double Tref = 0.01;
    double result = 0.730 * (Temp - Tref);
    return result;
}

// ASHRAE Enthalpies
static public double h_moistair(double Temp, double SH)
{
    double Tref = 0.0;
    double result = 1.006 * (Temp - Tref) + SH * (2501 + 1.86*(Temp -
Tref));
    return result;
}

static public double h_h2o(double Temp)
{
    double Tref = 0.01;
    double result = 2501 + 1.86 * (Temp - Tref);
    return result;
}

// Main enthalpy equation
static public double h_element(int Element, double Temp)
{
    double[] col = new double[4] { 0, 0, 0, 0 };
    if (Element == 1)           // Air
    {
        col[0] = 9.816e-1;
        col[1] = 1.245e-4;
    }
}

```

```

        col[2] = -1.08e-12;
        col[3] = -2.154e-12;
    }
    else if (Element == 2) // O2
    {
        col[0] = 8.974e-1;
        col[1] = 1.994e-4;
        col[2] = -7.432e-8;
        col[3] = 1.225e-11;
    }
    else if (Element == 3) // N2
    {
        col[0] = 1.015;
        col[1] = 1.037e-4;
        col[2] = 5.452e-9;
        col[3] = -6.693e-12;
    }
    else if (Element == 4) // Argon
    {
        col[0] = 5.205e-1;
        col[1] = 0;
        col[2] = 0;
        col[3] = 0;
    }
    else if (Element == 5) // CO2
    {
        col[0] = 8.437e-1;
        col[1] = 4.258e-4;
        col[2] = -1.705e-7;
        col[3] = 2.819e-11;
    }
    else if (Element == 6) // NO
    {
        col[0] = 8.861e-1;
        col[1] = 3.263e-4;
        col[2] = 0;
        col[3] = 0;
    }
    else if (Element == 7) // SO2
    {
        col[0] = 6.426e-1;
        col[1] = 1.850e-4;
        col[2] = 0;
        col[3] = 0;
    }
    }

    double result;
    result = col[0] * Temp + col[1] * (Temp * Temp) + col[2] * (Temp *
Temp * Temp) + col[3] * (Temp * Temp * Temp * Temp);
    return result;
}

// Other Enthalpies
static public double h_air(double Temp)
{
    double result = h_element(1, Temp);
    return result;
}

static public double h_o2(double Temp)

```

```

{
    double result = h_element(2, Temp);
    return result;
}

static public double h_n2(double Temp)
{
    double result = h_element(3, Temp);

    return result;
}

static public double h_argon(double Temp)
{
    double result = h_element(4, Temp);
    return result;
}

static public double h_co2(double Temp)
{
    double result = h_element(5, Temp);

    return result;
}

static public double h_no(double Temp)
{
    double result = h_element(6, Temp);
    return result;
}

static public double h_so2(double Temp)
{
    double result = h_element(7, Temp);
    return result;
}

// Flue Gas Enthalpy (mass fraction as input)
static public double h_fg(double Temp, double mfo2_fg, double mfco2_fg,
double mfn2_fg, double mfso2_fg, double mfh2o_fg, double mfubc_fg, double
mffa_fg, double mfno_fg, double mfar_fg)
{
    double result = mfo2_fg * h_o2(Temp) + mfco2_fg * h_co2(Temp) +
mfn2_fg * h_n2(Temp)
                    + mfso2_fg * h_so2(Temp) + mfh2o_fg * h_h2o(Temp) +
mfubc_fg * h_ubc(Temp)
                    + mffa_fg * h_FA(Temp) + mfno_fg * h_no(Temp) +
mfar_fg * h_argon(Temp);
    return result;
}

static public double f_hfg(double hfgc, double Temp, double mfo2_fg,
double mfco2_fg, double mfn2_fg, double mfso2_fg, double mfh2o_fg, double
mfubc_fg, double mffa_fg, double mfno_fg, double mfar_fg)
{
    double result = hfgc - h_fg(Temp, mfo2_fg, mfco2_fg,
mfn2_fg, mfso2_fg, mfh2o_fg, mfubc_fg, mffa_fg, mfno_fg, mfar_fg);
    return result;
}

// Used the Secant method to calculate the root of the function "desired
enthalpy" - "flue gas enthalpy equation @ Temperature"

```

```

    static public double root(double mfo2_fg, double mfco2_fg, double
mfn2_fg, double mfso2_fg, double mfh2o_fg, double mfubc_fg, double mffa_fg,
double mfno_fg, double mfar_fg, double hfgc)
    {

        double ta = 100;
        double tb = 250;
        double tc = 2000;
        double err = 0.001;
        double counter = 0;

        double result = 1500;

        while ((Math.Abs(f_hfg( hfgc, tc, mfo2_fg, mfco2_fg, mfn2_fg,
mfso2_fg, mfh2o_fg, mfubc_fg, mffa_fg, mfno_fg, mfar_fg)) > err) &&
(counter <= 2000))
        {
            counter = counter + 1;
            tc = (ta*f_hfg( hfgc, tb, mfo2_fg, mfco2_fg, mfn2_fg,
mfso2_fg, mfh2o_fg, mfubc_fg, mffa_fg, mfno_fg, mfar_fg) - tb*f_hfg( hfgc,
ta, mfo2_fg, mfco2_fg, mfn2_fg, mfso2_fg, mfh2o_fg, mfubc_fg, mffa_fg,
mfno_fg, mfar_fg))/
            (f_hfg( hfgc, tb, mfo2_fg, mfco2_fg, mfn2_fg, mfso2_fg,
mfh2o_fg, mfubc_fg, mffa_fg, mfno_fg, mfar_fg) - f_hfg( hfgc, ta, mfo2_fg,
mfco2_fg, mfn2_fg, mfso2_fg, mfh2o_fg, mfubc_fg, mffa_fg, mfno_fg,
mfar_fg));

            if (f_hfg( hfgc, tc, mfo2_fg, mfco2_fg, mfn2_fg, mfso2_fg,
mfh2o_fg, mfubc_fg, mffa_fg, mfno_fg, mfar_fg) > 0)
            {
                tb = tc;
            }
            else
            {
                ta = tc;
            }
        }
        result = tc;
        return result;
    }

//-----
//-----
//script main execution function - called every cycle
public override void Execute(double Time)
{
//=====
//-----Constants-----
//=====

//-----Air Concentration-----
// https://www.engineeringtoolbox.com/air-composition-d_212.html
// Mass basis
double N2mm = 0.755; // % kg /kg
double O2mm = 0.232; // % kg/ / kg
double Armm = 0.0128; // % kg / kg

// Volume Basis
double N2vv = 0.78117; // % m^3 / m^3
double O2vv = 0.2095; // % m^3 / m^3
double Arvv = 0.00933; // % m^3 / m^3

```

```

// Molar Basis
double N2mb = 0.78119; // % mol / mol
double O2mb = 0.20947; // % mol / mol
double Armb = 0.00934; // % mol / mol

//-----Molar Mass-----
double MC = 12.01; // g/mol
double MH = 1.00795; // g/mol
double MO = 15.9995; // g/mol
double MN = 14.0065; // g/mol
double MS = 32.07; // g/mol

double Rd = 287.05; // J/(kg.K)

double MN2 = 2*MN; // g/mol
double MO2 = 2 * MO; // g/mol
double MAr = 39.95; // g/mol
double MAIR = N2mb * MN2 + O2mb * MO2 + Armb * MAr; // g/mol

double MH2O = 2 * MH + MO; // g/mol
double MCO2 = MC + 2 * MO; // g/mol
double MNO = MN + MO; // g/mol
double MSO2 = MS + 2*MO; // g/mol
double MNO2 = MN + 2*MO; // g/mol

//-----Other-----
double hH2Ovap = 2441.7; // kJ/kg
double rho_ratio = MO2 / 30.262;
_T_amb.Value = 44; // °C

//=====
//-----INPUTS-----
//=====
//-----Input Constants-----
//Metrological inputs
double Patm = 83.5; // kPa
double RH = 0.1;

double P_H2O = p_h2o(RH, _AtmTemp.Value); // kPa
double xH2O = P_H2O / Patm;
double SH = (xH2O * MH2O) / (xH2O * MH2O + (1 - xH2O) * MAIR);

// Air/Flue Gas O2 concentration
double[] o2fgi = { 0.0437, 0.0316, 0.0316 };
double o2_ah_fg_inlet = Interpolation(o2fgi, _MW_Gen.Value);

double[] o2fgo = { 0.0536, 0.0411, 0.0408 };
double o2_ah_fg_outlet = Interpolation(o2fgo, _MW_Gen.Value);

double[] o2fi = { 0.041, 0.0285, 0.0285 };
double o2_furn_inlet = Interpolation(o2fi, _MW_Gen.Value);

double[] o2id = { 0.0555, 0.0431, 0.0429 };
double o2_id_inlet = Interpolation(o2id, _MW_Gen.Value);

// Air/Flue Gas Temperature
double[] TTfgi = { 305, 331, 334 };
double TfgAHin = Interpolation(TTfgi, _MW_Gen.Value); //°C

```

```

double[] TTfgo = { 113, 126, 127 };
double TfgAHout = Interpolation(TTfgo, _MW_Gen.Value); //°C

double[] TTai = { 268, 286, 288 };
double TairAHout = Interpolation(TTai, _MW_Gen.Value); //°C

//Ash Analysis
double Cfa = 0.01;
double Cba = 0.01;
double FA = 0.9;
double BA = 0.1;

double TBA_exit = 800; //°C

//Energy Losses
double Q_insul_loss = 0.008; // % (in decimal)
//=====
//-----Credits-----
//=====

//Mills
double NoOfMills = 5;
double MillMotorPower = 1550;
double Milleff = 0.5;
double MillPower = Milleff*MillMotorPower*NoOfMills; //kW

//PA Fans
double NoPAFans = 2;
double PAMotorFan = 1850;
double PA_Eff = 0.968;
double PA_Power = NoPAFans*PAMotorFan*PA_Eff; //kW

//Seal Air Fans
double NoSAFans = 2;
double SAMotorFan = 75.0;
double SA_Eff = 0.935;
double SA_Power = NoSAFans*SAMotorFan*SA_Eff; //kW

//FD fans
double NoFDFans = 2;
double FDMotorFan = 2386.0;
double FD_Eff = 0.658;
double FD_Power = NoFDFans*FDMotorFan*FD_Eff; //kW

//Total Power
double FanTotal = SA_Power; //kW
double FanTotalR = PA_Power + SA_Power + FD_Power; //kW

//Seal air
double SAVol_one = 2.65;
double SAVol_tot = SAVol_one*NoSAFans;
double SAm = SAVol_tot*rho_air(_T_amb.Value, Patm, Rd, P_H2O); //kg/s

//Oil and other things
double OtherPower = 0;

//=====
//-----Coal Properties-----
//=====

```



```

double CVmeasured = 0; // (kJ/kg)
double fnox = 0.7;

// Mass Fraction
double mfc = 0;
double mfh = 0;
double mfo = 0;
double mfn = 0;
double mfs = 0;

double mfh2o = 0;
double mfash = 0;

if (_Condition.Value == 1) // (Aug 2016)
{
    mfc = 0.3599;
    mfh = 0.0209;
    mfo = 0.1008;
    mfn = 0.0086;
    mfs = 0.0058;

    mfh2o = 0.044;
    mfash = 0.448;
    CVmeasured = 13640;
}
else if (_Condition.Value == 2) // (Nov 2003)
{
    mfc = 0.4215;
    mfh = 0.0247;
    mfo = 0.0845;
    mfn = 0.0108;
    mfs = 0.0071;

    mfh2o = 0.05;
    mfash = 0.382;
    CVmeasured = 16280;
    //
}
else if (_Condition.Value == 3) // (Sept 2003)
{
    mfc = 0.5315;
    mfh = 0.0247;
    mfo = 0.0515;
    mfn = 0.0134;
    mfs = 0.0077;

    mfh2o = 0.044;
    mfash = 0.3040;
    CVmeasured = 19240;
}
else
{
    mfc = 0.4394;
    mfh = 0.025;
    mfo = 0.0961;
    mfn = 0.0111;
    mfs = 0.01;

    mfh2o = 0.1051;

```

```

        mflash = 0.3133;
        CVmeasured = 16410;
    }

// Calorific Value (kJ/kg)
    double cvc = 32778.15;
    double cvh = 119931.72;
    double cvo = 0;
    double cvn = 0;
    double cvs = 9257.524;

    double cvh2o = 0;
    double cvash = 0;

// Stoichiometric Coefficient
    double stc = 1;
    double sth = 0.25;
    double sto = -0.5;
    double stn = 0.5*fnox;
    double sts = 1;

    double sth2o = 0;
    double stash = 0;

    double CVcoal = 0;
    ;

    if (_CVcalcMode.Value == 1)
    {
        CVcoal = mfc*cvc + mfo*cvo + mfh*cvh + mfn*cvn + mfs*cvs +
mfh2o*cvh2o + mflash*cvash; // kJ / kg

        _CV_Value.Value = CVcoal;
    }
    else if (_CVcalcMode.Value == 2)
    {
        CVcoal = CVmeasured; // kJ / kg

        _CV_Value.Value = CVcoal;
    }
    else
    {
        CVcoal = 16410; // kJ / kg

        _CV_Value.Value = CVcoal;
    }

//=====
//-----Mass Balances-----
//=====

    double C1 = mflash*(( Cfa*FA ) + ( Cba*BA ));

    double C2 = C1 / mfc;

    double C3 = cvc * ( C1 / CVcoal);

    double TAR = (MAIR / O2mb) *
        (stc * ((mfc - C1) / MC) + sto * (mfo / MO) + sth * (mfh /
MH) + stn * (mfn / MN) + sts * (mfs / MS));

```

```

// Excess Air at AH inlet
double EA_AH_fg_inlet = ((TAR + 1) / (TAR)) * (o2_ah_fg_inlet / ((O2mm / rho_ratio) -
o2_ah_fg_inlet));

//---
double per_Air_ing = EA_AH_fg_inlet - ((TAR + 1) / (TAR)) * ( (o2_furn_inlet) / (
(O2mm / rho_ratio) - o2_furn_inlet) );
//---

//DAR
double DAR = TAR * (1 + EA_AH_fg_inlet);

//HAR
double HAR = DAR * (1 + SH);

// Mole fractions
double mfc_1 = mfc - C1;

double nc = (mfc_1 / MC) * (MC / mfc_1);
double nh = (mfh / MH) * (MC / mfc_1);
double no = (mfo / MO) * (MC / mfc_1);
double nn = (mfN / MN) * (MC / mfc_1);
double ns = (mfs / MS) * (MC / mfc_1);
// -----
//Mass flow rates ber kg Coal
double FR_CO2 = nc * mfc_1 * (MCO2 / MC);
double FR_H2O = 0.5 * nh * mfc_1 * (MH2O / MC) + SH * DAR +
mfh2o;
double FR_O2 = EA_AH_fg_inlet * TAR * O2mb * (MO2 / MAIR);
double FR_N2 = 0.5 * (1 - fnox) * nn * mfc_1 * (MN2 / MC) + DAR
* N2mb * (MN2 / MAIR);
double FR_NO = fnox * nn * mfc_1 * (MNO / MC);
double FR_SO2 = ns * mfc_1 * (MSO2 / MC);

double FR_Ar = DAR * Armb * (MAr / MAIR);
double FR_FA = mfash * FA * (1 - Cfa);
double FR_UBC = mfash * (Cfa * FA);

double FGR = FR_CO2 + FR_H2O + FR_O2 + FR_N2 + FR_NO + FR_SO2 +
FR_Ar + FR_FA + FR_UBC;
// -----
//Mass fraction
double mfco2_fg = FR_CO2 / FGR;
double mfh2o_fg = FR_H2O / FGR;
double mfo2_fg = FR_O2 / FGR;

double mfn2_fg = FR_N2 / FGR;
double mfno_fg = FR_NO / FGR;
double mfso2_fg = FR_SO2 / FGR;

double mfar_fg = FR_Ar / FGR;
double mffa_fg = FR_FA / FGR;
double mfubc_fg = FR_UBC / FGR;
// -----
double MFG = mfo2_fg * MO2 + mfco2_fg * MCO2 + mfn2_fg * MN2
+ mfso2_fg * MSO2 + mfno_fg * MNO2 + mfh2o_fg * MH2O
+ mfar_fg * MAr + mfubc_fg * MC;

```

```

//=====
//-----Enthalpy Polynomials-----
//=====

//          All equations are in the methods above

//=====
//-----Global Boiler Energy Balance-----
//=====

    //kW
    double Q_steam = ((_msh.Value*_hsh.Value) +
(_mrhout.Value*_hrhout.Value))
                - ((_mfw.Value*_hfw.Value) + (_mrhin.Value*_hrhin.Value)
                + (_mshs.Value*_hshs.Value) + (_mrhs.Value*_hrhs.Value)
);

    double Q_credits = MillPower + FanTotal + OtherPower;

    double m_coal_top = Q_steam - Q_credits + SAM * ( h_moistair(TairAHout,
SH) - h_moistair(_T_amb.Value, SH) );

    double m_coal_bot = CVcoal * (1 - Q_insul_loss)
                + h_coal(_T_amb.Value)
                + HAR * per_Air_ing * h_moistair(_T_amb.Value,
SH)
                + HAR * (1 - per_Air_ing) *
h_moistair(TairAHout, SH)
                - FGR * h_fg(TfgAHin, mfo2_fg, mfco2_fg,
mfno2_fg, mfso2_fg, mfh2o_fg, mfubc_fg, mffa_fg, mfno_fg, mfar_fg)
                - mflash * BA * h_FA(TBA_exit);

// -----
double m_coal = m_coal_top/m_coal_bot;
// -----
_CoalFlow.Value = m_coal;

//Mass flowrates
double m_air_total = HAR * m_coal;
double m_fg_AH_inlet = m_coal * FGR;

double m_airing = m_air_total * per_Air_ing;
double m_air_ah_outlet = m_air_total - m_airing - SAM;

// -----
// Leakage calculations
double m_AH_leak = m_fg_AH_inlet * rho_ratio * ((o2_ah_fg_outlet -
o2_ah_fg_inlet)/
(O2mm - o2_ah_fg_outlet * rho_ratio));

double m_air_AH_inlet = m_air_ah_outlet + m_AH_leak;
double m_fg_AH_outlet = m_fg_AH_inlet + m_AH_leak;

double fghin = h_fg(TfgAHin, mfo2_fg, mfco2_fg, mfn2_fg,
mfso2_fg, mfh2o_fg, mfubc_fg, mffa_fg, mfno_fg, mfar_fg);

double mfg_rat = m_fg_AH_inlet/m_fg_AH_outlet;

```

```

        double mfo2_fg2 = ( m_fg_AH_inlet*mfo2_fg +
m_AH_leak*O2mm)/m_fg_AH_outlet;
        double mfn2_fg2 = ( m_fg_AH_inlet*mfn2_fg +
m_AH_leak*N2mm)/m_fg_AH_outlet;
        double mfar_fg2 = ( m_fg_AH_inlet*mfar_fg +
m_AH_leak*Armm)/m_fg_AH_outlet;

        double fghout = h_fg(TfgAHout, mfo2_fg2, mfco2_fg*mfg_rat,
mfn2_fg2, mfso2_fg*mfg_rat, mfh2o_fg*mfg_rat, mfubc_fg*mfg_rat, mffa_fg*mfg_rat,
mfno_fg*mfg_rat, mfar_fg2);

        double h_a_amb = h_moistair(_T_amb.Value, SH) ;
        double h_a_ah = h_moistair(TfgAHin, SH);

        double Q_AH = (fghin*m_fg_AH_inlet - fghout*m_fg_AH_outlet) +
m_AH_leak*h_a_amb;

//=====
//-----Outputs to Flownex-----
//=====

        double m_esp_leak = m_fg_AH_outlet * rho_ratio * ((o2_id_inlet -
o2_ah_fg_outlet)/
(O2mm - o2_id_inlet * rho_ratio));

        _mair_id.Value = m_esp_leak;
        _m_fg.Value = m_fg_AH_outlet + m_esp_leak;
        _m_fg_leak.Value = m_fg_AH_outlet - m_fg_AH_inlet;
        _m_air_ing.Value = m_airing;

        _Q_bhx.Value = Q_steam;
        _Q_AH.Value = Q_AH;

        double hat = fghin + (Q_steam / (m_fg_AH_inlet - m_airing) ) + (
m_airing / (m_fg_AH_inlet - m_airing) )*( h_a_ah - h_a_amb );
        _Furnace_Temp.Value = root( mfo2_fg, mfco2_fg, mfn2_fg, mfso2_fg,
mfh2o_fg, mfubc_fg, mffa_fg, mfno_fg, mfar_fg, hat);
//=====
//-----Efficiency -----
//=====

        double Q_in = m_coal*CVmeasured + Q_credits;
        _effD.Value = 100*Q_steam/Q_in;
// -----
//HHV losses
        double Q_fgL = m_fg_AH_inlet*fghin - (m_air_total*h_a_ah +
m_coal*h_coal(_T_amb.Value));
        double Q_ubcL = C3*m_coal*CVcoal;
        double Q_radL = Q_in*Q_insul_loss;
        double Q_ashL = m_coal*mfash*((BA*h_FA(TBA_exit)) + (FA*h_FA(TfgAHin)));
        double Q_H2OL = m_fg_AH_inlet*mfh2o_fg*hH2Ovap;
        double Q_evapL = m_coal*mfh2o_fg*hH2Ovap;

        double Q_totalHHV = Q_ubcL + Q_radL + Q_ashL + Q_H2OL + Q_fgL;
        double Q_totalLHV = Q_fgL + Q_ubcL + Q_radL + Q_ashL;
// -----
        _effHHV.Value = 100*(1 - Q_totalHHV/Q_in);

//=====
//=====

```

```

}

//any processing you want to do before steady state
public override void ExecuteBeforeSteadyState()
{
    Execute(0.0);
}

//any processing you want to do while solving steady state
public override void ExecuteSteadyState()
{
    Execute(0.0);
}

//any processing you want to do after steady state
public override void ExecuteAfterSteadyState()
{
    Execute(0.0);
}

//constructor initialises parameters
public Script()
{
    //-----Inputs-----
    _mfw = new IPS.Properties.Double();
    _mfw.Value = 0;

    _hfw = new IPS.Properties.Double();
    _hfw.Value = 0;

    _msh = new IPS.Properties.Double();
    _msh.Value = 0;

    _hsh = new IPS.Properties.Double();
    _hsh.Value = 0;

    _mshs = new IPS.Properties.Double();
    _mshs.Value = 0;

    _hshs = new IPS.Properties.Double();
    _hshs.Value = 0;

    _mrhin = new IPS.Properties.Double();
    _mrhin.Value = 0;

    _hrhin = new IPS.Properties.Double();
    _hrhin.Value = 0;

    _mrhout = new IPS.Properties.Double();
    _mrhout.Value = 0;

    _hrhout = new IPS.Properties.Double();
    _hrhout.Value = 0;

    _mrhs = new IPS.Properties.Double();
    _mrhs.Value = 0;

    _hrhs = new IPS.Properties.Double();
    _hrhs.Value = 0;
}

```

```

_MW_Gen = new IPS.Properties.Double();
_MW_Gen.Value = 618.5;

_AtmTemp = new IPS.Properties.Double();
_AtmTemp.Value = 19;

_CV_Value = new IPS.Properties.Double();
_CV_Value.Value = 16410;
//-----Outputs-----
_m_fg = new IPS.Properties.Double();
_m_fg.Value = 0;
_m_fg_leak = new IPS.Properties.Double();
_m_fg_leak.Value = 0;
_m_air_ing = new IPS.Properties.Double();
_m_air_ing.Value = 0;

_Q_bhx = new IPS.Properties.Double();
_Q_bhx.Value = 0;
_Q_AH = new IPS.Properties.Double();
_Q_AH.Value = 0;

_Furnace_Temp = new IPS.Properties.Double();
_Furnace_Temp.Value = 1850;
_T_amb = new IPS.Properties.Double();
_T_amb.Value = 44;

_mair_id = new IPS.Properties.Double();
_mair_id.Value = 0;

//-----
_Condition = new IPS.Properties.Double();
_Condition.Value = 1;

_CVcalcMode = new IPS.Properties.Double();
_CVcalcMode.Value = 1;

_CVcorr = new IPS.Properties.Double();
_CVcorr.Value = -7.55;

_CoalFlow = new IPS.Properties.Double();
_CoalFlow.Value = 0;

_effD = new IPS.Properties.Double();
_effD.Value = 0;
_effHHV = new IPS.Properties.Double();
_effHHV.Value = 0;
}
//-----
//property declarations to make
//parameters visible to outside world

/*----- VP Inputs -----*/

[PropertyUsage(UseProperty.DYNAMIC)]
[GridCategory(new String[]{"VP Inputs"})]
[GridOrder(0)]
public IPS.Properties.Double mfw
{
    get

```

```

        {
            return _mfw;
        }
    }

    [PropertyUsage(UseProperty.DYNAMIC)]
    [GridCategory(new String[]{"VP Inputs"})]
    public IPS.Properties.Double hfw
    {
        get
        {
            return _hfw;
        }
    }

    [PropertyUsage(UseProperty.DYNAMIC)]
    [GridCategory(new String[]{"VP Inputs"})]
    public IPS.Properties.Double msh
    {
        get
        {
            return _msh;
        }
    }

    [PropertyUsage(UseProperty.DYNAMIC)]
    [GridCategory(new String[]{"VP Inputs"})]
    public IPS.Properties.Double hsh
    {
        get
        {
            return _hsh;
        }
    }

    [PropertyUsage(UseProperty.DYNAMIC)]
    [GridCategory(new String[]{"VP Inputs"})]
    public IPS.Properties.Double mshs
    {
        get
        {
            return _mshs;
        }
    }

    [PropertyUsage(UseProperty.DYNAMIC)]
    [GridCategory(new String[]{"VP Inputs"})]
    public IPS.Properties.Double hshs
    {
        get
        {
            return _hshs;
        }
    }

    [PropertyUsage(UseProperty.DYNAMIC)]
    [GridCategory(new String[]{"VP Inputs"})]
    public IPS.Properties.Double mrhin
    {
        get

```



```

        {
            return _mrhin;
        }
    }

    [PropertyUsage(UseProperty.DYNAMIC)]
    [GridCategory(new String[]{"VP Inputs"})]
    public IPS.Properties.Double hrhin
    {
        get
        {
            return _hrhin;
        }
    }

    [PropertyUsage(UseProperty.DYNAMIC)]
    [GridCategory(new String[]{"VP Inputs"})]
    public IPS.Properties.Double mrhout
    {
        get
        {
            return _mrhout;
        }
    }

    [PropertyUsage(UseProperty.DYNAMIC)]
    [GridCategory(new String[]{"VP Inputs"})]
    public IPS.Properties.Double hrhout
    {
        get
        {
            return _hrhout;
        }
    }

    [PropertyUsage(UseProperty.DYNAMIC)]
    [GridCategory(new String[]{"VP Inputs"})]
    public IPS.Properties.Double mrhs
    {
        get
        {
            return _mrhs;
        }
    }

    [PropertyUsage(UseProperty.DYNAMIC)]
    [GridCategory(new String[]{"VP Inputs"})]
    public IPS.Properties.Double hrhs
    {
        get
        {
            return _hrhs;
        }
    }

    [PropertyUsage(UseProperty.DYNAMIC)]
    [GridCategory(new String[]{"VP Inputs"})]
    public IPS.Properties.Double MW_Gen
    {
        get

```

```

        {
            return _MW_Gen;
        }
    }
    [PropertyUsage(UseProperty.DYNAMIC)]
    [GridCategory(new String[]{"VP Inputs"})]
    public IPS.Properties.Double AtmTemp
    {
        get
        {
            return _AtmTemp;
        }
    }

/*----- Study Variables -----*/

    [PropertyUsage(UseProperty.DYNAMIC)]
    [GridCategory(new String[]{"Study Variables"})]
    [GridOrder(1)]
    public IPS.Properties.Double Condition
    {
        get
        {
            return _Condition;
        }
    }

    [PropertyUsage(UseProperty.DYNAMIC)]
    [GridCategory(new String[]{"Study Variables"})]

    public IPS.Properties.Double CVcalcMode
    {
        get
        {
            return _CVcalcMode;
        }
    }

/*----- Temperatures -----*/

    [PropertyUsage(UseProperty.DYNAMIC)]
    [GridCategory(new String[]{"Temperatures"})]
    [GridOrder(2)]
    public IPS.Properties.Double Furnace_Temp
    {
        get
        {
            return _Furnace_Temp;
        }
    }

    [PropertyUsage(UseProperty.DYNAMIC)]
    [GridCategory(new String[]{"Temperatures"})]
    public IPS.Properties.Double Tamb
    {
        get
        {
            return _T_amb;
        }
    }

```

```

    }

/*----- Flows -----*/

    [PropertyUsage(UseProperty.DYNAMIC)]
    [GridCategory(new String[]{"Flows"})]
    [GridOrder(4)]
    public IPS.Properties.Double mfg
    {
        get
        {
            return _m_fg;
        }
    }

    [PropertyUsage(UseProperty.DYNAMIC)]
    [GridCategory(new String[]{"Flows"})]
    public IPS.Properties.Double mfg_leak
    {
        get
        {
            return _m_fg_leak;
        }
    }

    [PropertyUsage(UseProperty.DYNAMIC)]
    [GridCategory(new String[]{"Flows"})]
    public IPS.Properties.Double mair_ing
    {
        get
        {
            return _m_air_ing;
        }
    }

    [PropertyUsage(UseProperty.DYNAMIC)]
    [GridCategory(new String[]{"Flows"})]
    public IPS.Properties.Double mesp_ing
    {
        get
        {
            return _mair_id;
        }
    }

    [PropertyUsage(UseProperty.DYNAMIC)]
    [GridCategory(new String[]{"Flows"})]
    [GridOrder(4)]
    public IPS.Properties.Double Coal_flow
    {
        get
        {
            return _CoalFlow;
        }
    }
}

/*----- Other -----*/

    [PropertyUsage(UseProperty.DYNAMIC)]
    [GridCategory(new String[]{"Other"})]
    [GridOrder(4)]
    public IPS.Properties.Double Qbhx
    {
        get

```

```

        {
            return _Q_bhx;
        }
    }

    [PropertyUsage(UseProperty.DYNAMIC)]
    [GridCategory(new String[]{"Other"})]
    public IPS.Properties.Double QAH
    {
        get
        {
            return _Q_AH;
        }
    }

    [PropertyUsage(UseProperty.DYNAMIC)]
    [GridCategory(new String[]{"Other"})]
    public IPS.Properties.Double CVvalue
    {
        get
        {
            return _CV_Value;
        }
    }

    /*----- Efficiency -----*/
    [PropertyUsage(UseProperty.DYNAMIC)]
    [GridCategory(new String[]{"Efficiency"})]
    [GridOrder(5)]
    public IPS.Properties.Double Efficiency_Direct
    {
        get
        {
            return _effD;
        }
    }

    [PropertyUsage(UseProperty.DYNAMIC)]
    [GridCategory(new String[]{"Efficiency"})]
    public IPS.Properties.Double Efficiency_HHV
    {
        get
        {
            return _effHHV;
        }
    }
}

```

## B.2 - VirtualPlant C# script

```
//script using directives
//css_ref IPS.Core.dll;
//css_ref IPS.PluginInterface.dll;
//css_ref IPS.Units.dll;
//css_ref IPS.Utilities.CSharp.dll;

// ----- VP libraries -----
//css_ref VP\\vp.api.dll;
//css_ref VP\\DevExpress.Utills.v14.1.dll;
//css_ref VP\\DevExpress.XtraEditors.v14.1.dll;
//css_ref VP\\GeneralPhysics.Applications.EtaPRO.Transfer.Common.dll;
//css_ref VP\\GeneralPhysics.Applications.VP.Base.dll;
//css_ref VP\\GeneralPhysics.Applications.VP.Common.dll;
//css_ref VP\\GeneralPhysics.Applications.VP.Components.dll;
//css_ref VP\\GeneralPhysics.Applications.VP.Connectivity.dll;
//css_ref VP\\GeneralPhysics.Applications.VP.Cycles.dll;
//css_ref VP\\GeneralPhysics.Common.dll;
//css_ref VP\\GeneralPhysics.Common.Licensing.dll;
//css_ref VP\\GeneralPhysics.Common.Versioning.dll;
//css_ref VP\\Transfer.KnownObjects.dll;
// -----

using System;
using System.IO;
using IPS.Properties;
using IPS.Scripting;

using System.Collections;
using System.Collections.Generic;
using System.Reflection;
using System.Runtime.CompilerServices;
using System.Threading;
using System.Windows.Forms;
using System.Xml.Serialization;

// ----- access llibraries -----
using GeneralPhysics.Applications.VP.Common;
using GeneralPhysics.Applications.VP.Components;
using GeneralPhysics.Applications.VP.Connectivity;
using GeneralPhysics.Applications.VP.Cycles;
using GeneralPhysics.Applications.EtaPRO.Transfer.Connectivity;
using GeneralPhysics.Applications.EtaPRO.Transfer.KnownObjects;
using GeneralPhysics.Common;
using GeneralPhysics.Common.Licensing;
using GeneralPhysics.Common.UnitConv;
using GeneralPhysics.Common.Versioning;
using Microsoft.VisualBasic;

using GeneralPhysics.Applications.VP.API;

//script must be derived from IComponentScript
public class Script: IPS.Scripting.IComponentScript
{
    // -----
    public double Spray_rh1(double[] Flow, double MW_Gen)
    {

```

```

    if (MW_Gen < 371.1)
    {
        double result1 = Flow[0];
        return result1;
    }
    else if ((371.1 <= MW_Gen) && (MW_Gen < 494.8))
    {
        double deltam_1 = (Flow[1] - Flow[0]) / (494.8 - 371.1);
        double result2 = deltam_1 * (MW_Gen - 371.1) + Flow[0];
        return result2;
    }
    else if ((494.8 <= MW_Gen) && (MW_Gen <= 618.5))
    {
        double deltam_2 = (Flow[2] - Flow[1]) / (618.5 - 494.8);
        double result3 = deltam_2 * (MW_Gen - 494.8) + Flow[1];
        return result3;
    }
    else
    {
        return Flow[2];
    }
}

// -----
public double Spray(double[] Flow, double MW_Gen)
{
    if (MW_Gen < 371.1)
    {
        double result1 = Flow[0];
        return result1;
    }
    else if ((371.1 <= MW_Gen) && (MW_Gen < 494.8))
    {
        double deltam_1 = (Flow[1] - Flow[0]) / (494.8 - 371.1);
        double result2 = deltam_1 * (MW_Gen - 371.1) + Flow[0];
        return result2;
    }
    else if ((494.8 <= MW_Gen) && (MW_Gen <= 618.5))
    {
        double deltam_2 = (Flow[2] - Flow[1]) / (618.5 - 494.8);
        double result3 = deltam_2 * (MW_Gen - 494.8) + Flow[1];
        return result3;
    }
    else
    {
        return Flow[2];
    }
}

// -----
public double Spray_sh(double[] Flow, double MW_Gen)
{
    if (MW_Gen < 424.291)
    {
        double result1 = Flow[0];
        return result1;
    }
    else if ((424.291 <= MW_Gen) && (MW_Gen < 599.945))
    {
        double deltam_1 = (Flow[1] - Flow[0]) / (599.945 - 424.291);
        double result2 = deltam_1 * (MW_Gen - 424.291) + Flow[0];
        return result2;
    }
}

```

```

    }
    else if ((599.945 <= MW_Gen) && (MW_Gen <= 618.5))
    {
        double deltam_2 = (Flow[2] - Flow[1]) / (618.5 - 599.945);
        double result3 = deltam_2 * (MW_Gen - 599.945) + Flow[1];
        return result3;
    }
    else
    {
        return Flow[2];
    }
}

// Inputs
IPS.Properties.Double _Input;
IPS.Properties.Double _AtmTemp;

// Outputs
IPS.Properties.Double _mfw;
IPS.Properties.Double _hfw;

IPS.Properties.Double _msh;
IPS.Properties.Double _hsh;

IPS.Properties.Double _mshs;
IPS.Properties.Double _hshs;

IPS.Properties.Double _mrhin;
IPS.Properties.Double _hrhin;

IPS.Properties.Double _mrhout;
IPS.Properties.Double _hrhout;

IPS.Properties.Double _mrhs;
IPS.Properties.Double _hrhs;

IPS.Properties.Double out1;
IPS.Properties.Double out2;

IPS.Properties.Double HPCond;
IPS.Properties.Double LPCond;

//do pre simulation initialisation here
public override void Initialise()
{
}

//do post simulation cleanup here
public override void Cleanup()
{
}

//script main execution function - called every cycle
public override void Execute(double Time)
{
    ModelHandler Model = new ModelHandler();
    //-----Load Model-----//

    string Path = "G:\\My Drive\\Post
Grad\\2018\\Masters\\Final_model\\Masters_Model_V7_BP_project\\VPmodel_v3_2.cyl"
;

```

```

Model.LoadModel(Path);

//-----Set parametric variables-----//
//Input Names
string VariableNameIn_1 = "MiscData.SetGeneration";
string ComponentIDIn_1 = "00000000-0000-0000-0000-000000000000";
string UnitGroupIn_1 = "LargePower";
string UnitIn_1 = "MW";
double ValueIn_1 = _Input;

string VariableNameIn_2 = "MiscData.SolveForGeneration";
string ComponentIDIn_2 = "00000000-0000-0000-0000-000000000000";
string UnitGroupIn_2 = "None";
string UnitIn_2 = "N/A";
double ValueIn_2 = 1;

string VariableNameIn_3 = "MiscData.AmbTemp";
string ComponentIDIn_3 = "00000000-0000-0000-0000-000000000000";
string UnitGroupIn_3 = "Temp";
string UnitIn_3 = "°C";
double ValueIn_3 = _AtmTemp;

string VariableNameIn_4 = "Boiler.Design.SetSHSspray";
string ComponentIDIn_4 = "a6069c93-68f8-4fd7-b183-b89f9ba3222b";
string UnitGroupIn_4 = "Flow";
string UnitIn_4 = "kg/s";
double[] flow_sh = {27.354, 25.654, 21.922};
double ValueIn_4 = Spray_sh(flow_sh, _Input.Value);
out1.Value = ValueIn_4;

string VariableNameIn_5 = "Boiler.Design.SetRHSspray";
string ComponentIDIn_5 = "a6069c93-68f8-4fd7-b183-b89f9ba3222b";
string UnitGroupIn_5 = "Flow";
string UnitIn_5 = "kg/s";
double[] flow_rh = {0, 1.389, 9.390};
double ValueIn_5 = Spray_rh1(flow_rh, _Input.Value);
out2.Value = ValueIn_5;

string VariableNameIn_6 = "Condenser, Main.Design.ConstBackPress(0)";
string ComponentIDIn_6 = "a4c66a79-bcf2-4237-a584-fc87cfb26624";
string UnitGroupIn_6 = "PressInHgaCmHga";
string UnitIn_6 = "kPaa";
double ValueIn_6 = LPCond;

string VariableNameIn_7 = "Condenser, Main.Design.ConstBackPress(1)";
string ComponentIDIn_7 = "a4c66a79-bcf2-4237-a584-fc87cfb26624";
string UnitGroupIn_7 = "PressInHgaCmHga";
string UnitIn_7 = "kPaa";
double ValueIn_7 = HPCond;

//Load Inputs
Model.SetVariable_Smart(VariableNameIn_1, ComponentIDIn_1, UnitGroupIn_1,
UnitIn_1, ValueIn_1);
Model.SetVariable_Smart(VariableNameIn_2, ComponentIDIn_2, UnitGroupIn_2,
UnitIn_2, ValueIn_2);
Model.SetVariable_Smart(VariableNameIn_3, ComponentIDIn_3, UnitGroupIn_3,
UnitIn_3, ValueIn_3);
Model.SetVariable_Smart(VariableNameIn_4, ComponentIDIn_4, UnitGroupIn_4,
UnitIn_4, ValueIn_4);

```



```

Model.SetVariable_Smart(VariableNameIn_5, ComponentIDIn_5, UnitGroupIn_5,
UnitIn_5, ValueIn_5);

Model.SetVariable_Smart(VariableNameIn_6, ComponentIDIn_6, UnitGroupIn_6,
UnitIn_6, ValueIn_6);
    Model.SetVariable_Smart(VariableNameIn_7, ComponentIDIn_7,
UnitGroupIn_7, UnitIn_7, ValueIn_7);

//-----Run Model-----//
    Model.RunModel();
//-----Collect Return variables-----//
//Output Names
    string CIDout = "a6069c93-68f8-4fd7-b183-b89f9ba3222b";

//FW
    string VNout_1 = "Boiler.StmWtrNode.ndFWInlet.massflow";
    string VNout_2 = "Boiler.StmWtrNode.ndFWInlet.enthalpy";

//SH
    string VNout_3 = "Boiler.StmWtrNode.ndSHOut.massflow";
    string VNout_4 = "Boiler.StmWtrNode.ndSHOut.enthalpy";

//SH Spray
    string VNout_5 = "Boiler.StmWtrNode.ndSHSspray.massflow";
    string VNout_6 = "Boiler.StmWtrNode.ndSHSspray.enthalpy";

//RH
    string VNout_7 = "Boiler.StmWtrNode.ndRHInlet.massflow";
    string VNout_8 = "Boiler.StmWtrNode.ndRHInlet.enthalpy";
    string VNout_9 = "Boiler.StmWtrNode.ndRHOutlet.massflow";
    string VNout_10 = "Boiler.StmWtrNode.ndRHOutlet.enthalpy";

//RH Spray
    string VNout_11 = "Boiler.StmWtrNode.ndRHSspray.massflow";
    string VNout_12 = "Boiler.StmWtrNode.ndRHSspray.enthalpy";

//Getting Values
    VariableInfo OV1 = Model.GetSingleVariable_Smart(VNout_1, CIDout);
    VariableInfo OV2 = Model.GetSingleVariable_Smart(VNout_2, CIDout);

    VariableInfo OV3 = Model.GetSingleVariable_Smart(VNout_3, CIDout);
    VariableInfo OV4 = Model.GetSingleVariable_Smart(VNout_4, CIDout);

    VariableInfo OV5 = Model.GetSingleVariable_Smart(VNout_5, CIDout);
    VariableInfo OV6 = Model.GetSingleVariable_Smart(VNout_6, CIDout);

    VariableInfo OV7 = Model.GetSingleVariable_Smart(VNout_7, CIDout);
    VariableInfo OV8 = Model.GetSingleVariable_Smart(VNout_8, CIDout);

    VariableInfo OV9 = Model.GetSingleVariable_Smart(VNout_9, CIDout);
    VariableInfo OV10 = Model.GetSingleVariable_Smart(VNout_10, CIDout);

    VariableInfo OV11 = Model.GetSingleVariable_Smart(VNout_11, CIDout);
    VariableInfo OV12 = Model.GetSingleVariable_Smart(VNout_12, CIDout);

    string temp = OV1.DisplayValue.ToString();
    _mfw.Value = Convert.ToDouble(temp);
    temp = OV2.DisplayValue.ToString();
    _hfw.Value = Convert.ToDouble(temp);

```

```

temp = OV3.DisplayValue.ToString();
_msh.Value = Convert.ToDouble(temp);
temp = OV4.DisplayValue.ToString();
_hsh.Value = Convert.ToDouble(temp);

temp = OV5.DisplayValue.ToString();
_mshs.Value = Convert.ToDouble(temp);
temp = OV6.DisplayValue.ToString();
_hshs.Value = Convert.ToDouble(temp);

temp = OV7.DisplayValue.ToString();
_mrhin.Value = Convert.ToDouble(temp);
temp = OV8.DisplayValue.ToString();
_hrhin.Value = Convert.ToDouble(temp);

temp = OV9.DisplayValue.ToString();
_mrhout.Value = Convert.ToDouble(temp);
temp = OV10.DisplayValue.ToString();
_hrhout.Value = Convert.ToDouble(temp);

temp = OV11.DisplayValue.ToString();
_mrhs.Value = Convert.ToDouble(temp);
temp = OV12.DisplayValue.ToString();
_hrhs.Value = Convert.ToDouble(temp);
}

//any processing you want to do before steady state
public override void ExecuteBeforeSteadyState()
{
    Execute(0.0);
}

//any processing you want to do while solving steady state
public override void ExecuteSteadyState()
{
    Execute(0.0);
}

//any processing you want to do after steady state
public override void ExecuteAfterSteadyState()
{
    Execute(0.0);
}

//constructor initialises parameters
public Script()
{
    _mfw = new IPS.Properties.Double();
    _mfw.Value = 0;

    _hfw = new IPS.Properties.Double();
    _hfw.Value = 0;

    _msh = new IPS.Properties.Double();
    _msh.Value = 0;

    _hsh = new IPS.Properties.Double();
    _hsh.Value = 0;
}

```

```

    _mshs = new IPS.Properties.Double();
    _mshs.Value = 0;

    _hshs = new IPS.Properties.Double();
    _hshs.Value = 0;

    _mrhin = new IPS.Properties.Double();
    _mrhin.Value = 0;

    _hrhin = new IPS.Properties.Double();
    _hrhin.Value = 0;

    _mrhout = new IPS.Properties.Double();
    _mrhout.Value = 0;

    _hrhout = new IPS.Properties.Double();
    _hrhout.Value = 0;

    _mrhs = new IPS.Properties.Double();
    _mrhs.Value = 0;

    _hrhs = new IPS.Properties.Double();
    _hrhs.Value = 0;

    _Input = new IPS.Properties.Double();
    _Input.Value = 618;

    _AtmTemp = new IPS.Properties.Double();
    _AtmTemp.Value = 19;

    out1 = new IPS.Properties.Double();
    out2 = new IPS.Properties.Double();

    HPCond = new IPS.Properties.Double();
    HPCond.Value = 10.107;

    LPCond = new IPS.Properties.Double();
    LPCond.Value = 6.494;

}

//property declarations to make
//parameters visible to outside world
//Inputs
[PropertyUsage(UseProperty.DYNAMIC)]
[GridCategory(new String[]{"General Inputs"})]
[GridOrder(1)]
public IPS.Properties.Double MW_Gen
{
    get
    {
        return _Input;
    }
}
[PropertyUsage(UseProperty.DYNAMIC)]
[GridCategory(new String[]{"General Inputs"})]
[GridOrder(2)]
public IPS.Properties.Double AtmTemp
{

```

```

        get
        {
            return _AtmTemp;
        }
    }

//-----
//Outputs
[PropertyUsage(UseProperty.DYNAMIC)]
[GridCategory(new String[]{"VP Outputs"})]
[GridOrder(3)]
public IPS.Properties.Double mfw
{
    get
    {
        return _mfw;
    }
}

[PropertyUsage(UseProperty.DYNAMIC)]
[GridCategory(new String[]{"VP Outputs"})]
[GridOrder(4)]
public IPS.Properties.Double hfw
{
    get
    {
        return _hfw;
    }
}

[PropertyUsage(UseProperty.DYNAMIC)]
[GridCategory(new String[]{"VP Outputs"})]
[GridOrder(5)]
public IPS.Properties.Double msh
{
    get
    {
        return _msh;
    }
}

[PropertyUsage(UseProperty.DYNAMIC)]
[GridCategory(new String[]{"VP Outputs"})]
[GridOrder(6)]
public IPS.Properties.Double hsh
{
    get
    {
        return _hsh;
    }
}

[PropertyUsage(UseProperty.DYNAMIC)]
[GridCategory(new String[]{"VP Outputs"})]
[GridOrder(7)]
public IPS.Properties.Double mshs
{
    get

```

```

        {
            return _mshs;
        }
    }

    [PropertyUsage(UseProperty.DYNAMIC)]
    [GridCategory(new String[]{"VP Outputs"})]
    [GridOrder(8)]
    public IPS.Properties.Double hshs
    {
        get
        {
            return _hshs;
        }
    }

    [PropertyUsage(UseProperty.DYNAMIC)]
    [GridCategory(new String[]{"VP Outputs"})]
    [GridOrder(9)]
    public IPS.Properties.Double mrhin
    {
        get
        {
            return _mrhin;
        }
    }

    [PropertyUsage(UseProperty.DYNAMIC)]
    [GridCategory(new String[]{"VP Outputs"})]
    [GridOrder(10)]
    public IPS.Properties.Double hrhin
    {
        get
        {
            return _hrhin;
        }
    }

    [PropertyUsage(UseProperty.DYNAMIC)]
    [GridCategory(new String[]{"VP Outputs"})]
    [GridOrder(11)]
    public IPS.Properties.Double mrhout
    {
        get
        {
            return _mrhout;
        }
    }

    [PropertyUsage(UseProperty.DYNAMIC)]
    [GridCategory(new String[]{"VP Outputs"})]
    [GridOrder(12)]
    public IPS.Properties.Double hrhout
    {
        get
        {
            return _hrhout;
        }
    }

```

```

[PropertyUsage(UseProperty.DYNAMIC)]
[GridCategory(new String[]{"VP Outputs"})]
[GridOrder(13)]
public IPS.Properties.Double mrhs
{
    get
    {
        return _mrhs;
    }
}

[PropertyUsage(UseProperty.DYNAMIC)]
[GridCategory(new String[]{"VP Outputs"})]
[GridOrder(14)]
public IPS.Properties.Double hrhs
{
    get
    {
        return _hrhs;
    }
}

//-----
//Debug
[PropertyUsage(UseProperty.DYNAMIC)]
[GridCategory(new String[]{"Study inputs"})]
[GridOrder(0)]
public IPS.Properties.Double HP_Condenser
{
    get
    {
        return HPCond;
    }
}

[PropertyUsage(UseProperty.DYNAMIC)]
[GridCategory(new String[]{"Study inputs"})]
[GridOrder(1)]
public IPS.Properties.Double LP_Condenser
{
    get
    {
        return LPCond;
    }
}
}

```

## Appendix C. Model design

### C -1 Steady state controller flowchart

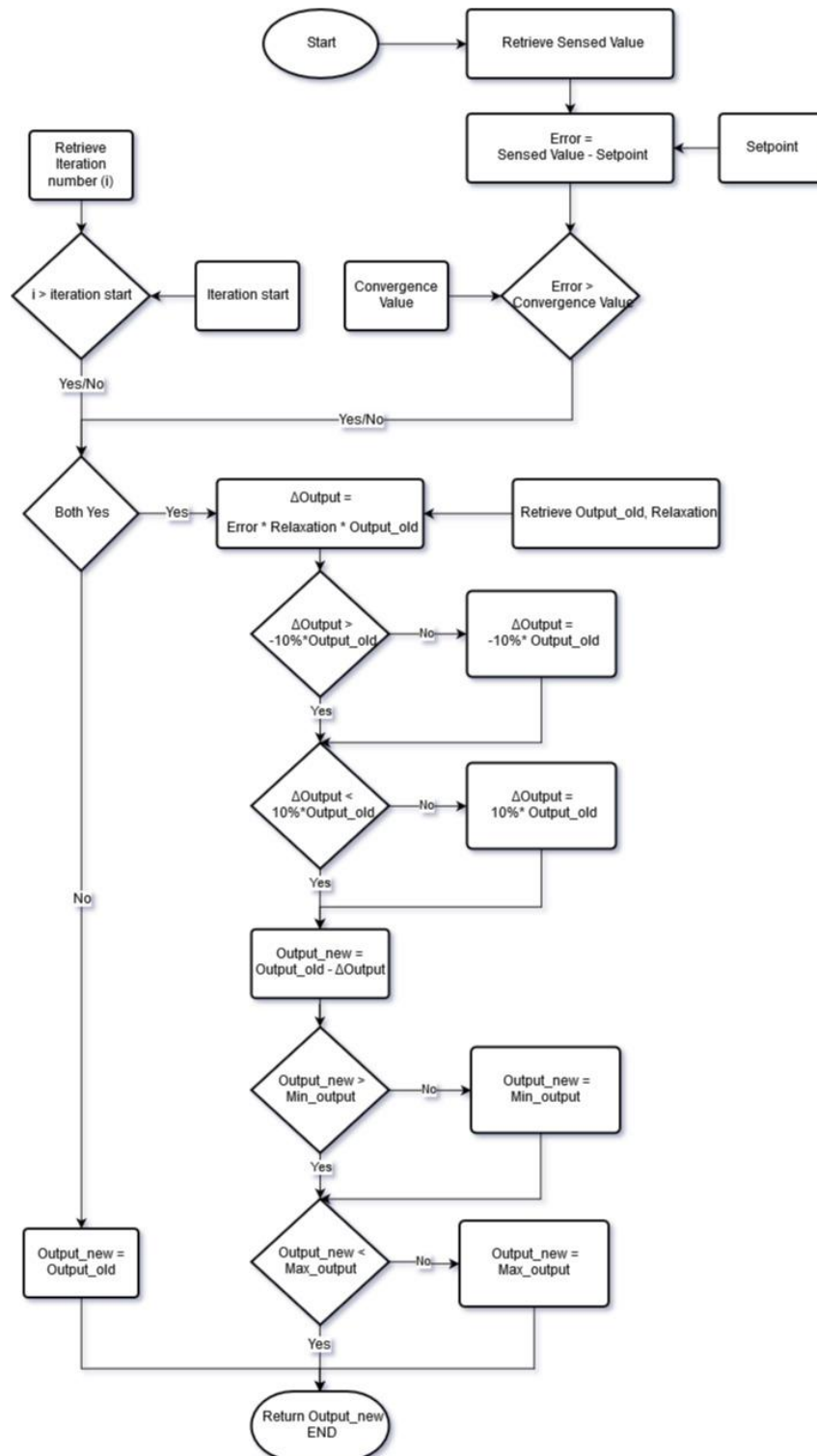


Figure 54: Steady-state controller program flowchart